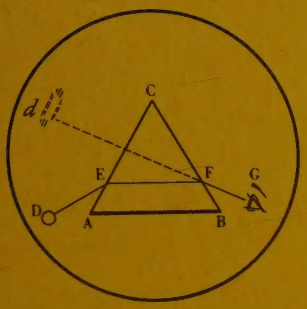

optics and spectroscopy

UNIVERSITY OF ILLINOIS
LIBRARY
FEB 7 1961
CHICAGO

volume ix
number 4
october 1960

OPTICAL SOCIETY OF AMERICA

USSR ACADEMY OF SCIENCES

RUSSIAN EDITORIAL STAFF FOR
OPTIKA I SPEKTROSKOPIYA sponsored by
USSR ACADEMY OF SCIENCES

Editor: S. E. FRISH

Assistant Editor: P. P. FEOFILOV
Corresponding Secretary: L. S. SAZONOV

Associate Editors:

M. M. GUREVICH M. A. EL'IASHEVICH A. A. LEBEDEV V. P. LINNIK
S. L. MANDEL'SHTAM I. V. OBREIMOV V. K. PROKOF'EV
N. N. SOBOLEV A. N. TERENIN A. I. TUDOROVSKII

Translated from *OPTIKA I SPEKTROSKOPIYA* on the initiative of THE OPTICAL SOCIETY OF AMERICA, INC. with a grant-in-aid from THE NATIONAL SCIENCE FOUNDATION. *Optics and Spectroscopy* is a cover-to-cover translation of *Optika i Spektroskopiya* and no attempt is made to edit the material other than to correct obvious misprints. The views are those of the original authors and do not represent the Optical Society of America.

TRANSLATION EDITORIAL STAFF

Scientific Editors

CYRUS FELDMAN, *Oak Ridge National Laboratory*

CARL W. GARLAND, *Massachusetts Institute of Technology*

MATHEW G. GIBBONS, *Oakland, California*

Administrative Editor: PATRICIA R. WAKELING, *OSA*

Published monthly by the Optical Society of America, Inc. Executive office: 1155 Sixteenth Street, N.W., Washington, D.C. Subscriptions for one year to members of the Society: Associates $13.00; Regular members and Fellows $17.00. Subscriptions for non-members of the Society: One year U. S. and Possessions, $25.00; Foreign $28.00. Back numbers: $3.00 per copy. Subscriptions, changes of address and undeliverable copies should be referred to the Executive offices in Washington, D.C. The office of publication is 2500 South State Street, Ann Arbor, Michigan. Second class postage paid at Ann Arbor, Michigan.

Printed in the U.S.A. by Edwards Brothers, Inc., Ann Arbor, Michigan.

A SPECTROSCOPIC METHOD FOR STUDYING THE DIFFUSION OF ATOMS IN AN ELECTRIC ARC

Ya. D. Raikhbaum and V. D. Malykh

Received 19 January 1960

A method is proposed for the determination of the mean time τ spent by atoms in an arc discharge. This method is based on measurement of the intensity of spectral lines after the introduction of atoms into the discharge has ceased. The elements to be investigated are introduced into the arc column with the help of moving probes. The measured values of τ are given for various elements in the dc arc. The effective magnitudes of diffusion coefficients are computed from the τ values.

In spectral analysis the use of the electric arc as a ce of excitation of spectra is related to the measment of the line intensities of elements that are orated during the arc discharge. In this case N, number of atoms of the element in the arc, is deter-ed from the equation

$$\frac{dN}{dt} = n - \beta N, \qquad (1)$$

re n is the number of atoms entering the arc per time and β is the probability that the atoms will e the discharge. In the steady state, the number of ms in the arc is equal to[1]

$$N = \frac{n}{\beta} = n\tau, \qquad (2)$$

re τ is the mean time spent by the atoms in the arc. s the line intensity of an element in the arc spectrum etermined by its rate of vaporization as well as by mean time spent by its atoms in the excitation zone he discharge. In view of this, it is interesting to meas-τ and to investigate the dependence of τ on various ors. In order to solve this problem, we used the im-e method to introduce the vapors of a substance into arc with the help of rotating probes, and measured intensity of the spectral lines during the impulse.

The probes were prepared from 0.2 mm diam Ni-ome wire and were attached to the shaft of a synchro-s motor. As the motor rotated, the probes traversed arc column in the middle of the discharge gap at a ed of 120 cm/sec. The experiments were carried out h a dc arc in air between spectrally pure 6 mm diam -bon electrodes. The arc gap was 5 mm. The probes re connected to the cathode and had a negative poten-of 80 volts with respect to it in order to decrease the -turbation of the arc plasma by the probe.[2] The ele-nts, which were introduced on the probe surfaces in form of chlorides, evaporated in the arc when it was versed by the probe. The lines of the elements were lated from the arc spectrum with the help of a KC-55 ectrograph which had glass optics and a two-channel otoelectric attachment with FEU-19 photomultipliers. order to illuminate the slit of the spectrograph, we ed a double lens condensing system with an intermedi-e image projected onto a diaphraghm.

A simultaneous record of the probe current and the otomultiplier signals, made with various elements de-sited on the probes, showed that after the probe had left e arc (i.e., after the vapors had stopped entering the c) the emission of the spectral lines continued for 10^{-3} 10^{-2} sec, corresponding to the time it took the atoms leave the discharge. The shape and height of the sig-ls at the output of the multipliers were measured during the impulse with the help of an EO-7 cathode ray oscilloscope; the signal was fed directly to the input of the latter. The oscilloscope screen was photographed while the arc was being traversed by the probes (Fig. 1). All calculations were made from oscillograms obtained in the middle of the oscillograph screen, since for large ray deflections the signal shape may be distorted.

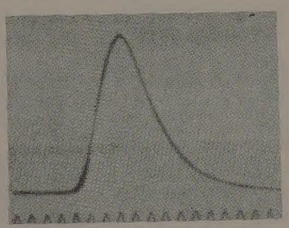

Fig. 1. Oscillogram of thallium line (5360.46 A) intensity during impulse (EO-7 oscilloscope). Time markers correspond to 0.001 sec.

The measurements showed that the decrease in line intensity at the end of the impulse follows the exponential law

$$I = I_0 e^{-\frac{t}{\tau}}, \qquad (3)$$

as is illustrated in Fig. 2. Under a given set of discharge conditions, the spread of the measured τ values for a

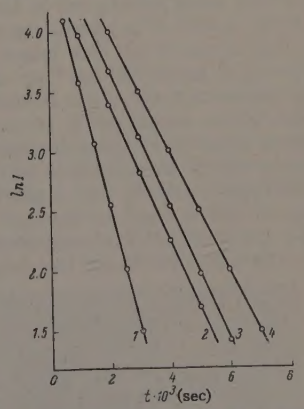

Fig. 2. The change of the line intensity of various elements with time at the end of the impulse. Curve 1—lithium (4602.86 A); curve 2—cadmium (4799.92 A); curve 3—cadmium (5085.22 A); curve 4—thallium (5350.46 A).

Mean Time (τ) Spent by Atoms of Different Elements in the Arc Discharge

Element	Atomic weight	Wave length of line used in measurements (A)	$\tau \cdot 10^3$ (sec)	D (cm²/sec)
Lithium	6.94	4602.86	1.05	20.2
Sodium	22.99	5688.22	1.40	15.2
Calcium	40.08	4454.78	1.58	13.4
Zinc	65.38	4810.53	1.75	12.1
Silver	107.88	5209.07	1.85	11.5
Cadmium	112.41	4799.92	1.90	11.1
Cadmium	112.41	5085.22	1.90	11.1
Thallium	204.39	5350.46	2.10	10.1

given element was about 5 to 7% (mean relative deviation).

The Table shows the mean values of τ obtained for several elements for an arc current of 10 amp. The increase of τ with the increasing atomic weight indicates the importance of the part played by the diffusion process when the atoms leave the discharge. Calculation of the diffusion coefficient D from the measured τ values presents some difficulties. These difficulties arise from the nonuniformity of the discharge and from intense convection. An order of magnitude estimate of the effective value of D was carried out with the help of following equation

$$D = \frac{r_0^2}{(2.405)^2 \tau}, \qquad (4)$$

Equation (4) holds for a cylindrical diffusion zone and for the diffusion of the particles in the radial direction[3,4] (r_0 is the zone radius). The radius of the arc was estimated by a photographic method. The arc was photographed (using a "Zenith" camera without filters) on "Kinonegativ A-2" film (sensitivity: 90 GOST units) with a 1/500 sec exposure. For an arc current of 10 amp, the measured value of r_0 was 0.35 cm. If the possible variations in the size of the zone of spectral line excitations are ignored, and we substitute this value of r_0 in (4), we obtain the effective D values given in the Table.

Since the diffusion time depends on the dimensions of the diffusion zone, an increase in the arc current or in

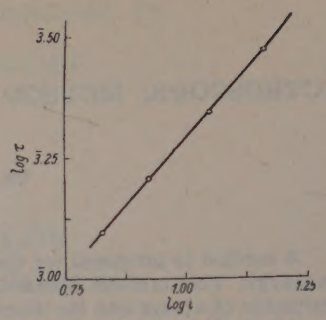

Fig. 3. The dependence of the average time spent by the atoms in the arc on current (cadmium line 5085.22 A).

the radius of the discharge column should lead to an increase in τ. The variation of τ with the current i was determined over the range 6 to 20 amp. Experiments with different elements showed that as the arc current i increases, τ varies as i^k, with k having the value 1 to 1.3 (Fig. 3 shows this dependence for cadmium).

This type of dependence can be explained by the fact that according to Engel's data,[5] the current density for arc in air decreases somewhat with increasing current for the current values shown, and the cross section of the arc column increases disproportionately.

REFERENCES

1. S. L. Mandelshtam, "Introduction to Spectral Analy OGIZ, Moscow, Leningrad, 1946.
2. G. Müller, Z. Physik 151, 460, 1958.
3. V. L. Granovskii, "Electric Current in a Gas 1. Go darst. Izol. Tekh.-Teoret. Lit., Moscow, Leningrad 1952.
4. W. Jost, "Diffusion in Solids, Liquids, and Gases." Academii Press, New York, 1952.
5. A. Engel', "Ionized Gases," Fizmatgiz., Moscow,

ISOTOPE EFFECT IN THE SINGLET SPECTRAL BANDS OF THE BF MOLECULE

A. A. Mal'tsev

Received 31 December 1959

With the vacuum spectrograph DFS-5, the spectrum was obtained in the 1300 to 2090 A region of the discharge in boron trifluoride of a natural isotopic composition, as well as of a composition enriched to 92% with the isotope B^{10}. The use of the latter permitted to obtain a more detailed spectrum of the singlet bands of the BF molecule. A new band system of BF was found and assigned to the transition $E^1\Sigma^+ - X^1\Sigma^+$. The vibrational constants of the $D^1\Pi$ state were determined more accurately.

The spectrum of the BF molecule contains singlet[1-3] triplet[4-6] band systems. The singlet systems (transi-ns $A^1\Pi - X^1\Sigma^+$, $B^1\Sigma^+ - X^1\Sigma$, $C^1\Sigma^+ - X^1\Sigma^+$, and $D^1\Pi - X^1\Sigma^+$) re found and analyzed by Chretien and Mischer[1,2] in emission spectrum (1300 to 2100 A range). The spec- were obtained with a vacuum spectrograph having in first order a dispersion of 8.3 A/mm. As a source, ordinary discharge tube was used through which boron fluoride continuously circulated. Helium served as a rier gas. The system $A^1\Pi - X^1\Sigma^+$ (with a rotational lysis) was investigated most thoroughly. Next, Onaka,[3] ng a spectrograph with a dispersion of 0.3 A/mm, im-ved considerably the values of the molecular con-nts obtained by Chretien for the system $A^1\Pi - X^1\Sigma^+$, the rest of the singlet systems of the BF bands were investigated. Furthermore, the paper by Chretien was complete in several respects. For instance, the tope effect in the spectrum $D^1\Pi - X^1\Sigma^+$ was not ob-rved, and a number of bands in the region 1300 to 1350 A re not assigned. In addition to the spectrum of BF, retien found several bands in the 1650-1800 A region, ch he attributed to the BO molecule. However, the ence of the isotope shifts in these bands did not per-t him to make a definite assignment.

In order to clarify all the above-mentioned points, have obtained the emission spectrum of BF with the cuum spectrograph DFS-5[7] with a 3 meter concave fraction grating, having a dispersion of 2.8 A/mm and heoretical resolving power of 120,000. The experi-ental procedure and the discharge tube were the same those used by Chretien, with the only difference being at instead of a circulating pump, one with a piston and system of valves was applied. Schumann plates made Agfa were used. The wavelengths of the bands were easured with a IZA-Z comparator using the atomic nes of boron, silicon,[9] carbon, oxygen, and helium.[10] or the investigation of the isotope effect, boron tri-uoride was used enriched to 92% with the isotope B^{10} he naturally occurring boron contains 18% of the iso-pe B^{10}).

The spectra of BF which we have obtained in the 800-1850 A region and which correspond to different ontents of the isotopes B^{10} and B^{11}, are shown in the Figure. We have not recorded the band system $A^1\Pi - X^1\Sigma^+$ because it had already been thoroughly studied by other authors.[2,3]

The bands of BO are also observed in the 1650-1800 A region. They appear as a result of the interaction of boron trifluoride with the walls of the discharge tube. The presence of the isotope effect in these bands confirms the correctness of the assignment of these bands to the BO molecule, which has been discussed by us in detail in another paper.[9] All the measured band heads of the molecules $B^{11}F$ and $B^{10}F$ are given in the Table. It can be seen from these data that the values of the isotope shift determined for all bonds agree with the calculated ones and confirm the correctness of the vibrational analysis given by Chretien. In addition to the bands studied by Chretien, we have obtained the bands 1—6, 2—7, 0—4, 1—5, 2—6, 3—7, 2—0, and 3—1 of the system $B^1\Sigma^+ - X^1\Sigma^+$; the bands 0—3, 1—4, and 2—0 of the system $C^1\Sigma - X^1\Sigma^+$; as well as the bands 0—1, 1—2, 2—3, 2—2, 3—2 and 2—0 of the system $D^1\Pi - X^1\Sigma$. Although a number of additional bands were obtained for the first two systems, and the positions of the bands measured previously were more accurately measured, the values of the vibrational constants could not be significantly improved, inasmuch as the error introduced by measuring the heads of the P-branches, and not the zero lines (or even the heads of the Q-branches, as in the $D^1\Pi - X^1\Sigma^+$), is considerable, and the distance between the zero line and the head varies for different bands. The lack of accuracy in the analysis using the heads of the P-branches can be seen also from the fact that the value of the vibrational constant of the ground state $X^1\Sigma^+$, as determined with the zero lines ($\omega_e'' = 1402.1$ cm^{-1}),[3] differs from that determined with the P-heads ($\omega_e'' = 1398.8$ cm^{-1} and $\omega_e'' = 1397.5$ cm^{-1} for the bands $B^1\Sigma^+ - X^1\Sigma^+$ and $C^1\Sigma^+ - X^1\Sigma^+$, respectively). More accurate values of the vibrational constants of the higher states can be obtained only after a rotational analysis of these bands; however, to do this it will be necessary to obtain a spectrum with an apparatus having a still greater dispersion and resolving power, because we were unable to separate the lines of the P-branches forming the head, although the rotational structure of the R-branches was well resolved.

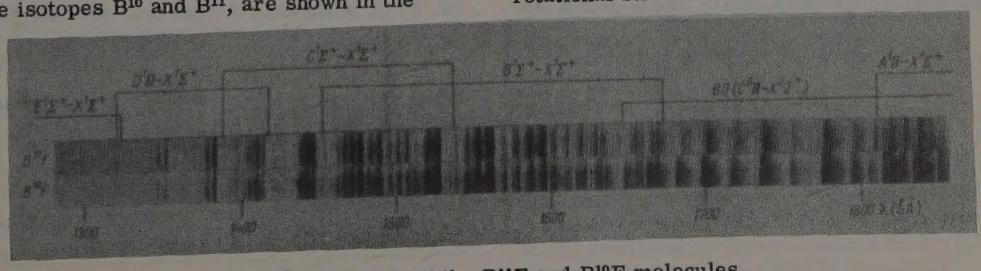

Singlet bands of the $B^{11}F$ and $B^{10}F$ molecules.

The Band Heads of the $B^{11}F$ and $B^{10}F$ Molecules (Frequencies in cm^{-1})

Band	$\nu(B^{11}F)$	$\nu(B^{10}F)$	$\Delta\nu=\nu(B^{11}F)-\nu(B^{10}F)$ experiment	calculation
system $B^1\Sigma^+-X^1\Sigma^+$				
1—6	59227.3	—	—	—
2—7	59625.8	—	—	—
0—4	60112.2	—	—	—
1—5	60492.3	—	—	—
2—6	60869.9	60743.3	+126.6	+125.6
3—7	61242.7	—	—	—
0—3	61421.1	61303.1	+118.0	+117.0
1—4	61779.0	61674.6	+104.4	+103.9
2—5	62134.8	62042.9	+ 91.8	+ 90.8
0—2	62752.0	62673.4	+ 78.6	+ 78.0
1—3	63087.9	63020.9	+ 67.0	+ 66.2
2—4	63421.4	63365.9	+ 55.5	+ 54.5
3—5	63751.1	63706.2	+ 44.9	+ 43.2
0—1	64105.7	64067.8	+ 37.9	+ 37.5
1—2	64419.0	64391.4	+ 27.6	+ 27.1
2—3	64730.2	64712.1	+ 18.1	+ 16.8
3—4	65037.4	65029.0	+ 8.4	+ 6.9
0—0	65483.0	65486.9	— 3.9	— 4.5
1—1	65772.5	65784.8	— 12.3	— 13.4
1—0	67148.3	67202.3	— 54.0	— 55.4
2—1	67413.8	67475.3	— 61.5	— 62.8
3—2	67676.0	—	—	—
2—0	68789.0	68891.9	—102.9	—104.7
3—1	69028.2	—	—	—
system $C^1\Sigma^+-X^1\Sigma^+$				
0—3	65054.3	64935.1	+119.2	+118.3
1—4	65328.8	65220.0	+108.8	+107.8
0—2	66384.8	66305.0	+ 79.8	+ 79.2
1—3	66636.6	66566.4	+ 70.2	+ 70.2
2—4	66882.4	66820.9	+ 61.5	+ 61.5
3—5	67121.8	67070.9	+ 50.9	+ 53.2
0—1	67738.1	67698.0	+ 40.1	+ 38.7
1—2	67966.8	67935.2	+ 31.6	+ 31.1
2—3	68189.5	68166.2	+ 23.3	+ 24.3
3—4	68407.4	68390.0	+ 17.4	+ 17.0
4—5	68619.8	—	—	—
0—0	69113.4	69116.1	— 2.7	— 3.2
1—1	69319.3	69327.7	— 8.4	— 9.4
2—2	69520.0	69534.2	— 14.2	— 15.3
1—0	70693.4	70742.2	— 48.8	— 51.3
2—1	70870.5	70924.3	— 53.8	— 55.7
3—2	71041.5	71105.0	— 63.5	— 59.7
4—3	71209.9	71285.3	— 75.4	— 63.2
5—4	71379.7	—	—	—
2—0	72240.7	—	—	—
system $D^1\Pi-X^1\Sigma^+$				
0—1 (P)	70889.3	70851.5	—	—
1—2 (P)	71197.2	71168.3	—	—
2—3 (P)	71503.7	71485.6	—	—
0—0 (P)	72265.7	72269.1	—	—
(Q)	72286.8	72292.2	— 5.4	— 4.4
1—1 (P)	72549.5	72560.9	—	—
(Q)	72570.8	72583.3	—12.5	—13.4
system $D^1\Pi-X^1\Sigma^+$				
2—2 (P)	72833.3	72854.9	—	—
(Q)	72854.9	—	—	—
1—0 (P)	73924.3	73976.5	—	—
(Q)	73949.1	74003.4	—54.3	—55.3
2—1 (P)	74185.1	74245.1	—	—
(Q)	74209.2	74270.9	—61.7	—62.9
3—2 (P)	74445.9	74514.0	—	—
(Q)	74470.7	74539.4	—68.7	—70.7
2—0 (P)	75557.2	—	—	—
(Q)	75588.0	—	—	—
system $E^1\Sigma^+-X^1\Sigma^+$				
0—1	75697	75658	+39	+38
0—0	77070	77073	— 3	— 3

A more accurate measurement of the Q-heads in the system $D^1\Pi-X^1\Sigma$ permitted us to obtain a considerably more precise value of the energy of the electronic transition of the molecule $B^{11}F$ (T_e = 72145.6 cm^{-1}), and of the values of the vibrational constants of the higher state $D^1\Pi$ (ω_e' = 1685.5 cm^{-1} and $\omega_e'x_e'$ = 11.7 cm^{-1}), as compared with the values of Chretien. As a result, the Q-heads can be represented (accurately to 0.3 cm^{-1}) by the equatio

$$\nu_Q = 72145.6 + 1685.5\left(v' + \frac{1}{2}\right) - 11.7\left(v' + \frac{1}{2}\right)^2$$

$$- 1402.7\left(v'' + \frac{1}{2}\right) + 12.1\left(v'' + \frac{1}{2}\right)^2.$$

The small deviations between ω_e'' determined with the Q-heads (1402.7 cm^{-1}) and with the zero lines (140 cm^{-1}) indicates that the vibrational constants of the up per state are determined quite accurately. The deviat between the values of the measured isotope shifts (see Table) and those calculated according to the formula $\rho = \sqrt{\mu/\mu^1}$ (μ and μ^1 are the reduced masses of the B^{11} and B^{10} molecules) are due to the influence of the isot substitution on the position of the Q-head, and to a cer tain inaccuracy in the determination of the vibrational constants of $B^{11}F$.

In the 1300 cm^{-1} region we have found two weak bands shaded to the violet which have an isotope shift (see Table). The low intensity of these bands and the absence of the spectrum in the wavelength region belo 1300 A are due to a strong absorption of the fluorite l The band (1297.5 A), having the shorter wavelength of two mentioned above, was previously observed by Chr tien; however, it was not assigned by him to any of the known systems. A very small isotope shift (−3 cm^{-1}) the 1297.5 A band, and a large one (−38 cm^{-1}) in the 1321.1 A band, and the distance between these two ban (1373 cm^{-1}) which correspond to the distance between vibrational levels $v''=0$ and $v''=1$ of the ground sta $X^1\Sigma^+$ enable us to assign these bands to a new electro transition of the BF molecule. Since these bands have single head, the upper state of the new system must b the $^1\Sigma^+$. From the characteristics of these bands it w also possible to estimate the values of the constants o the upper state $E'\,^1\Sigma^+$: $T_e \approx 76955$ cm^{-1}, $\omega_e' \approx 1630$ cm and $\omega_e'x_e' \approx 12$ cm^{-1}.

REFERENCES

1. M. Chretien and E. Miescher, Helv. Phys. Acta 2 588 (1949).
2. M. Chretien, Helv. Phys. Acta 23, 259 (1950).
3. R. Onaka, J. Chem. Phys. 27, 374 (1957).
4. H. M. Strong and H. P. Knauss, Phys. Rev. 49, 74 (1936).
5. F. W. Paul and H. P. Knauss, Phys. Rev. 54, 107 (1938).
6. R. F. Barrow, D. Premaswarup, J. Winternitz, a P. B. Zeeman, Proc. Phys. Soc. 71, 61 (1958).
7. B. K. Prokof'ev, Izvest. Akad. Nauk SSSR, Ser. F 22, 737 (1958).
8. I. G. Katsnel'son, B. P. Bruns, and D. Iu. Gambu Zavodskaya Lab. 12, 379 (1946).
9. A. A. Mal'tsev, D. I. Kataev, and B. M. Tatevskii Opt. i Spektr. (in press).
10. P. G. Wilkinson, J. Opt. Soc. Am. 45, 862 (1955).

VIBRATIONAL SPECTRA OF UNSATURATED HYDROCARBONS
IX. Calculation and Interpretation of the Vibrational Spectra of Methylallene and the Deuterioallenes

L. M. Sverdlov and M. G. Borisov

Received 24 December 1959

A frequency calculation has been carried out and a full interpretation is given for the vibrational spectra of methylallene and the deuterioallenes. The characteristic frequencies of the monoalkyl substitution products of allene have been established.

1. In our previous works[1, 2] on the elucidation of the culiarities of the vibrational spectra of compounds with mulated double bonds, we considered allene, tetra-uterioallene, and 1,1-dimethylallene. It was shown in f. 2 that the force constants of allene and of olefins may used to calculate the alkyl substitution products of ene. In continuation of these investigations, it was of erest to carry out a calculation of the vibrational spec-a of partially deuterated allenes—monodeuterioallene, 1-dideuterioallene, 1,3-dideuterioallene, and trideuterio-ene—and also of methylallene. The calculation of the rmal vibration frequencies was carried out according the procedure of El'yashevich and Stepanov.[3]

2. The molecules C_3H_3D, C_3HD_3, and methylallene long to the symmetry group C_s. The molecules 1,1-$_2H_2D_2$ and 1,3-$C_3H_2D_2$ are assigned respectively to the mmetry groups C_{2v} and C_2. The molecules just enerated possess vibrations of the following symmetry pes: C_3H_3D and C_3HD_3, $\Gamma = 10A' + 5A''$; 1,3-$C_3H_2D_2$, = 8A + 7B; 1,1-$C_3H_2D_2$, $\Gamma = 6A_1 + 4B_2 + 4B_1 + A_2$; ethylallene, $\Gamma = 15A' + 9A''$.

We shall choose as internal vibrational coordinates e changes in the bond lengths and angles.

Deuterioallenes: q_i, β_i (i = 1-4), α_{12}, α_{34}, Q_a, Q_b, $_{ab}$, γ''_{ab} (Figs. 1, 2), $\rho^a_{CH_2}$, ρ^b_{CHD}, $\chi^{CH_2}_{CHD}$ (in the case of $_3D$). Here $\rho^a_{CH_2}$ is the departure of the bond $(C{=}C)_a$ om the CH_2 plane, ρ^b_{CHD} is the departure of the bond $C{=}C)_b$ from the CHD plane, and $\chi^{CH_2}_{CHD}$ is the coordinate haracterizing the rotation of the CH_2 and CHD groups ith respect to each other. There are two additional con-tions among the coordinates.

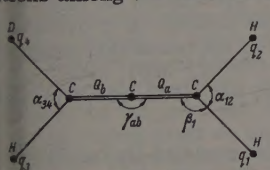

Fig. 1

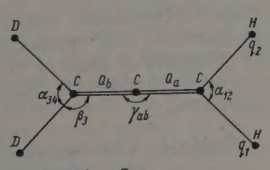

Fig. 2

Fig. 1. Vibrational coordinates of monodeuterioallene.

Fig. 2. Vibrational coordinates of 1,1-dideuterioallene.

Methylallene: q_i, β_i (i = 1-6), Q_a, Q_b, Q_c, α_{12}, α_{45}, $_{46}$, α_{56}, γ'_{ab}, γ''_{bc}, γ_{bc} (Fig. 3), $\rho^a_{CH_2}$, ρ^b_{CCH}, $\chi^{CCH}_{CH_2}$ (the last hree coordinates have the same meaning as in the case f C_3H_3D).* There are three additional conditions among he coordinates.

*The coordinate characterizing the restricted rotation of he CH_3 group was not considered in the calculation.

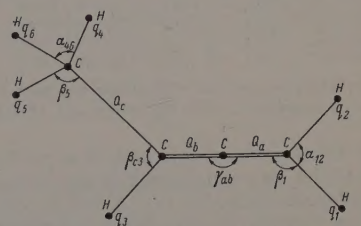

Fig. 3. Vibrational coordinates of methylallene.

The vibrational spectra of 1,1-dideuterioallene have been studied in several works.[4-6] In ref. 4, a brief description of the infrared and Raman spectra of the molecule is given. Shuler and Fletcher,[5] having studied the infrared spectrum in the 1.6-38μ region, carried out an interpretation of the spectrum and a calculation of the frequencies of the 1,1-$C_3H_2D_2$ molecule. However, in doing so they committed errors in the interpretation of some frequencies. The lines 924 and 1176 cm^{-1} were assigned respectively to the vibrations $Q^+(C{=}C)^{A_1}$ and $\alpha(DCD)^{A_1}$. On the basis of the results of our calculation, we make the opposite assignment. The authors[5] assign the lines 668 and 1022 cm^{-1} to symmetry type B_1 and the lines 826 and 845 cm^{-1} to symmetry type B_2, while on the basis of our computed data we make the opposite assignment in this case also.

In Thompson's work,[6] only certain infrared bands of the 1,1-$C_3H_2D_2$ molecule were studied with the help of an apparatus of high resolving power. The Raman spectra of methylallene have been studied in refs. 7 and 8, the polarization of the lines also being determined in the latter work. The authors[8] made an attempt to carry out an interpretation of the spectrum; however, many frequencies were incorrectly assigned (cf. Table 2). The infrared spectra of methylallene in the 2-15μ region have been investigated in a work by Rasmussen and Brattain.[9]

3. For the evaluation of the kinematic coefficient matrices of the deuterioallenes, the geometric parameters of allene[1] were taken. In the case of methylallene, the following geometric parameters were used: r(=C–H) = 1.07A, r(C=C) = 1.308A, r(C–H) = 1.09A, r(C–C) = 1.54A, $\theta_{12} = \theta_{c3} = 117°$, $\theta_{c4} = \theta_{45} = 109° 28'$.

The force constants necessary for the evaluation of the potential energy matrices of the deuterioallenes were taken from the allene calculation.[1] For the methylallene molecule, the force constants for allene[1] and propylene[10] were used.

On the basis of the symmetry of the molecules, we introduced symmetry coordinates with the help of which we set up symmetrized matrices of the kinematic and force coefficients. By multiplication of these matrices, symmetrized secular equations of the 15th, 10th, 8th, 7th,

Table 1. Interpretation of the Vibrational Spectra of the Deuterioallenes

C_3H_3D			$1,3\text{-}C_3H_2D_2$			$1,1\text{-}C_3H_2D_2$				C_3HD_3		
Coordinate	Symmetry	$\nu_{calc.}$ (cm^{-1})	Coordinate	Symmetry	$\nu_{calc.}$ (cm^{-1})	Coordinate	Symmetry	$\nu_{calc.}$ (cm^{-1})	$\nu^*_{obs.}$ according to refs. 5, 6 (cm^{-1})	Coordinate	Symmetry	$\nu_{calc.}$ (cm^{-1})
q (C—D)	A'	2267	q (C—D)	A	2258	q^+ (C—D)	A_1	2228	2227	q^+ (C—D)	A'	2222
α (HCH)	A'	1435	α (HCD)	A	1338	α (HCH)	A_1	1433	1418	α (DCD)	A'	941
Q^+ (C=C)	A'	1048	Q^+ (C=C)	A	1047	Q^+ (C=C)	A_1	1161	1176	Q^+ (C=C)	A'	1147
$\gamma^{CHD}_{CH_2}$	A''	851	γ^{CHD}_{CHD}	A	683	$\gamma^{CD_2}_{CH_2}$	A_2	750	—	$\gamma^{CHD}_{CD_2}$	A''	641
q^+ (C—H)	A'	2995	q (C—D)	B	2277	q^+ (C—H)	A_1	2995	3013	q (C—D)	A'	2272
Q^- (C=C)	A'	1955	Q^- (C=C)	B	1941	Q^- (C=C)	A_1	1937	1940	Q^- (C=C)	A'	1924
α (HCD)	A'	1319	α (DCD)	B	1279	α (DCD)	A_1	938	924 ***	α (HCD)	A'	1320
q (C—H)	A'	3045	q (C—H)	A	3045	q^- (C—D)	B_1	2319	2318	q (C—H)	A'	3045
β (CCD)	A'	830	β (CCD)	A	860	β^- (CCD)	B_1	806	826 **	β (CCD)	A'	859
ρ_{CH_2}	A'	860	ρ_{CHD}	A	808	ρ_{CH_2}	B_1	851	845 **	ρ_{CD_2}	A'	684
γ (CCC)	A'	337	γ (CCC)	A	322	γ (CCC)	B_1	326	327 **	γ (CCC)	A'	310
q^- (C—H)	A''	3089	q (C—H)	B	3046	q^- (C—H)	B_2	3089	3084	q^- (C—D)	A''	2319
β^- (CCH)	A''	1025	β (CCD)	B	890	β^- (CCH)	B_2	1025	1022	β (CCD)	A''	796
ρ_{CHD}	A''	712	ρ_{CHD}	B	754	ρ_{CD_2}	B_2	678	668 **	ρ_{CDH}	A''	832
γ (CCC)	A''	338	γ (CCC)	B	325	γ (CCC)	B_2	332	336 **	γ (CCC)	A''	311

Note: *Infrared absorption spectrum. **Determined from analysis of overtones:[5] $1653 = 2\nu_9$; $1690 = 2\nu_{10}$; $654 = 2\nu_{11}$; $672 = 2\nu_{15}$; $1336 = 2\nu_{14}$. ***Raman spectrum.[4]

5th, and 4th degrees were obtained. The roots of the secular equations were computed by the method of progressive diagonalization.

In Tables 1 and 2 the calculated and observed frequency values for the molecules under consideration are presented and an interpretation of the vibrational spectra of $1,1\text{-}C_3H_2D_2$ and of methylallene is given. The agreement of the experimental and the calculated data is quite good—the maximum error for $1,1\text{-}C_3H_2D_2$ equals 20 cm^{-1} and the average error is 8 cm^{-1}; for methylallene, the values are 39 and 16 cm^{-1} respectively.

The accuracy of the calculation of the frequency values for the deuterioallenes is confirmed by the excellent fulfillment of the sum rules[11] for the calculated frequencies of the various symmetry types:

$$\frac{3}{4}\sum\nu_i^2(C_3H_4)+\frac{1}{4}\sum\nu_i^2(C_3D_4)=\sum\nu_i^2(C_3H_3D);$$

$$\frac{1}{4}\sum\nu_i^2(C_3H_4)+\frac{3}{4}\sum\nu_i^2(C_3D_4)=\sum\nu_i^2(C_3HD_3);$$

$$\frac{1}{2}\sum\nu_i^2(C_3H_4)+\frac{1}{2}\sum\nu_i^2(C_3D_4)=\sum\nu_i^2(1,1\text{-}C_3H_2D_2);$$

$$\frac{1}{2}\sum\nu_i^2(C_3H_4)+\frac{1}{2}\sum\nu_i^2(C_3D_4)=\sum\nu_i^2(1,3\text{-}C_3H_2D_2).$$

Table 3. Interpretation of the Overtones and Combination Frequencies of Methylallene (Frequency in cm^{-1})

IR according to ref. 9	Assignment	Ram. according to ref. 7	Assignment
670 (w)	876 − 210 = 666	957 (vw)	1961 − 1003 = 958
727 (vw)	523 + 210 = 733	2870	1439 + 1439 = 2878
760 (vw)	555 + 210 = 765	2931 (m)	1462 + 1462 = 2924
1040 (m)	523 + 523 = 1046		
1055 (m)	842 + 210 = 1052		
1167 (w)	842 + 322 = 1164		
1183 (w)	859 + 322 = 1184		
1198 (vw)	876 + 322 = 1198		
1266 (w)	1462 − 210 = 1252		
1285 (w)	1072 + 210 = 1282		
1372 (w)	842 + 523 = 1365		
1570 (w)	1003 + 555 = 1558		
1692 (m)	842 + 842 = 1684		
1704 (m)	859 + 859 = 1718		
1890 (w)	1327 + 555 = 1882		
2180 (vw)	1102 + 1072 = 2174		
2260 (vw)	1132 + 1132 = 2264		
2480 (w)	1374 + 1102 = 2476		
2540 (w)	1439 + 1102 = 2541		
2675 (vw)	2993 − 322 = 2671		
2775 (w)	1439 + 1327 = 2766		
3300 (vw)	1961 + 1327 = 3288		
3510 (vw)	2993 + 523 = 3516		
3955 (vw)	2954 + 1003 = 3957		
4055 (vw)	2954 + 1102 = 4056		
4365 (w)	2910 + 1462 = 4372		
4465 (vw)	2993 + 1462 = 4455		

Note: For symbols, see note to Table 2.

Table 2. Interpretation of the Vibrational Spectrum of Methylallene*

Coordinate	Symmetry	$\nu_{calc.}$ (cm^{-1})	$\nu_{obs.}$ (cm^{-1})		Assign
			Ram. (liquid) according to refs. 7, 8	IR (gas) from ref. 9	from re
$q^-_{CH_2}$ (C—H)	A''	3089	3061 (m)	—	**
$q^+_{CH_2}$ (C—H)	A'	2995	2993 (vs)	3010 (s)	**
σ_{CH_2} (HCH)	A'	1434	1439 (w)	1437 (m)	13
$\beta^-_{CH_2}$ (CCH)	A''	1021	1003 (vw)	~ 1011 (m)	11
Q^+ (C=C)	A'	1133	1132 (vs)	—	10
Q^- (C=C)	A'	1982	1961 (vw)	1970 (s)	19
γ'_{ab} (C=C=C)	A'	202	210 (vs) b	—	2
γ''_{ab} (C=C=C)	A''	328	322 (vw)	—	3
ρ_{CH_2}	A'	836	—	859 (vs)	8
ρ_{CCH}	A''	486	523 (vw)	—	8
q_{CH} (C—H)	A'	3045	3061 (m)	—	**
β_{C_2} (CCH)	A'	1310	1327 (w) p	~ 1330 (m)	13
γ_{bc} (CCC)	A'	551	555 (m) p	—	5
Q (C—C)	A'	859	876 (vs) p	—	8
$\gamma^{CH_2}_{CCH}$	A''	848	842 (w)	—	5
$q^-_{CH_2}$ (C—H)	A'	2976	2954 (vw)	2965 (s)	**
$q^+_{CH_2}$ (C—H)	A'	2899	2910 (m)	2905 (s)	**
q''_{CH_2} (C—H)	A''	2975	2954 (vw)	2965 (s)	**
$\sigma^-_{CH_2}$ (HCH)	A'	1473	1462 (m) d	1453 (m)	14
σ''_{CH_2} (HCH)	A''	1470	1462 (m) d	1453 (m)	14
$\sigma^+_{CH_2}$ (HCH)	A'	1404	1374 (m)	1389 (w)	13
$\beta^-_{CH_2}$ (CCH)	A'	1042	1072 (s) p	~ 1074 (m)	11
β''_{CH_2} (CCH)	A''	1063	1102 (m) d	~ 1110 (m)	10

Note: *Symbols: IR—infrared absorption spectrum; Ram.—Raman spectrum (b line, p—polarized line, d—double). Intensities (in parentheses): vs—very strong s—strong; m—medium; w—weak; vw—very weak. **The frequencies 3061, 2993, 2931, 2910, and 2870 cm^{-1} were assigned to C-H vibrations.

At the same time, the so-called order rules[12] are also well fulfilled. The order rule consists in this: if the frequencies ν of a light molecule are arranged in increasing order, and likewise the frequencies ν' of a heavier isotopic molecule, the following relationships are obtained: $\nu'_1 \leq \nu_1$, $\nu'_2 \leq \nu_2$, ..., $\nu'_n \leq \nu_n$, where n is the number of vibrational degrees of freedom.

On the basis of the assignment carried out for the fundamental frequencies of methylallene, the remaining frequencies may be interpreted as overtones or combination frequencies (Table 3). The calculation carried out for the methylallene frequencies enables us to determine the characteristic frequencies of the monoalkyl substitution products of allene, RCH=C=CH_2: 3061, 2993, 1443, 1003, 1132, 1964, 200, 325, 850, 540, 1338, 555, 840, and 1100 cm^{-1}.

Table 4. Characteristic Frequencies (in cm^{-1}) of Monoalkylallenes, RCH=C=CH_2

Coordinate	Propylallene Ram. from ref. 7	Butylallene Ram. from ref. 7	Coordinate	Propylallene Ram. from ref. 7	Butyla Ram. ref.
$q^-_{CH_2}$ (CH), q_{CH_3} (CH)	3061 (m)	3062 (s)	γ''_{ab} (C=C=C)	325 (w)	326
$q^+_{CH_2}$ (CH)	2992 (vs)	2993 (s)	ρ_{CH_2}	–	~848
α_{CH_2} (HCH)	1445 (s)	1441 (s)	ρ_{CCH}	537 (w)	547
$\beta^-_{CH_2}$ (CCH)	–	1009 (vw)	β_{CH} (CCH)	1332 (vw)	1345
Q^+ (C=C)	1131 (s)	1132 (s)	γ_{bc} (CCC)	548 (w)	563
Q^- (C=C)	1964 (vw)	1964 (vw)	$\gamma^{CCH}_{CH_2}$	839 (m)	842
γ'_{ab} (C=C=C)	198 (s)	196 (s)	$\beta''_{>CH_2}$ (CCH)	1098 (s)	1099

Note: For symbols, see note to Table 2.
*Line in the infrared absorption spectrum (according to ref. 13).

By analogy with methylallene, the lines 850 and 1964 cm^{-1} should have the greatest intensity in the infrared ectrum, and the lines 2993, 1132, 200, and 1100 cm^{-1} the Raman spectrum. The available experimental evi- nce gives good confirmation of the conclusions of the eory (Table 4).

EFERENCES

.. L. M. Sverdlov, Opt. i Spektr. 2, 540 (1957).
.. L. M. Sverdlov, M. G. Borisov, and N. V. Tarasova, Opt. i Spektr. 5, 354 (1958).
.. M. V. Vol'kenshtein, M. A. El'yashevich, and B. I. Stepanov. "Kolebaniya molekul" (Molecular Vibrations), Vol. 1. Gosudarst Izd. Tekh.-Teoret. Lit., Moscow, 1949.
.. J. Evans, J. Wilmshurst, and H. Bernstein, Can. J. Chem. 34, 1139 (1956).
5. W. E. Shuler and W. H. Fletcher, J. Mol. Spectroscopy 1, 95 (1957).
6. D. R. Eaton and H. W. Thompson, Proc. Roy. Soc. A250, 39 (1959).
7. H. Bourguel and L. Piaux, Bull. Soc. chim. France 51, 1041 (1932).
8. G. Szasz, J. S. McCartney, and D. H. Rank, J. Am. Chem. Soc. 69, 3150 (1947).
9. R. S. Rasmussen and R. R. Brattain, J. Chem. Phys. 15, 131 (1947).
10. L. M. Sverdlov, Doklady Akad. Nauk SSSR 106, 80 (1956).
11. L. M Sverdlov, Doklady Akad. Nauk SSSR 78, 1115 (1951).
12. R. Courant and D. Hilbert, "Metody matematicheskoi fiziki" (Methods of Mathematical Physics), Vol. 1. Gosudarst. Izd. Tekh., Moscow, 1951.
13. J. Wotiz, J. Am. Chem. Soc. 73, 698 (1951).

TEMPERATURE DEPENDENCE OF THE INTENSITIES OF THE INFRARED ABSORPTION BANDS OF LIQUID CHLOROFORM

M. P. Lisitsa and Yu. P. Tsyashchenko

Received 4 January 1960

We have studied quantitatively the course of the temperature dependence of the integrated absorption in the bands of the fundamental vibrations ν_1 and ν_4, of the most intense overtones $2\nu_1$ and $2\nu_4$, and of the combination frequencies $\nu_1 + \nu_4$, $\nu_2 + \nu_6$, and $\nu_3 + \nu_6$ of the infrared spectrum of liquid chloroform. In almost all cases, the measurements were carried out at five temperature values over the entire range of existence of the liquid phase. An improved construction of a cryostat for low-temperature measurements is described. A discussion of the results in comparison with the data for other substances ($CHBr_3$, CCl_4, and CBr_4) is given.

TRODUCTION

The present work was undertaken for the purpose of rther quantitative study of the regularities and nature the temperature dependence of the intensities in the frared absorption spectra of molecular liquids. In one the previous works,[1] the authors investigated the influ- nce of temperature on the integrated absorption of cer- in vibrational bands of liquid bromoform. In the present ork, the temperature dependence of the integrated ab- rption (mainly in the bands of the same vibrations) of quid chloroform has been studied. Such a sequence and arallelism in the choice of objects of study enables us o follow, on the one hand, the influence of the properties f the vibration itself on the effect under study. On the ther hand, there arises the possibility of a quantitative omparison of the temperature dependence of the inten- ities of identical vibrations in the spectra of liquids of he same type with regard to molecular structure and ature; i.e., the possibility of studying the dependence of he phenomenon on the properties of the liquid itself.

EXPERIMENTAL PROCEDURE

The liquid cell used in the present measurements has been described in ref. 1. It was heated, in the temperature range 20-60°C, by cylindrical electric ovens with temperature regulation, and was cooled (in the interval -20 to -60°C) in a cryostat whose arrangement is shown in Fig. 1. Cryostats in which the metal block for cooling the cell is joined to the remaining glass parts by Kovar-glass or copper-glass seals have been described in a whole series of works.[2-5] Their common defect is that the cooling of the cell takes place through contact with the bottom of the metal cup-block into which the refrigerant is poured. Such a method of lowering the temperature inevitably brings about the appearance of a considerable thermal gradient along the vertical axis of the cell, which is especially inconvenient when the liquid freezes and one goes over to studies in the crystalline phase; it also raises the attainable lower temperature limit (the minimum temperature obtained with liquid nitrogen at a pressure of 10^{-3} mm Hg in the cryostat lies between the limits of -150 to -175°C[4,5]). To eliminate this defect, the cooling block 1 was made hollow in our construction, so that in this way the refrigerant poured into it could flow around all sides of the cell 2 contained in the block. By means of the Kovar-glass seal 3, the block was joined to the glass part of the cryostat, which was arranged in the ordinary way. A thermocouple was introduced through an opening in the glass stopper 4, which was covered with picein to ensure a vacuum. The rock-salt windows 5 were secured to the glass vessel also with the help of picein. To bring about good thermal contact with the walls of the block, the ends of the cell were covered with a layer of vacuum grease.

The above-described construction ensured both the practically complete absence of a temperature gradient along the cell and also its rapid cooling. At a pressure of the order of 10^{-3} mm Hg in the cryostat and under cooling with liquid nitrogen, the lowest temperature

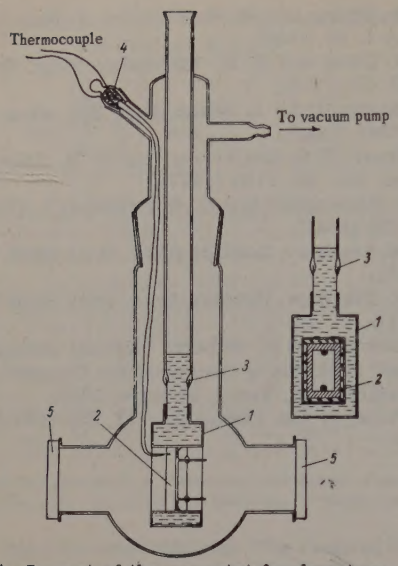

Fig. 1. Layout of the cryostat for low-temperature studies.

which we succeeded in reaching did not exceed −185 to −190°C; i.e., it was substantially less than the temperature obtained using ordinary cryostats. In the measurements which we undertook, the cell was cooled with a mixture of acetone and solid carbon dioxide. By changing the quantity of the latter, it was possible to obtain several sufficiently stable temperature points in the interval from +20 to −60°C.

A detailed consideration and estimate of the errors of the measurements has been given in the preceding work.[1] Here there is reason to dwell only on the effect (pointed out in ref. 6) of the change in cell thickness in consequence of the temperature variation of the vapor pressure of the liquid under study. A direct check, which we carried out in the cryostat at room temperature for the band of the vibration ν_4 (cell thickness 7.5μ), did not reveal the presence of such an effect. Evidence regarding its occurrence (at least within the limits of experimental error) is also given by the fact that no breaks are observed in the temperature dependences obtained (Fig. 4) on going through the +20°C point; i.e., they are always linear. If there were a change in cell thickness exceeding the limits of random errors (5-7%), the linearity would be disturbed, since at temperatures below room temperature all the measurements were made in the cryostat with a single cell, while above it they were made with two cells of different thickness, placed in two ovens heated simultaneously.* The use of two cells enables us

*The band of the vibration ν_4 constitutes an exception.

to exclude the effect under consideration (if it actually takes place) as being independent of the thickness.

The results of the measurements have been corrected for the relative temperature variation in the density of $CHCl_3$, which amounts to 15-16% over the entire range of existence of the liquid phase. The magnitude of the integrated absorption is given with an error of 10-15%; however, its relative change with temperature was obtained with an error only half as great.

RESULTS AND DISCUSSION OF THE MEASUREMENTS

The absorption bands of liquid $CHCl_3$ (the spectrum of which has been studied by us in detail in ref. 7) investigated in the present work are the most convenient for temperature measurements—in the majority of cases they do not overlap other bands and they are distinguis by relatively low intensity values. The results of the measurements are represented in part in Fig. 2, in wh are given the bands of the fundamental vibrations ν_1 a ν_4, those of the combination frequencies $\nu_1 + \nu_4$ and ν_2 ν_6, and that of the overtone $2\nu_1$ at various temperature As follows from the data presented, the absorption diminishes with an increase in temperature for the funda mental vibrations and the combination frequencies. At the same time, the intensities of both overtones remai constant (in Fig. 2e only the one curve corresponding t the overtone $2\nu_1$ is presented as an example). The greatest temperature dependence is observed for the totally symmetric valence vibration* of the C—H bond,

*In the calculation of the integrated absorption in the band of the vibration ν_1, the latter was assumed to be symmetrical, and the absorption of its unidentified sho wavelength satellite was not taken into account. The in tegrated absorption in the band of the combination frequency $\nu_1 + \nu_4$ is also given after graphical separation i.e., without the absorption of the short-wavelength component.

ν_1, the integrated absorption in the band of which diminishes by 32% in the interval from −58 to +60°C. Th value agrees satisfactorily with the data of ref. 8, fron which it follows that, on heating chloroform from −10 +50°C, the molar absorption coefficient in this band diminishes by 14.1%. The 49% reduction of absorption given in ref. 6 for the band of this same vibration seen to us to be too high. For the remaining bands, the observed fall in intensity has a markedly lower value and fluctuates within the limits of 17-25%.

The curves of the temperature dependence of the i tegrated intensity of most of the bands studied are rep sented in Figs. 3 and 4. In contrast to bromoform,[1] the intensity of the deformation vibration of the C—H bond in chloroform depends less on the temperature than tha of the vibration ν_1. Qualitatively, this agrees with the

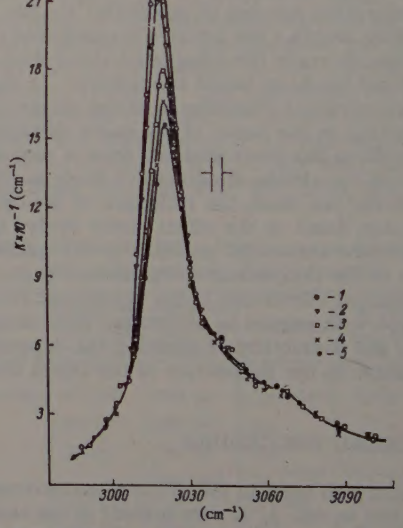

Fig. 2a. Influence of temperature on various infrared absorption bands of liquid $CHCl_3$. Vibration: Fig. a—ν_1; b—ν_4; c—$\nu_2 + \nu_6$; d—$\nu_1 + \nu_4$; e—$2\nu_1$.

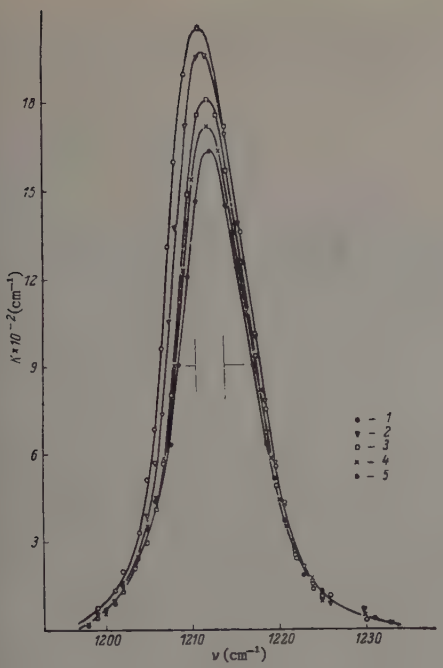

Fig. 2b

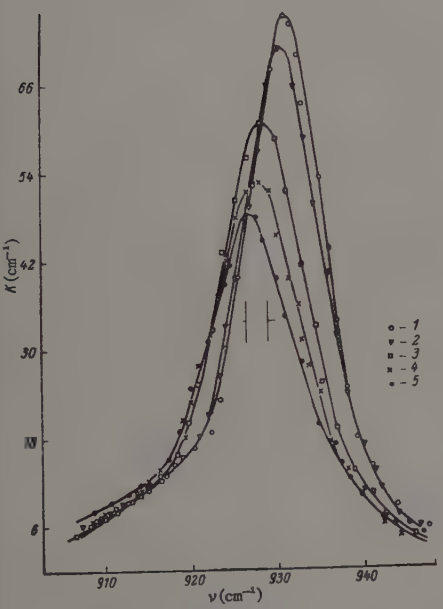

Fig. 2c

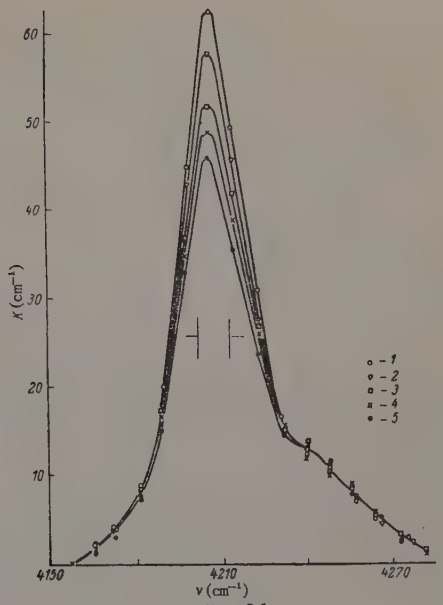

Fig. 2d

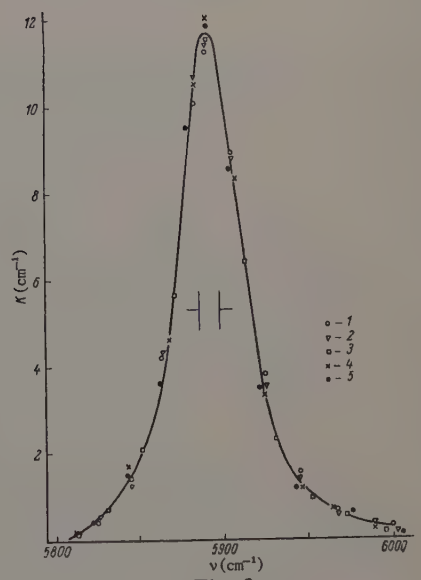

Fig. 2e

data of ref. 6, although no temperature dependence of the absorption in the band of this vibration was detected at all by these authors. With the exception of the discrepancy just cited, there is otherwise a marked parallelism between the temperature dependences studied in the spectra of chloroform and of bromoform. In both cases the intensities of the overtones ($2\nu_1$ and $2\nu_4$ in the $CHCl_3$ spectrum and $2\nu_1$, $2\nu_4$, and $2\nu_5$ in the $CHBr_3$ spectrum) do not depend on the temperature, while for the fundamental frequencies such a dependence is observed. We note that the intensity of the band of the overtone $2\nu_3$ of liquid CBr_4 is practically invariant with temperature.[9] The behavior of the band of the combination frequency $\nu_1 + \nu_4$ is also the same in both cases—its intensity is less strongly dependent on temperature (for chloroform, the integrated absorption in the band of this vibration diminishes by 18%) than the intensity of each of the fundamental vibrations ν_1 and ν_4 separately (in the $CHCl_3$ spectrum, their integrated intensity diminishes by 32 and 20% respectively).

At present it is still premature to form an opinion as to the generality of the above-noted weak temperature dependence of combination frequencies and overtones in comparison with fundamental vibrations (all the more so since CCl_4 is characterized by the reverse phenomenon[10]). Aside from the influence of the Boltzmann factor, which to some extent smooths out the decrease in vibration intensities with an increase in temperature which is associated with the weakening of the intermolecular interactions, an increase in temperature

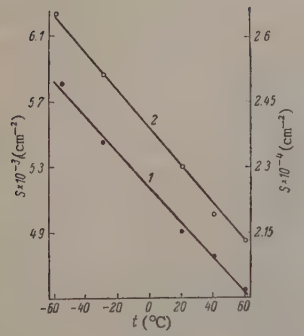

Fig. 3

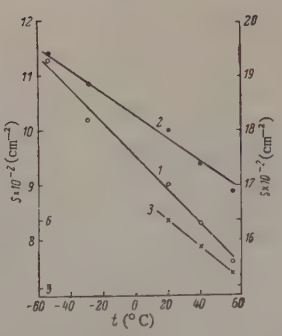

Fig. 4

Fig. 3. Temperature dependence of the integrated absorption in the bands of the vibrations ν_1 (curve 1) and ν_4 (curve 2) of liquid $CHCl_3$. Scale for curve 1 at the right, for curve 2 at the left.

Fig. 4. Temperature dependence of the integrated absorption in the bands of the combination frequencies $\nu_1 + \nu_4$ (curve 1), $\nu_2 + \nu_6$ (curve 2), and $\nu_3 + \nu_6$ (curve 3) of liquid chloroform. Scale for curve 1 at the right, for curve 2 at the left, for curve 3 in the middle.

may be accompanied by an intensification of the anharmonicity of the vibrations, which must in turn lead to an increase in the intensity of the combination frequencies and overtones. According to the estimate made for diatomic molecules in ref. 6, the temperature role of the anharmonicity is insignificant; however, for complex molecules in the liquid phase, it apparently increases considerably.

The data of Figs. 3 and 4 indicate the linearity of the temperature dependence of the intensities of the vibrational absorption bands. The bands of other molecular liquids also observe such a regularity, namely carbon tetrachloride,[10] bromoform,[1] carbon tetrabromide,[9] and certain paraffin hydrocarbons and esters.[11] However, in the latter case the unfavorable choice of objects of study (complex molecules allowing of rotational isomerism and association) does not permit one to deal unequivocally with the results of the investigation. Nevertheless, it may be considered established at the present time that the phenomenon is general,* and that

*For solutions, a similar effect has been observed in refs. 8 and 12.

the temperature decrease of the integrated absorption of vibrational bands in the infrared spectra of molecular liquids follows a linear law. It is understood that we are speaking of bands located in the relatively short-wavelength ($\lambda < 25\mu$) region of the infrared spectrum.

It may also be considered definitely established that the observed temperature dependence is governed by intermolecular interactions. Although the causes leading to the established dependence are already clear at present, for the time being still no quantitative theory has been worked out. A statistical theory,[13] which is qualitatively confirmed for gases,[14,15] does not in principle explain the phenomenon in the case of a liquid, inasmuch as it does not take account of intermolecular interactions and it leads to an increase of absorption with temperature. The ideas developed in refs. 16 and 17 likewise cannot be accepted as satisfactory. Starting from a statistical distribution of collisional perturbations of the molecules in the liquid and a dispersion form of the vibrational bands, the author of ref. 16 obtained a diminution with temperature proportional to $1/\sqrt{T}$ in the integrated absorption. One of the principal conditions which must here be fulfilled consists of the temperature invariance of the parameter $A = (1/4)\Gamma^2 D_{max}$, where Γ is the actual half-width of the band on the optical density scale and D_{max} is the actual optical density at the absorption maximum. A numerical check carried out on the basis of our data for $CHCl_3$, corrected for the spectral slit width of the apparatus, and of the data[6] for the deformation vibration of the CH_3 group in acetone shows that this condition is not fulfilled: although the halfwidth, as a rule, increases with an increase in temperature, the quantity A does not remain constant. In the temperature interval studied, the value of this parameter changes in general by 15-25%, which exceeds the errors of measurement.

The author of ref. 17 attempts to partially explain the observed decrease in the band intensity with an increase in temperature by the change in dielectric constant of the liquid, as determined by the Lorenz-Lorentz relation. The calculations are based on a formula resulting from Onsager's theory[18] which describes the connection between the integrated absorption in the gas and in the liquid. In the majority of cases, this formula finds experimental confirmation (see the list of references in ref. 19), so that its use is hardly justified.

The explanation put forward in ref. 9 is apparently to be considered as the most probable as well as the most general explanation of the mechanism of the influence of molecular interaction on the observed temperature dependence. Its essence is this: the increase in the average distance between molecules during thermal expansion of the liquid diminishes the induced dipole moment of the interaction and consequently the magnitude of the absorption. This indicates a direct connection between the values of the temperature coefficients of cubical expansion of liquids of the same type (in the sense of interaction forces and the structure of the intermolecular force field) and the temperature dependences of the intensities of corresponding vibrations. Such a parallelism is actually observed. The infrared absorption in $CHBr_3$, the coefficient of cubical expansion of which equals 0.905×10^{-3},[20] in general varies only slightly with temperature, while in $CHCl_3$, whose temperature coefficient of cubical expansion is substantially greater, equalling 1.26×10^{-3}, the same vibrations display a significant temperature dependence. An analogous phenomenon may also be noted when one compares the effect of temperature on the infrared absorption of CCl_4[10] and CBr_4.[9]

CONCLUSIONS

1. The diminution of the intensities of the vibration absorption bands of liquid chloroform with an increase in temperature is subject to a linear law.

2. The band of the totally symmetric valence vibration of the C—H bond, ν_1, undergoes the greatest change with temperature. The intensities of the bands of the overtones $2\nu_1$ and $2\nu_4$ do not depend on the temperature, although the intensities of the combinations $\nu_1 + \nu_4$, $\nu_2 + \nu_6$, and $\nu_3 + \nu_6$ diminish substantially with an increase in temperature.

3. Due to the fact that the structures of the $CHCl_3$ and $CHBr_3$ molecules are of the same type, as are the intermolecular force fields in liquid chloroform and bromoform, a parallelism is observed in the temperature variations of the intensities of corresponding vibrations (the deformation vibration of the C—H bond, ν_4, constitutes an exception).

4. Comparison of the temperature variations in the

ntensity of the vibrational absorption bands of $CHCl_3$, HBr_3, CCl_4, and CBr_4 enables us to establish a correlation between the coefficient of cubical expansion of a quid and the average temperature coefficient of diminution of the band intensities.

EFERENCES

1. M. P. Lisitsa and Yu. P. Tsyashchenko, Opt. i Spektr. 9, 188 (1960), Optics and Spectroscopy 9, 99 (1960).
2. E. Wagner and D. Hornig, J. Chem. Phys. 18, 296 (1950).
3. R. Lord, R. McDonald, and F. Miller, J. Opt. Soc. Am. 42, 149 (1952).
4. L. Bovey, J. Opt. Soc. Am. 41, 381 (1951).
5. I. I. Novak and E. S. Solov'ev, Opt. i Spektr. 2, 62 (1957).
6. P. A. Bazhulin and V. N. Smirnov, Opt. i Spektr. 6, 745 (1959), Optics and Spectroscopy 6, 485 (1959).
7. M. P. Lisitsa and Yu. P. Tsyashchenko, Opt. i Spektr. 6, 605 (1959), Optics and Spectroscopy 6, 396 (1959).
8. U. Liddel and E. Becker, J. Chem. Phys. 25, 173 (1956).
9. M. P. Lisitsa, V. N. Malinko, and I. N. Khalimonova, Opt. i Spektr. 7, 638 (1959), Optics and Spectroscopy 7, 386 (1959).
10. M. P. Lisitsa and V. N. Malinko, Izvest. Akad. Nauk SSSR, Ser. Fiz. 22, 1117 (1958).
11. G. Dijkstra, Proc. Colloq. Spectroscop. Internat. 6, 618 (1957).
12. R. Hughes, R. Martin, and N. Coggeshall, J. Chem. Phys. 24, 489 (1956).
13. M. V. Vol'kenshtein, M. A. El'yashevich, and B. I. Stepanov, "Kolebaniya molekul" (Molecular Vibrations), Vol. 2. Gosudarst. Izd. Tekh. Moscow-Leningrad, 1949.
14. M. P. Lisitsa and V. N. Malinko, Ukrain. Fiz. Zhur. 3, 773 (1958); Opt. i Spektr. 6, 694 (1959), Optics and Spectroscopy 6, 450 (1959).
15. V. N. Smirnov and P. A. Bazhulin, Opt. i Spektr. 7, 193 (1959), Optics and Spectroscopy 7, 123 (1959).
16. T. Brown, J. Chem. Phys. 24, 1281 (1956).
17. W. Person, J. Chem. Phys. 28, 319 (1958).
18. S. Polo and M. Wilson, J. Chem. Phys. 23, 2376 (1955).
19. J. Jaffe and S. Kimmel, J. Chem. Phys. 25, 374 (1956).
20. A. Weissberger, "Organicheskie rastvoriteli" (Organic Solvents). Izd. Inostrannoi Lit., Moscow, 1958.

THE VIBRATIONAL SPECTRUM AND MOLECULAR STRUCTURE OF CRYSTALLINE ARSENIC OXIDE

N. N. Sobolev and V. P. Cheremisinov

Received 26 December 1959

The Raman and infrared absorption spectra of crystalline arsenic oxide were investigated. The Raman spectrum contains thirteen lines, the most intense of which are at 305 and 440 cm^{-1}. In the infrared absorption spectrum, seven bands were observed between 2.5 and 36μ; only one of these bands is weak. Analysis of the activities of the frequencies in the Raman and infrared absorption spectra verified the hypothesis that the molecule of crystalline arsenic oxide is characterized by the formula As_4O_{10}, and belongs to the point group T_d. An interpretation of the vibrational spectrum of this compound was carried out.

INTRODUCTION

A series of previous papers[1-5] by the authors was devoted to the investigation of the vibrational spectra of a number of vitreous oxides, which, according to the hypothesis of Zachariasen,[6] can give single-component glasses. It was shown that some of these oxides have a molecular structure in the crystalline and vitreous state. This result was obtained not only by studying vibrational spectra, but also by analyzing the physico-chemical and structural properties of the oxides (x-ray and electron diffraction). The present work is devoted to a discussion and interpretation of the results of an investigation of the vibrational spectrum of arsenic oxide.

According to the hypothesis of Zachariasen, this material is a vitreous oxide; in ref. 7 arsenic oxide was actually obtained in the form of a glass. In the crystalline state, arsenic oxide exists in only one modification. In the monograph of Ormont[8] it is pointed out that the structure of arsenic oxide is analogous to the structure of phosphorus pentoxide, and that in the crystalline state it therefore consists of molecules of As_4O_{10}. We also started with this picture of the molecular structure of crystalline arsenic oxide in discussing the experimental results obtained from an investigation of its vibrational spectrum.

EXPERIMENTAL PART

Because of the lack of a single crystal of arsenic oxide, the investigation of the Raman spectrum was performed by the powder method[3] with the aid of an ISP-51 spectrograph. The exposure times were 50 to 100 hr. The thickness of the layer of the material investigated varied from 1 to 3 mm. The spectra were photographed on Orthochrome Agfa Raman Plates.

The infrared absorption spectrum of arsenic oxide between 2.5 and 20μ was investigated by Sidorov[9] in our laboratory. We supplemented his data by studying the infrared spectrum of the oxide from 20 to 36μ. This investigation was carried out with powders suspended in paraffin oil, using a dual-beam KRS-5 prism spectrophotometer. The crystalline modification of arsenic oxide was obtained in the Institute of Glass as chemically pure.

EXPERIMENTAL RESULTS

The results obtained from a study of the Raman and infrared absorption spectra of arsenic oxide are given in Table 1, along with approximate estimates of the band intensities. As is evident from the table, thirteen lines were observed in the Raman spectrum of arsenic oxide.

Table 1. Vibrational Spectrum of Arsenic Oxide

ν (cm^{-1}) R. p.	ν (cm^{-1}) IR.	ν (cm^{-1}) R. p.	ν (cm^{-1}) IR.
305 (m)	—	—	858 (s)
—	395 (m)	954 (w)	—
440 (m)	—	1060 (w)	—
535 (w)	527 (m)	1140 (w)	1131 (m)
580 (w)	574 (m)	1205 (w)	
640 (w)	—	1245 (vw)	1243 (w)
695 (w)	—	1358 (vw)	—
777 (w)	(775 (m)		

The following notation is used in Tables 1 to 4: R – Raman spectrum; IR – infrared absorption spectrum. Intensities of the bands (indicated in parentheses): vw – very weak; w – weak; m – medium; s – strong.

There is a possibility that some of the lines were not recorded because of the presence of a strong background as far as 400 cm^{-1}. The background was caused by the exciting mercury line $\lambda = 4358$ A and swamped out the weak lines.

The infrared absorption spectrum between 2.5 and 36μ (see the Figure) has seven absorption bands. Only one of these bands is weak; the remaining ones have approximately the same intensities. The band near 3μ is attributed to the OH vibration, which indicates the presence of a small quantity of water in the sample.*

*The hypothesis that we obtained the spectrum of arsenic acid and not the oxide is not valid, since the spectrum we obtained differs strongly from the spectrum of the acid. Besides, during the preparation of the powder–oil suspension, the oxide came in contact with the atmosphere for only a short time (< 30 sec) which is insufficient for the formation of the acid.

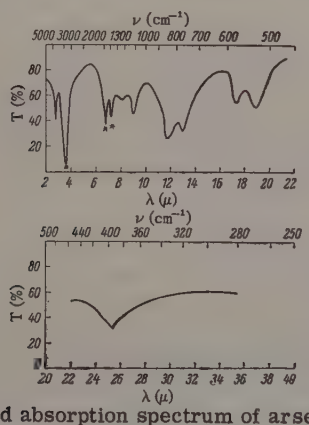

Infrared absorption spectrum of arsenic oxide from 2.5 to 36μ. (The bands marked with asterisks belong to paraffin oil.)

DISCUSSION OF THE RESULTS

From Table 1 and the Figure it follows that the infrared absorption spectrum contains six bands with intensities higher than "weak." Obviously, these must be the frequencies of the fundamental vibrations. The Raman spectrum showed thirteen lines; eleven were estimated as "weak" and "very weak," and two had higher intensities. It should be pointed out that in view of the appreciable molecular weight of arsenic oxide, it is hardly necessary to take account of lines with frequencies higher than 1200 cm^{-1} in determining the frequencies of the fundamental vibrations. Therefore, one may consider the principal lines in the Raman spectrum to be all of the lines lying below the indicated limit, since their intensities are approximately the same. Thus ten or eleven fundamental vibration frequencies appear in the Raman spectrum. I us also include the line at 1205 cm^{-1} among the fundamental frequencies.

From a consideration of the Raman and infrared ab sorption spectra of arsenic oxide and also from the activity of the vibrational frequencies in these spectra, on can draw the following conclusions:[10]

1. The molecule cannot belong to the point groups C_2, C_3, C_6, C_{3v}, and $C_{\infty v}$, since the number of lines in th Raman spectrum (10-11) considerably exceeds the number of lines in the infrared absorption spectrum (6).

2. The molecule cannot belong to the point groups C_1, C_{2h}, D_{2h}, S_6, C_{4h}, C_{6h}, D_{3d}, D_{4d}, D_{4h}, D_{5h}, D_{6h}, $D_{\infty h}$, or O_h, since there are frequencies occurring in both spectra (535, 580, 777, and 1140 cm^{-1}).

3. There are lines in the infrared absorption spectrum which are absent from the Raman spectrum (395 and 858 cm^{-1}). We calculated the number of frequencies for molecules of those point groups which are characterized by the existence of lines which are forbidden in the Raman spectrum and permitted in the infrared absorption spectrum. (This includes the groups D_3, D_4, D_5, D_6, C_{3h}, C_{5h}, and D_{3h}).*

*Since the formulas determining the number of vibratio for the symmetries of the point groups D_5 and C_{5h} are n derived in Herzberg's book,[10] these formulas were derived by us.

The results of the calculation of the number of frequencies for the indicated point groups are given in Table 2, where the experimental data are given in the lower line. The possible models of the molecule were chosen in such a way that they corresponded to the smallest number of frequencies. The calculation of the frequencies was made for various positions of the atom in the molecule of a given point group; but, as is eviden from the table, this fact had little effect on the results. The model for the point group D_{3h} gives the best agreement, but it also differs from the experimental data in the number of frequencies. The divergence is still greater for the other groups. Thus these models are scarcely acceptable; we therefore had to assume that th frequencies 395 and 858 cm^{-1} are permitted in the Ram spectrum by the selection rules, although they were not observed by us experimentally. Apparently, because of the weakness of these lines, it is difficult to bring them out by the powder method (in addition, as already pointe out above, the effect of the background produced by the exciting line is evident for the line at 395 cm^{-1}).

Thus if one assumes that all the lines of the infra-

Table 2. Selection Rules for Models of Molecules Belonging to Point Groups D_3, D_4, D_5, D_6, C_{3h}, C_{5h}, and C_{3h}

Sym. group	No. of freq. in R	No. of freq. in IR	No. of freq. active in both spectra	Molecular model
D_3	18	18	12	As_4O_{10}
	19	17	12	
D_4	23	13	9	As_4O_{10}
	22	14	10	
D_5	19	11	8	As_4O_{10}
	18	12	8	
D_6	25	20	13	As_6O_{15}
	26	19	13	
C_{3h}	18	13	7	As_4O_{10}
	18	12	6	
	19	17	7	
C_{5h}	18	8	4	As_4O_{10}
D_{3h}	8	5	3	As_2O_5
Experiment	10—11	6	4	—

ed absorption are also present in the Raman spectrum, hen, according to the calculation, the latter must con- ain twelve or thirteen fundamental vibration frequen- ies, instead of the ten or eleven fundamentals observed xperimentally.

4. A molecule, for which all the frequencies of the nfrared spectrum are present in the Raman spectrum, nust belong to one of the following point groups: C_{2v}, D_2, C_4, C_5, C_6, S_4, C_{4v}, C_{5v}, C_{6v}, D_{2d}, T, or T_d. The results f a calculation of the number of frequencies for molec- lar models of the groups indicated above are given in able 3. The experimental data, it is easy to see, agree ost completely with the model As_4O_{10} of the point group T_d, and are presented in the last line of the table.

Table 3. Selection Rules for Models of Molecules Belonging to Point Groups C_{2v}, D_2, C_4, C_5, C_6, S_4, C_{4v}, C_{5v}, C_{6v}, D_{2d}, T, and T_d

Sym. group	No. of freq. in R	No. of freq. in IR	No. of freq. active in both spectra	No. of freq. active only in R	Molecular model
. . . . .	15	14	14	1	As_2O_5
. . . . .	15	11	11	4	As_2O_5
. . . . .	27	18	18	9	As_4O_{10}
. . . . .	22	16	16	6	As_4O_{10}
. . . . .	18	12	12	6	As_4O_{10}
. . . . .	11	7	7	4	As_2O_5
. . . . .	11	8	8	3	As_2O_5
. . . . .	9	6	6	3	As_2O_5
. . . . .	21	18	18	3	As_4O_{10}
. . . . .	11	7	7	4	As_2O_5
. . . . .	23	15	15	8	As_6O_{15}
. . . . .	12	6	6	6	As_3O_{15}
xperiment . .	12—13	6	6	6—7	—

NTERPRETATION OF THE VIBRATIONAL SPECTRUM OF THE ARSENIC OXIDE MOLECULE

The selection rules for the As_4O_{10} molecule, belonging to the point group T_d, require the presence of three totally symmetrical vibrations of the type A_1 active in the Raman spectrum; three doubly degenerate vibrations of type E, active in the Raman spectrum; three triply degenerate vibrations of the type F_1, forbidden in both spectra; and six triply degenerate vibrations of type F_2 allowed in both spectra.

One can interpret the frequencies of the vibrational spectrum of arsenic oxide on the basis of the activity of the various frequencies and their intensities in both spectra. Since the totally symmetrical lines are active only in the Raman spectrum and have high intensity, one must assign the most intense of them (305 and 440 cm^{-1}) to vibrations of type A_1. The frequencies 395, 535, 580, 777, 858, and 1131 cm^{-1} must be assigned to vibrations of type F_2, since they are active in both spectra.

By analogy with phosphorous pentoxide, which has a similar structure, the highest frequency (1205 cm^{-1}), which lies near the boundary of the fundamental frequency region, must be assigned to a totally symmetrical vibration of type A_1. The frequencies of 954 and 1060 cm^{-1} are assigned by us to vibrations of type E, since with their help the frequencies 640 and 1358 cm^{-1} are interpreted satisfactorily, and the absence of these frequencies in the infrared absorption spectrum is explained. The frequency 695 cm^{-1} must apparently be assigned to a third fundamental vibration of type E. The weak frequency 1245 cm^{-1}, active in both spectra, is interpreted well by combination of frequencies 395 and 858 cm^{-1}.

An interpretation of all the frequencies of the vibrational spectrum of arsenic oxide is given in Table 4. One must note that the interpretation of certain lines (vibrations of type E) cannot be considered unique because of the absence of data on the polarization of the Raman lines. Unfortunately, a study of the polarization of the lines is not practical in an investigation of Raman spectra by the powder method.

Table 4. Interpretation of the Vibrational Spectrum of Molecules of Arsenic Oxide

ν (cm^{-1}) R	ν (cm^{-1}) IR	Interpretation	Computed freq.	Sym. of the upper vibrational state
305 (m)	—	ν_3	—	A_1
—	395 (m)	ν_{15}	—	F_2
440 (m)	—	ν_2	—	A_1
535 (w)	527 (m)	ν_{14}	—	F_2
580 (w)	574 (m)	ν_{13}	—	F_2
640 (w)	—	$\nu_5 - \nu_3$	649	E
695 (w)	—	ν_6	—	E
777 (w)	775 (m)	ν_{12}	—	F_2
—	858 (s)	ν_{11}	—	F_2
954 (w)	—	ν_5	—	E
1060 (w)	—	ν_4	—	E
1140 (w)	1131 (m)	ν_{10}	—	F_2
1205 (w)	—	ν_1	—	A_1
1245 (vw)	1243 (w)	$\nu_{11} + \nu_{15}$	1253	$A_1 + E + F_1 + F_2$
1358 (vw)	—	$\nu_3 + \nu_4$	1365	E

CONCLUSION

In this work the vibrational spectrum of only the crystalline modification of arsenic oxide was investigated. The results best fit the structure of the molecule As_4O_{10}, which belongs to the point group T_d. We did not investigate vitreous arsenic oxide. However, since crystalline arsenic oxide exists in only one modification, one may assume that the vitreous modification will also have a molecular structure with the basic structural unit As_4O_{10}; and hence, the vibrational spectra of these modifications must be analogous. This assumption, which, of course, must be verified, agrees with the known fact of analogous vibrational spectra of crystals and glasses in a number of vitreous oxides (see, for example, ref. 3).

In conclusion, let us note that in spite of the fact that the spectroscopic data verify the assumption of Ormont about the molecular structure of crystalline arsenic oxide, it is necessary to make a careful x-ray structural investigation of this compound for a final answer to the question.

REFERENCES

1. T. A. Sidorov and N. N. Sobolev, Opt. i Spektr. 2, 711 (1957).
2. T. A. Sidorov and N. N. Sobolev, Opt. i Spektr. 2, 713 (1957).
3. V. P. Cheremisinov, Opt. i Spektr. 7, 454 (1959), Optics and Spectroscopy 7, 293 (1959).
4. E. N. Lotkova, V. V. Obukhov-Denisov, N. N. Sobolev, and V. P. Cheremisinov, Opt. i Spektr. 1, 772 (1956).
5. T. A. Sidorov and N. N. Sobolev, Opt. i Spektr. 3, 560 (1957).
6. W. H. Zachariasen, J. Am. Chem. Soc. 54, 3841 (1932).
7. Mellor, Vol. IX, pp. 137-138, Longmans Green, London, 1929.
8. B. F. Ormont, "Structure of Inorganic Materials." Moscow-Leningrad, 1950.
9. T. A. Sidorov, Kand. Diss., Fiz. Inst. Akad. Nauk, 1957.
10. G. Herzberg, "Vibrational and Rotational Spectra of Polyatomic Molecules" Izd. Inostrannoi Lit., Moscow, 1949.

VIBRATIONAL SPECTRA OF SILICATES
III. Equations of the Vibrations of Planar Silicon-Oxygen Rings in Silicates

A. M. Prima

Received 4 January 1960

A theoretical study of the vibrations of silicon-oxygen rings of symmetry D_{nh} has been carried out. By using complex coordinates to take account of symmetry, we have obtained in general form the matrices of the reduced kinematic coefficients and dynamic coefficients (force constants) and the selection rules applicable to various structures and symmetry types. We have determined the symmetry types for which the vibrational frequencies do not depend on the number of Si atoms in the ring.

At the present time there exist a number of experimental investigations of the infrared absorption and reflection spectra of cyclic silicates.[1-5] In consequence of the absence of theoretical computations of the vibrations of the corresponding structures, the authors have in the majority of cases limited themselves to a discussion of the spectra without interpretation of the bands, and the existing attempts at interpretation are almost without foundation. Recently experimental data have appeared on the reflection spectra of monocrystals of cyclic silicates with planar rings,[4,5] the interpretation of which is made somewhat easier as a result of the high symmetry as well as of the appearance of dichroism in the lines. The experiments usually determine the spectrum of the stretching frequencies of the Si—O bonds. Since these differ to a considerable degree from the other frequencies (among which are the vibrational frequencies of the metal atoms) in consequence of the weak coupling with the vibrations of the metal, one can carry out an interpretation of the spectra of silicates to quite a good approximation by starting from an analysis of the vibrations of the isolated silicon-oxygen skeleton.

The present work consists of a theoretical analysis of the vibrations of the planar silicon-oxygen rings which are contained in the structure of many silicates (e.g., catapleite, beryl, aquamarine) and which are linked by metal atoms to form a crystal lattice. It was of interest to determine which bands remained unchanged during a change in the number of SiO_4 tetrahedra in the ring—i.e., to find the characteristic frequencies and also the directions of displacement of those bands which depend mainly on the vibrations of the ring. Treatment of the symmetry by means of the complex variables previously applied to infinite crystal lattices[6-8] enables us to obtain a general expression for the secular equations of various symmetry types and for all the structures considered.

The general appearance of the structures belonging to the symmetry groups D_{nh} and the internal coordinates are depicted in the figure. All the SiO_4 tetrahedra and the coordinates corresponding to them are numbered in the order in which they follow one another: q_i^s is the change in the i-th Si—O bond of the tetrahedron numbered s, and γ_{ik}^s and α_{12}^s are the changes in the corresponding O—Si—O and Si—O—Si angles. Assuming all the O—Si—O angles to be tetrahedral, we have determined the values of the Si—O—Si angle as a function of the number of silicon atoms in the ring, n. For $n > 3$, the vibrations of the atoms constituting the ring are divided into planar and nonplanar. The torsional coordinates describing these nonplanar vibrations were not taken into account because of their weak interaction with the remaining coordinates. The matrix of the potential energy constants (Table 1) includes nondiagonal interactions between coordinates belonging to the same SiO_4 tetrahedron. All the remaining nondiagonal elements of this matrix not contained in Table 1 have been equated to zero.

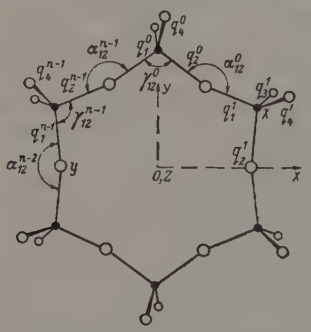

General appearance of the silicon-oxygen rings (black and white circles represent Si and O atoms respectively).

Table 1

	q_1^s	q_2^s	q_3^s	q_4^s	γ_{12}^s	γ_{23}^s	γ_{34}^s	γ_{13}^s	γ_{24}^s	α
q_1^s	K_{q_1}	h	h	h	a	0	a	0	a	0
q_3^s			K_{q_3}	h	0	0	0	a	a	a
γ_{12}^s					K_γ	l	l	l	l	0
γ_{23}^s						K_γ	l	l	0	l
γ_{34}^s										K_γ
γ_{14}^s										

The elements of the matrix of the kinematic coefficients, which was determined with the help of the procedure described in ref. 9, depend on the angle $\varphi_n = 2\pi$ (which is equal to the minimum angle of rotation during the symmetry operation C_n), on the values of ε_x and ε (which are the reciprocals of the masses of the corresponding atoms), and on the quantity $\sigma = 1/s$, where s the equilibrium length of the Si—O bond (x and y are respectively atoms of Si and O).

The symmetry axis C_n was taken into account with the help of the complex symmetry coordinates x_j and α_{12}, which are connected with the internal coordinates the following way

$$x_j^s = x_j e^{ik s}, \quad \alpha_{12}^s = \alpha_{12} e^{ik\left(s+\frac{1}{2}\right)},$$

Table 2

	$\mathrm{Re}\, q_1'$	$\mathrm{Im}\, q_1'$	q_3'	γ_{12}'
$\mathrm{Re}\, q_1'$	$\frac{2}{3}\varepsilon_x + \varepsilon_y - \frac{1}{3}(\cos\varphi_n + \sqrt{8}\sin\varphi_n)\varepsilon_y \cos k$	$\frac{1}{3}(\cos\varphi_n + \sqrt{8}\sin\varphi_n)\varepsilon_y \sin k$	$-\frac{2}{3}\varepsilon_x$	$-\frac{4}{3}\varepsilon_x a + \frac{\sqrt{2}}{3}[\sin\varphi_n - \sqrt{8}\cos\varphi_n]\varepsilon_y a \cos k$
$\mathrm{Im}\, q_1'$	$\frac{1}{3}(\cos\varphi_n + \sqrt{8}\sin\varphi_n)\varepsilon_y \sin k$	$\frac{4}{3}\varepsilon_x + \varepsilon_y + \frac{1}{3}(\cos\varphi_n + \sqrt{8}\sin\varphi_n)\varepsilon_y \cos k$	0	$-\frac{\sqrt{2}}{3}[\sin\varphi_n - \sqrt{8}\cos\varphi_n]\varepsilon_y a \sin k$
q_3'	$-\frac{2}{3}\varepsilon_x$	0	$\varepsilon_y + \frac{2}{3}\varepsilon_x$	$\frac{4}{3}\varepsilon_x a$
γ_{12}'	$-\frac{4}{3}\varepsilon_x a + \frac{\sqrt{2}}{3}[\sin\varphi_n - \sqrt{8}\cos\varphi_n]\varepsilon_y a \cos k$	$-\frac{\sqrt{2}}{3}[\sin\varphi_n - \sqrt{8}\cos\varphi_n]\varepsilon_y a \sin k$	$\frac{4}{3}\varepsilon_x a$	$\left\{2\varepsilon_y + \frac{8}{3}\varepsilon_x + \frac{2}{3}(\sqrt{8}\sin\varphi_n + \cos\varphi_n)\cos k\varepsilon_y\right\}a^2$
$\mathrm{Re}\, \gamma_{14}'$	$\frac{\sqrt{2}}{6}[\sqrt{8}\cos\varphi_n - \sin\varphi_n]\varepsilon_y a \cos k$	$-\frac{\sqrt{2}}{6}[\sqrt{8}\cos\varphi_n - \sin\varphi_n]\varepsilon_y a \sin k$	0	$-\varepsilon_y a^2\left[1 + \frac{1}{3}(\sqrt{8}\sin\varphi_n + \cos\varphi_n)\cos k\right]$
$\mathrm{Im}\, \gamma_{14}'$	$-\frac{\sqrt{2}}{6}[\sqrt{8}\cos\varphi_n - \sin\varphi_n]\varepsilon_y a \sin k$	$-\frac{8}{3}\varepsilon_x a - \frac{\sqrt{2}}{6}[\sqrt{8}\cos\varphi_n - \sin\varphi_n]\varepsilon_y a \cos k$	0	$\frac{1}{3}(\sqrt{8}\sin\varphi_n + \cos\varphi_n)\varepsilon_y a^2 \sin k$
γ_{34}'	$\frac{4}{3}\varepsilon_x a$	0	$-\frac{4}{3}\varepsilon_x a$	$-\frac{8}{3}\varepsilon_x a^2$
α_{12}'	$-\frac{1}{3}a\cos\frac{k}{2}[4\varepsilon_x + \sqrt{2}(\sqrt{8}\cos\varphi_n - \sin\varphi_n)\varepsilon_y]$	$-\frac{1}{3}a\sin\frac{k}{2}[4\varepsilon_x - \sqrt{2}(\sqrt{8}\cos\varphi_n - \sin\varphi_n)\varepsilon_y]$	$\frac{4}{3}\varepsilon_x a\cos\frac{k}{2}$	$\frac{2}{3}[4\varepsilon_x + (3 + \cos\varphi_n + \sqrt{8}\sin\varphi_n)\varepsilon_y]a^2\cos\frac{k}{2}$

	$\mathrm{Re}\, \gamma_{14}'$	$\mathrm{Im}\, \gamma_{14}'$	γ_{34}'	α_{12}'
$\mathrm{Re}\, q_1'$	$\frac{\sqrt{2}}{6}[\sqrt{8}\cos\varphi_n - \sin\varphi_n[\varepsilon_y a \cos k$	$-\frac{\sqrt{2}}{6}[\sqrt{8}\cos\varphi_n - \sin\varphi_n]\varepsilon_y a \sin k$	$\frac{4}{3}\varepsilon_x a$	$-\frac{1}{3}[4\varepsilon_x + \sqrt{2}(\sqrt{8}\cos\varphi_n - \sin\varphi_n)\varepsilon_y]a\cos\frac{k}{2}$
$\mathrm{Im}\, q_1'$	$-\frac{\sqrt{2}}{6}[\sqrt{8}\cos\varphi_n - \sin\varphi_n]\varepsilon_y a \sin k$	$-\frac{8}{3}\varepsilon_x a - \frac{\sqrt{2}}{6}[\sqrt{8}\cos\varphi_n - \sin\varphi_n]\varepsilon_y a \cos k$	0	$-\frac{1}{3}[4\varepsilon_x - \sqrt{2}(\sqrt{8}\cos\varphi_n - \sin\varphi_n)\varepsilon_y]a\sin\frac{k}{2}$
q_3'	0	0	$-\frac{4}{3}\varepsilon_x a$	$\frac{4}{3}\varepsilon_x a\cos\frac{k}{2}$
γ_{12}'	$-\varepsilon_y a^2\left[1 + \frac{1}{3}(\sqrt{8}\sin\varphi_n + \cos\varphi_n)\cos k\right]$	$\frac{1}{3}(\sqrt{8}\sin\varphi_n + \cos\varphi_n)\varepsilon_y a^2 \sin k$	$-\frac{8}{3}\varepsilon_x a^2$	$\frac{2}{3}[4\varepsilon_x + (3 + \cos\varphi_n + \sqrt{8}\sin\varphi_n)\varepsilon_y]a^2\cos\frac{k}{2}$
$\mathrm{Re}\, \gamma_{14}'$	$\varepsilon_y a^2\left[1 + \frac{1}{6}(\cos\varphi_n + \sqrt{8}\sin\varphi_n)\cos k\right]$	$-\frac{1}{6}(\cos\varphi_n + \sqrt{8}\sin\varphi_n)\varepsilon_y a^2 \sin k$	$-\varepsilon_y a^2$	$-\frac{1}{3}\varepsilon_y a^2\cos\frac{k}{2}(3 + \cos\varphi_n + \sqrt{8}\sin\varphi_n)$
$\mathrm{Im}\, \gamma_{14}'$	$-\frac{1}{6}(\cos\varphi_n + \sqrt{8}\sin\varphi_n)\varepsilon_y a^2 \sin k$	$\left\{2\varepsilon_y + \frac{16}{3}\varepsilon_x - \frac{1}{6}(\cos\varphi_n + \sqrt{8}\sin\varphi_n)\varepsilon_y \cos k\right\}a^2$	0	$\frac{1}{3}[8\varepsilon_x + (3 + \cos\varphi_n + \sqrt{8}\sin\varphi_n)\varepsilon_y]a^2\sin\frac{k}{2}$
γ_{34}'	$-\varepsilon_y a^2$	0	$\left(2\varepsilon_y + \frac{8}{3}\varepsilon_x\right)a^2$	$-\frac{8}{3}\varepsilon_x a^2\cos\frac{k}{2}$
α_{12}'	$-\frac{1}{3}\varepsilon_y a^2\cos\frac{k}{2}(3 + \cos\varphi_n + \sqrt{8}\sin\varphi_n)$	$\frac{1}{3}[8\varepsilon_x + (3 + \cos\varphi_n + \sqrt{8}\sin\varphi_n)\varepsilon_y]\sin\frac{k}{2}a^2$	$-\frac{8}{3}\varepsilon_x a^2\cos\frac{k}{2}$	$\frac{2}{3}[\varepsilon_x(3 + \cos k) + \varepsilon_y(3 + \cos\varphi_n + \sqrt{8}\sin\varphi_n)]a^2$

where x_j^s is any vibrational coordinate except α_{12}^s. The parameter k is determined from the cyclic condition

$$x_j^{s+n} = x_j^s, \tag{2}$$

in consequence of which we have

$$k = \frac{2\pi l}{n} \qquad (l = 0, \pm 1, \pm 2, \ldots). \tag{3}$$

The real and imaginary parts of the expressions (1) for an integral value of l located, for example, in the following interval,

$$0 \leqslant l \leqslant \frac{n}{2}\ (n - \text{even}), \qquad 0 \leqslant l \leqslant \frac{n-1}{2}\ (n - \text{odd}), \tag{4}$$

give a complete set of different vibrations (doubly degenerate in the general case).

By going over to the new coordinates determined by the relations†

†The sign * denotes the taking of the complex conjugate.

$$\left.\begin{aligned} q_1' &= 2^{-\frac{1}{2}}(q_1 + q_2^*), \quad q_3' = 2^{-\frac{3}{2}}(q_3 + q_3^* + q_4 + q_4^*), \\ q_3'' &= 2^{-\frac{3}{2}}(q_3 + q_3^* - q_4 - q_4^*), \quad \gamma_{12}' = 2^{-1}(\gamma_{12}' + \gamma_{12}^*), \\ \gamma_{34}' &= 2^{-1}(\gamma_{34} + \gamma_{34}^*), \quad \gamma_{14}' = 2^{-\frac{3}{2}}(\gamma_{14} + \gamma_{13} + \gamma_{24}^* + \gamma_{23}^*), \\ \gamma_{14}'' &= 2^{-\frac{3}{2}}(\gamma_{14} - \gamma_{13} + \gamma_{24}^* - \gamma_{23}^*), \quad \alpha_{12}' = 2^{-1}(\alpha_{12} + \alpha_{12}^*), \end{aligned}\right\} \tag{5}$$

complete account is taken of the symmetry. When the values of the real and imaginary parts are equal for q_1, q_2, γ_{13}, γ_{14}, ... we obtain from the relationships (5) a

Table 3

	q''_5	$\mathrm{Re}\gamma''_{14}$	$\mathrm{Im}\gamma''_{14}$
q''_5	$\varepsilon_y + \frac{4}{3}\varepsilon_x$	$\frac{8}{3}\varepsilon_x\sigma$	0
$\mathrm{Re}\gamma''_{14}$	$\frac{8}{3}\varepsilon_x\sigma$	$\left(2\varepsilon_y + \frac{16}{3}\varepsilon_x\right)\sigma^2 + \frac{3}{2}\varepsilon_y\sigma^2\cos k$	$-\frac{3}{2}\varepsilon_y\sigma^2\sin k$
$\mathrm{Im}\gamma''_{14}$	0	$-\frac{3}{2}\varepsilon_y\sigma^2\sin k$	$3\varepsilon_y\sigma^2\left[1-\frac{1}{2}\cos k\right]$

Table 4

	$\mathrm{Re}q'_1$	$\mathrm{Im}q'_1$	q'_2	γ'_{12}	$\mathrm{Re}\gamma'_{14}$	$\mathrm{Im}\gamma'_{14}$	e'_{12}
$\mathrm{Re}q'_1$	$K_{q_1}+h$	0	$2h$	$\sqrt{2}a$	$\sqrt{2}a$	0	0
$\mathrm{Im}q'_1$	0	$K_{q_1}-h$	0	0	0	$\sqrt{2}a$	0
q'_2	$2h$	0	$K_{q_2}+h$	$-\sqrt{2}a$	$-\sqrt{2}a$	0	0
γ'_{12}	$\sqrt{2}a$	0	$-\sqrt{2}a$	$2K_\gamma$	$2K_\gamma$	0	0
$\mathrm{Re}\gamma'_{14}$	$\sqrt{2}a$	0	$-\sqrt{2}a$	$2K_\gamma$	$5K_\gamma-6l$	0	0
$\mathrm{Im}\gamma'_{14}$	0	$\sqrt{2}a$	0	0	0	K_γ	0
e'_{12}	0	0	0	0	0	0	K_e

Table 5

	q''_5	$\mathrm{Re}\gamma''_{14}$	$\mathrm{Im}\gamma''_{14}$
q''_5	$K_{q_2}-h$	$-\sqrt{2}a$	0
$\mathrm{Re}\gamma''_{14}$	$-\sqrt{2}a$	K_γ	0
$\mathrm{Im}\gamma''_{14}$	0	0	$K_\gamma-2l$

simple orthogonal normalized transformation.

For vibrations of all the symmetry types, within the given class of structures, which are symmetric with respect to the horizontal plane of symmetry σ_h, the elements of the matrices of the reduced kinematic and dynamic coefficients are represented in Tables 2 and 4 respectively. The coordinate γ'_{34} has been taken as dependent and excluded from the matrix of the dynamic coefficients in accordance with the supplementary condition

$$\gamma'_{12} + 2(\mathrm{Re}\,\gamma'_{14}) + \gamma'_{34} = 0. \qquad (6)$$

To eliminate it from the matrix of the kinematic coefficients, it is necessary to cancel the column and the row corresponding to γ'_{34}. The following two supplementary conditions belong to separate symmetry types:

$$\gamma'_{12} - \alpha'_{12} = 0 \qquad (\text{when } l = 0), \qquad (7)$$

$$\alpha'_{12} - \gamma'_{12}\left(\cos\frac{\pi}{n} + \frac{1}{\sqrt{2}}\sin\frac{\pi}{n}\right)$$

$$-\sigma\sin\frac{\pi}{n}\left[\sqrt{2}(\mathrm{Re}\,q'_1) - (\mathrm{Im}\,q'_1)\right] = 0 \qquad (\text{when } l = 1). \qquad (8)$$

All the supplementary conditions have been deduced geometrically on the basis of the method of ref. 9. For symmetry types which are antisymmetric with respect to σ_h, the matrices of the reduced kinematic and dynamic coefficients are presented in Tables 3 and 5 respectively.

To find the selection rules, the standard symbols for all the symmetry types were obtained by comparison of the characters of the transformations of coordinates under the symmetry operations C_n, σ_h, and σ_v with the characters of the symmetry types presented in ref. 9 or ref. 10, n taking on the values 3, 4, 5, and 6, since rings with $n > 6$ are not encountered. The symmetry of the dipole moments and polarizability tensors, which determines the selection rules, the dichroism, and the direction of polarization of the lines, was established as a function of the values of l and of the symmetry with respect to σ_h, with the help of the table of selection rules, no. 55 in ref. 10. The results of the theoretical investigation of the vibrations of the given class of structures are collected in Table 6.

When $l = 0$, vibrations of four nondegenerate A types always exist. The imaginary components of the coordinates (5), which are designated in Tables 2-5 by the symbol Im, differ from the real components in their different behavior under the operation σ_v, as a result of which, in the matrices of the tables cited, they are automatically separated from the remaining coordinates when the substitution $k = 0$ is made, and they represent separate symmetry types. Thus to obtain the matrices of the reduced kinematic or dynamic coefficients of the nondegenerate symmetry types, it is sufficient, in the matrices of Tables 2-5, first to reject the columns and rows corresponding to coordinates with the symbol Im, and then, on the contrary, to leave the columns and rows with the symbol Im, rejecting all the rest.

In the general case when $l \neq 0$, there are only 2 degenerate symmetry types (respectively symmetric and antisymmetric with respect to σ_h), from the matrices of which the division just noted is absent. Depending on the even or odd nature of n, the symbols of the symmetry types are somewhat different, since when n is even there is a center of symmetry. Under this condition the case $l = n/2$ constitutes an exception and, in accordance with expression (1), the vibrations remain nondegenerate and are divided into four B symmetry types in complete analogy to the case $l = 0$. For example, when $n = 4$, there exist in place of E_{2g} the two types B_{2g} and B_{1g} which have the components α_{xy} and α_{xx}, α_{yy} respectively of the polarizability tensor different from zero, and which are active in the Raman spectrum. When $n = 6$, all the additional symmetry types B_{1g}, B_{2u}, B_{1u}, and B_{2u} for which $l = 3$ are inactive in the vibrational spectra, as a result of which symmetry types with the value $l = 3$ are missing from Table 6.

According to the data of Table 6, an increase in the degree of polymerization neither complicates nor simplifies the vibrational spectra in regard to the number

Table 6

Value of		Real or imaginary part of the complex symmetry coordinates	Symbols of the symmetry type		Symmetry with respect to σ_h*	Nonzero components of the dipole moment	Nonzero components of the polarizability tensor	N be di en qu ci
l	n		n even	n odd				
0	3—6	Re	A_{1g}	A'_1	+		$\alpha_{xx}, \alpha_{yy}, \alpha_{zz}$	
0	3—6	Im	A_{2g}	A'_2	+			
0	3—6	Re	A_{2u}	A''_2	—	M_z		
0	3—6	Im	A_{1u}	A''_1	—			
1	3	Re, Im		E'	+	M_x, M_y	$\alpha_{xz}, \alpha_{yz}, \alpha_{xy}$	
1	4	Re, Im	E_u		+	M_x, M_y		
1	5.6	Re, Im	E_{1u}	E'_1	+	M_x, M_y		
1	3.4	Re, Im	E_g	E''	—		α_{xz}, α_{yz}	
1	5.6	Re, Im	E_{1g}	E''_1	—		α_{xz}, α_{yz}	
2	4	Re	B_{1g}		+		α_{xx}, α_{yy}	
		Im	B_{2g}		+		α_{xy}	
2	5.6	Re, Im	E_{2g}	E'_2	+		$\alpha_{xx}, \alpha_{yy}, \alpha_{xy}$	
2	4	Re	B_{2u}		—			
		Im	B_{1u}		—			
2	5.6	Re, Im	E_{2u}	E''_2	—			

*The symbols + and — indicate that the vibrations are respectively symmetric antisymmetric.

**The frequencies of the torsional vibrations, which belong to symmetry types w are antisymmetric with respect to σ_h, are not taken into account in Table 6.

different bands. In the infrared spectrum only two symetry types are active: (1) when l = 1, one which is degenerate and symmetric with respect to σ_h, with the direction of oscillation of the dipole moment perpendicular to the Z direction, and (2) when l = 0, an A_{2u} or A_2'' nondegenerate symmetry type, antisymmetric with respect to σ_h, with the direction of oscillation of the moment along the Z axis. Judging from the expressions for the elements of the kinematic coefficient matrices in tables 2 and 3, the position of the infrared bands (especially the stretching ones) for the first type depend strongly on the number of SiO_4 tetrahedra linked into the ring. The frequencies of the second symmetry type, A_2, do not depend on n at all and would remain practically unchanged on going over to different structures if the force constants were the same. Hence these vibrations may be considered to be characteristic.

The stretching frequency of type A_2'' or A_{2u} is fundamentally determined by the magnitude of the quasi-elastic constant, K_{q3}, of an Si—O bond linked to a metal by means of the free O atom. Its value does not depend at all on the magnitude of the constant K_{q1}, which corresponds to an Si—O bond not linked to a metal. The matrices of the coefficients of kinematic and dynamic interaction of this type do not include elements corresponding to torsional vibrations.

In the general case, three symmetry types are active in the Raman spectrum, except for the case n = 4, where there is no degeneracy when l = 2. However, the total number of Raman lines remains unchanged.

The results of this work will be applied to the interpretation of the spectra of crystalline silicates.

In conclusion, I express my profound gratitude to B. I. Stepanov and N. A. Borisevich for their valuable counsel and interest in the work.

REFERENCES

1. C. Schaefer, F. Matossi, and K. Wirtz, Z. Physik 89, 210 (1934).
2. F. Matossi and H. Kruger, Z. Physik 99, 1 (1936).
3. O. Reinkober, Ann. Phys. 34, 343 (1911).
4. G. B. Bokii and I. I. Plyusnina, Nauch. Doklady Vyssh. Shkoly, Geol.-Geogr. Nauki, No. 3, 116 (1958).
5. I. I. Plyusnina and G. B. Bokii, Kristallografiya 3, 752 (1958).
6. B. I. Stepanov and O. P. Girin, Trudy Gosudarst. Opt. Inst. 23, no. 139 (1953).
7. B. I. Stepanov and A. M. Prima, Opt. i Spektr. 4, 734 (1958).
8. A. M. Prima, Kand. diss., Belorussk. Gosudarst. Univ. (Thesis, White Russian State Univ.), 1958.
9. M. V. Vol'kenshtein, M. A. El'yashevich, and B. I. Stepanov, "Kolebaniya molekul" (Molecular vibrations), Vol. 1. Gosudarst. Izd. Tekh.-Teoret. Lit., Moscow, 1949.
10. G. Herzberg, "Kolebatel'nye i vrashchatel'nye spektry mnogoatomnykh molekul" (Vibrational and Rotational Spectra of Polyatomic Molecules). Izd. Inostrannoi Lit., Moscow, 1949.

INFRARED ABSORPTION SPECTRA OF THE COMPLEXES OF UREA AND THIOUREA WITH TIN CHLORIDE AND TIN BROMIDE

D. S. Bystrov, T. N. Sumarokova and V. N. Filimonov

Received 12 January 1960

The infrared spectra of the complexes of urea with $SnCl_4$, $SnBr_4$, $TiCl_4$ and of thiourea with $SnCl_4$ and $SnBr_4$ were investigated. It was shown that in the complexes of urea with $SnCl_4$ and $TiCl_4$ the addition takes place via linkage with oxygen, with $SnBr_4$ via linkage with nitrogen, whereas in the complexes of the thiourea with $SnCl_4$ and $SnBr_4$ it takes place via linkage with sulphur.

The urea complexes with stannic chloride and bromide were first obtained and described by Yarmukhamedova and Sumarokova.[1,2] As is known, stannic chloride is a strong acceptor of electron pairs—a Lewis acid[3,4]—and therefore may form complexes with molecules containing atoms which may serve as donors of electron pairs. Stannic bromide possesses similar though weaker electron-acceptor properties. It was shown in the case of ketones and complex esters of carboxylic acids[5,6] that in the complexes of metallic halides with carbonyl containing molecules, the linkage with the acceptor atom may take place only via the oxygen of carbonyl group. On the other hand, a great number of complexes of metallic halides with ammonia and amines are known, in which the donor-acceptor linkage may take place only with the participation of the unshared pair of electrons on the nitrogen atom. In the complexes of urea coordination bonds both with oxygen and nitrogen are possible. Similarly one may expect coordinate bonds both with sulphur and nitrogen in the complexes of thiourea.

To determine the site of linkage in the complexes of metallic halides with urea and thiourea as well as any changes which take place in the ligand molecules, the infrared absorption spectra of the following complexes were investigated in the present work: $2(NH_2)_2CO \cdot SnCl_4$, $2(NH_2)_2CS \cdot SnCl_4$, $2(NH_2)_2CO \cdot SnBr_4$, and $2(NH_2)_2CS \cdot SnBr_4$.

The technique previously described[5] was used in obtaining the infrared spectra. Thin layers of complexes, produced by the method described,[1,2] were prepared by vacuum sublimation in a specially constructed cell which permitted one to take the spectra of the samples without subjecting them to contact with atmosphere. The complexes with stannic chloride were obtained by reaction of a sublimed layer of urea or thiourea with $SnCl_4$ vapors. The spectra of complexes obtained in this way were found to be identical with the spectra of sublimed complexes. In order to be sure that the sublimation of thiourea complex with $SnBr_4$ did not result in its decomposition, the spectra of thin layers of the complex obtained by the

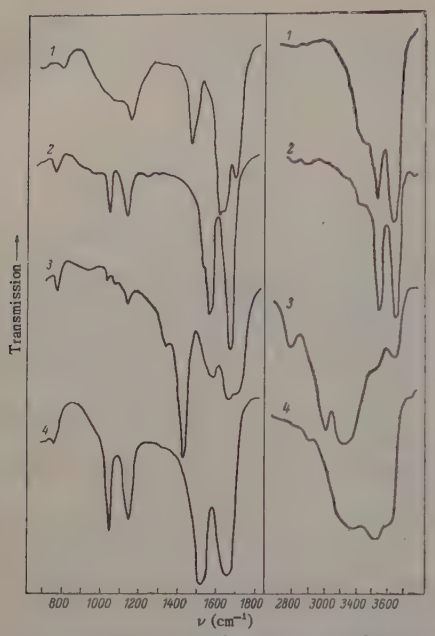

Fig. 1. The spectra of the urea complexes. Curve 1—$(NH_2)_2CO$; curve 2—$2(NH_2)_2CO \cdot SnCl_4$; curve 3—$2(NH_2)_2CO \cdot SnBr_4$; curve 4—$(NH_2)_2CO + TiCl_4$.

evaporation of its acetic acid solution were investigated. The infrared IKS-14 spectrophotometer was used to examine these spectra.

We shall now proceed to the actual results of the investigation.

$2(NH_2)_2CO \cdot SnCl_4$. As can be seen from Fig. 1 and Table 1, the absorption frequencies 3440 and 3330 cm^{-1}, corresponding to the stretching vibrations of the NH_2 groups of the urea molecule, are somewhat shifted towards higher frequencies in the spectrum of the complex. Such an effect could not take place if the linkage were made via the nitrogen atom; for in this case, one would expect a considerable decrease in the vibrational frequencies of the NH bonds as was found in the spectra of $[Pt\{(NH_2)_2CO\}_2Cl_2]$ and $[Pd\{(NH_2)_2CO\}_2Cl_2]$, investigated by Mizushima and co-workers.[7] The observed relative increase of the investigated frequencies in the spectrum of this complex may be explained by the ruptures of hydrogen bonds between the urea molecules that take place with the addition of $SnCl_4$ to the oxygen atom of the carbonyl groups of these molecules. The behavior of the remaining frequencies in the urea spectrum is also in good agreement with the hypothesis of a linkage via oxygen. In the 1700-1600 cm^{-1} region, in which the urea spectrum possesses two absorption bands, there is one band around

Table 1. Frequencies of Bands in the Spectra of the Urea Complexes with $SnCl_4$ and $TiCl_4$ (in cm^{-1})

Assignment[8]	$(NH_2)_2CO$	$2(NH_2)_2CO \cdot SnCl_4$	$(NH_2)_2CO + TiCl_4$
νNH_2	3440	3470	3435
	3330	3360	3330
	3260	3260	
			3195
δNH_2, νCN, $\nu C{=}O$	1687		
		1635	1642
δNH_2	1630		
$\nu C{=}O$, δNH_2	1590	1540	1530
νCN	1460	1510	
δNH_2, $\nu C{=}O$	1153	1135	1135
	1050		
νCN, $\nu C{=}O$	1000	1030	1035
	792	765	750

1635 cm^{-1} in the case of this complex which can be nat rally interpreted as the almost unshifted absorption ba corresponding to the NH deformation frequencies. The disappearance of the 1687 cm^{-1} absorption band, corre sponding to the normal vibration including the CN, CO stretching frequencies and NH deformation frequencie may be explained by its superposition with the 1635 cm band, following the lowering of the corresponding fre- quency. The supposed decrease in the 1687 cm^{-1} fre- quency may be caused by the weakening of the CO bond resulting from the coordinate linkage between the oxyg and $SnCl_4$ molecule. The lowering of the 1590 and 1153 cm^{-1} frequencies must be explained in the same way; the spectrum of the complex these apparently corresp to the intense absorption bands at 1540 and 1135 cm^{-1}. The 1510 and 1030 cm^{-1} absorption bands of the compl may be interpreted as the 1460 and 1000 cm^{-1} bands of urea corresponding to the symmetric and asymmetric NCN group vibrations, which have been displaced towa higher frequencies. Such an increase in frequencies of both vibrations apparently points to the stabilization of the CN bonds in the urea molecules following the com- plex formation.

$2(NH_2)_2CO \cdot SnBr_4$. The spectrum of the urea com plex with stannic bromide is sharply different from th urea complex with stannic chloride. As can be seen fr Fig. 1 and Table 2, in the region of NH stretching vibr tion frequencies the spectrum of this complex exhibits two pairs of bands. The 3030 and 3130 cm^{-1} bands are strongly displaced towards lower frequencies in comp son with the corresponding NH bands in the pure urea. Such lowering is to be expected if the acceptor ligand molecule is coordinated to the nitrogen atom of urea. The 3330 and 3450 cm^{-1} bands are approximately locat at the same frequencies as the corresponding NH band in pure urea; they must be assigned to the vibrations NH_2 groups which are not coordinated to $SnBr_4$. Thus, the lowering of the absorption bands of the NH bonds points in this case to the fact that the coordination link in the complex is taking place via one of the nitrogen atoms of urea.

Table 2. Frequencies of Bands in the Spectra of the U Complexes with $SnBr_4$ (in cm^{-1})

$\nu NH_2(-NH_2)$	3450	$\delta NH_2(H_2N:SnBr_4)$	15
	3330	$\nu NCN_{asym.}$	14
$\nu NH_2(H_2N:SnBr_4)$	3130	$\delta NH_2(H_2N:SnBr_4)$	13
	3030	$\delta NH_2(-NH_2)$	11
	2800		10
$\nu C{=}O$	1680	$\nu NCN_{sym.}$	10
$\delta NH_2(-NH_2)$	1630		7

The addition of the electron acceptor molecule (th metallic halide) to the nitrogen atom of urea disrupts conjugation of the free electron pair on the nitrogen at with the π-electron bond in C=O; this must result in t significant weakening of the CN bond, which is convert from a partially double bond (the double bond characte being 0.3)[9] to a single bond. The molecule of urea whi is perturbed in this way may be looked upon as one wh consists of an amide group ($CO \cdot NH_2$) similar to the amide group of a primary amide and a NH_2 group sing bonded to it. The nitrogen of this group forms a coord nation linkage with the acceptor molecule and therefor carries a positive charge.

Since the force constants of the single bonds CN, $\overset{+}{C}N$, and CC do not differ very much in magnitude, it i natural to make a comparison between the spectrum o the urea molecule in the complex with $SnBr_4$ and the spectrum of acetamide, as well as the spectrum of the urea cation $H_2NC\overset{+}{O}NH_3$,[10] in which the unshared pair o

lectrons of one of the nitrogen atoms participates in the ormation of a coordination bond in the same way as in ne complex. As can be seen from Fig. 2, the spectrum f urea in its complex with $SnBr_4$ is indeed similar to ne spectra of acetamide and of a urea cation.* This fact ignificantly facilitates the interpretation of the spectrum f this complex.

*The exception to this is presented by the frequencies of ne perturbed $\overset{+\delta}{NH_2}$ group, which are naturally different rom the frequencies of the CH_3 and $\overset{+}{N}H_3$ groups.

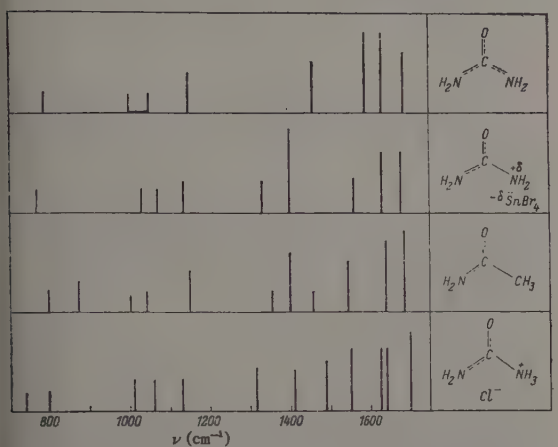

Fig. 2. The positions of the absorption maxima in the spectra of urea, urea complex with $SnBr_4$, acetamide, and hydrochloride of urea.[10]

It is logical to correlate the 1680 cm^{-1} absorption and in the spectrum of the complex with the band Amide observed in the spectrum of acetamide around 1685 cm^{-1} and essentially corresponding to the C=O stretching ibration.[11] To the intense 1400 cm^{-1} band corresponds he 1403 cm^{-1} band in acetamide. This acetamide band s practically unshifted by deuteration,[12] and is consequently due to the skeletal vibration (probably it is either he asymmetric vibration of the NCC group or the stretching vibration of the CN group). The band in the spectrum of the complex in the vicinity of 1030 cm^{-1}, which corresponds to either 1062 or 1012 cm^{-1} band in the spectrum of the urea cation, may be assigned to the symmetric ibration of the NCN group or to the stretching vibration of the C—N bond. This assignment is confirmed by the act that the absorption bands of the stretching vibrations of CN and $\overset{+\delta}{C}N$ of the spectra of methylamine and methylammonium iodide have the frequencies 1044 cm^{-1} [13] and 1003 cm^{-1},[14] respectively. A weak band in the acetamide spectrum around 1045 cm^{-1} is usually ascribed to the external deformational vibration of the CH_3 group, but some authors[15] interpret it as one arising from the CC stretching vibration.

The band observed in the spectrum of the complex around 1630 cm^{-1} must be assigned to the internal deformation vibrations of the unperturbed NH_2 groups by analogy with the spectrum of pure urea. In the spectra of primary amides the band Amide II, essentially corresponding to the deformation vibrations in the NH_2 group, also lies in the same region of the spectrum (cf., for example, ref. 11). The 1135 cm^{-1} band in the spectrum of the complex probably corresponds to the external deformation vibrations in the unperturbed NH_2 group. The analogous band in the acetamide spectrum lies in the vicinity of 1150 cm^{-1}.

The 1560 cm^{-1} absorption band must be assigned to the internal deformation vibration of the $\overset{+\delta}{NH_2}$ group, which has been perturbed by the addition of the acceptor. The correctness of this assignment is confirmed by comparison with the spectra of the compounds containing $\overset{+}{N}H_2$ group, in which the frequency under consideration lies in the region from 1580 cm^{-1} (in the spectrum of $(CN_3)_2\overset{+}{N}H_2$)[14] to 1540-1505 cm^{-1} (in the spectra of $(Hg\overset{+}{N}H_2)_n$).[16] The weakness in intensity of the 1560 cm^{-1} band in comparison to the 1630 cm^{-1} band may be ascribed to the effect of the acceptor. The external deformation vibrations of NH_2 usually possess a frequency not exceeding 1150 cm^{-1}, but in the spectrum of the $(CH_3)_2\overset{+}{N}H_2$ ion the band of the out-of-plane deformation vibration of NH_2 is observed around 1421 cm^{-1},[14] in view of which we feel that it is possible to interpret the 1330 cm^{-1} band in the complex as corresponding to the deformation vibration in the perturbed $\overset{+\delta}{NH_2}$ group.

Besides the complexes of urea with $SnCl_4$ and $SnBr_4$, we investigated the product of a reaction between urea and $TiCl_4$, obtained by the direct contact of $TiCl_4$ vapors with a sublimed layer of urea. As can be seen from Table 1, the spectrum of this compound is nearly identical with that of the complex of urea with $SnCl_4$ in the region of frequencies below 3000 cm^{-1}. This allows us to conclude that under the experimental conditions a complex of urea with $TiCl_4$ is formed, and that the oxygen of the carbonyl group participates in the coordination linkage. However, in the region of NH stretching vibration frequencies, the $TiCl_4$-urea complex spectrum differs significantly from the spectra of other complexes which we have investigated (Fig. 1). In it we observe a wide, strong, diffuse band which is somewhat displaced towards lower frequencies, in comparison with the spectrum of pure urea and of its complex with $SnCl_4$. Such a change in the spectrum may be explained by the formation of hydrogen bonds which are significantly more stable than those occurring in pure urea. Apparently these bonds are of the type N—H ... N, inasmuch as the oxygen of the complex is blocked by the addition of $TiCl_4$ molecule.

$2(NH_2)_2CS \cdot SnCl_4$, $2(NH_2)_2CS \cdot SnBr_4$. The spectra of the complexes of thiourea with stannic chloride and bromide (Fig. 3), differ but little from one another, in contrast with the corresponding spectra of the urea complexes. At the same time the spectrum of the thiourea

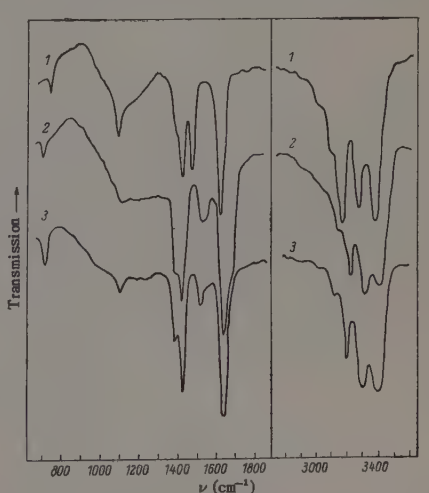

Fig. 3. The spectra of the thiourea complexes. Curve 1—$(NH_2)_2CS$; curve 2—$2(NH_2)_2CS \cdot SnCl_4$; curve 3—$2(NH_2)_2CS \cdot SnBr_4$.

complex with $SnBr_4$ is more similar to that of pure thiourea than the spectrum of the thiourea complex with $SnCl_4$, which is in line with the weaker electron-acceptor properties of the stannic bromide. The comparison between the frequencies of the pure thiourea with those of its complexes is shown in Table 3. The absence in the spectra of the complexes of shifts in bands corresponding to the NH stretching vibrations towards lower frequencies points to the fact that the coordination bond between thiourea and the acceptor molecule takes place via a sulphur atom. The increase in the 1470 cm^{-1} frequency, which apparently corresponds to the asymmetric stretching vibration of NCN,[17] may be brought about by the stabilization of the CN bond. Similar changes in the frequency of the CN bond vibrations and decreases in the intensity of the corresponding bands are observed in those complexes of urea in which the coordination takes place via the carbonyl oxygen atom. The 1610 cm^{-1} absorption band, which is usually ascribed to the NH deformation vibration, is considerably increased in frequency on forming the complex; apparently this must be explained by a certain admixture of the CN bond vibration in the corresponding normal vibration. The shift towards lower frequencies of the 727 cm^{-1} band apparently indicates that in this vibration, which includes the valence vibrations of the CN and CS bonds as well as the deformation vibrations of NH,[17] the admixture of the CS valence vibration is quite significant.

Table 3. Frequencies of Bands in the Spectra of the Thiourea Complexes (in cm^{-1})

Assignment[17]	$(NH_2)_2CS$	$2(NH_2)_2CS \cdot SnCl_4$	$2(NH_2)_2CS \cdot SnBr_4$
νNH_2	3380	3400	3410
	3275	3315	3315
	3175	3220	3210
δNH_2	1610	1640	1630
νNCN_{asym}	1470	1525	1510
δNH_2	1415	1425	1425
		1390	1385
νNCN, $\nu C{=}S$	1085	1100	1105
	730	683	700

In conclusion it must be observed that the spectra investigated in this work are very similar to the spectra of the urea and thiourea complexes with a series of metallic chlorides which have been investigated by Mizushima and co-workers. Thus the urea complex with the stannic chloride has a spectrum similar to the spectra of its complexes with $FeCl_3$, $CrCl_3$, $CuCl_2$, and $ZnCl_2$, the investigation of which indicated the formation of a coordination linkage via the carbonyl oxygen.[7] The spectral shifts, which are observed on the reaction of urea with stannic bromide, possess the same characteristics as those observed during the formation of urea complexes with $PtCl_2$ and $PdCl_2$, in which the coordination linkage apparently takes place via a nitrogen atom.[7] The spectra of complexes of thiourea which we have investigated show a great deal of similarity with the spectra of the thiourea complexes with $PtCl_2$, $PdCl_2$, and $ZnCl_2$, the analysis of which by Mizushima and co-workers[17] point to the coordination of these chlorides to the sulphur atom of thiourea.

The present work was done under the direction of A. N. Terenin, to whom the authors extend their deep gratitude.

REFERENCES

1. E. Sh. Yarmukhamedova and T. N. Sumarokova, Zhur. Obshchei Khim. **28**, 1410 (1958).
2. T. N. Sumarokova and E. Sh. Yarmukhamedova, Zhur. Obshchei Khim. **26**, 3291 (1956).
3. V. Lyuder and S. Tsuffanti, "Electronic Theory of Acids and Bases." Moscow, Leningrad, 1950.
4. M. Usanovich, Zhur. Obshchei Khim. **9**, 182 (1939); M. Usanovich and E. Kalabanovskaya, Byull. Srednеaziat. Gosudarst. Univ. No. **23** (1945); M. Usanovich, Izvest. Akad. Nauk Kazakh.SSR, Ser. Khim. No. **3** (1949); Izvest. Sektora Platiny Drug. Blagorod. Metal., Inst. Obshchei i Neorg. Khim., Akad Nauk SSSR No. **25**, 76 (1950); What are acids and bases. Alma-Ata, 1953.
5. V. N. Filimonov, D. S. Bystrov, and A. N. Terenin, Opt. i Spektr. **3**, 480 (1957); A. N. Terenin, V. N. Filimonov, and D. S. Bystrov, Izvest. Akad. Nauk SSSR, Ser. Fiz. **22**, 1100 (1958); D. S. Bystrov and V. N. Filimonov, Doklady Akad. Nauk SSSR **131**, 338 (1960).
6. P. Chalandon and B. P. Susz, Helv. Chim Acta **41**, 697 (1958).
7. R. B. Penland, S. Mizushima, C. Curran, and J. V. Quagliano, J. Am. Chem. Soc. **79**, 1575 (1957).
8. A. Yamaguchi, T. Miyasawa, T. Shimanoushi, and S Mizushima, Spectrochim. Acta **10**, 170 (1957).
9. P. Vaughan and J. Donohue, Acta Cryst. **5**, 530 (195
10. M. Davies and L. Hopkins, Trans. Faraday Soc. **53**, 1563 (1957); E. Spinner, Spectrochim. Acta 95 (1958).
11. "Application of Spectroscopy to Chemistry." Izd. Inostrannoi Lit., Moscow, 1959.
12. H. Lenormant, Ann. chim. (Paris) **5**, 459 (1950).
13. J. R. Barcelo and J. Bellanato, Spectrochim. Acta 27 (1956).
14. E. A V. Ebsworth and N. Sheppard, Spectrochim. Acta **13**, 261 (1959).
15. M. Davies and H. E. Hallam, Trans. Faraday Soc. **47**, 1170 (1951).
16. S. Mizushima, I. Nakagawa, and D. M. Sweeny, J. Chem. Phys. **25**, 1006 (1956); J. Nakagawa, R. B. Penland, S. Mizushima, T. J. Lane, and J. V. Quagliano, Spectrochim. Acta **9**, 19 (1957).
17. A. Yamaguchi, R. B. Penland, S. Mizushima, T. J. Lane, C. Curran, and J. V. Quagliano, J. Am. Chem Soc. **80**, 527 (1958).

CALCULATION OF THE OPTICAL ACTIVITY OF MOLECULES

M. V. Vol'kenshtein and M. P. Kruchek

Received 5 February 1960

A theoretical calculation of the optical activity of 3-methylcyclopentanone has been carried out. It is shown that the induction term in the expression for the gyration, computed on the basis of polarizability theory, plays an important role. The "internal" gyration, computed on the basis of the one-electron model, proves to be very small if one starts from the correct set of excited levels of the carbonyl group and from reasonable wave functions.

According to the quantum-mechanical theory of optical activity, the molecular rotation of a substance is expressed by the formula[1]

$$[M]_\nu = \frac{288\pi^2 N_A \nu^2}{c^2} \frac{n_\nu^2 + 2}{3} g_\nu, \qquad (1)$$

where N_A is Avogadro's number, c the velocity of light, ν the frequency of the incident light, n_ν the refractive index of the medium for this frequency, and g_ν the average gyration,

$$g_\nu = \frac{c}{3\pi h} \sum_r^\nu \frac{\mathrm{Im}\,(\mathbf{p}_{0r} \cdot \mathbf{m}_{r0})}{\nu_{r0}^2 - \nu^2}. \qquad (2)$$

Here $\mathbf{p}_{0r}$ and $\mathbf{m}_{r0}$ are the matrix elements of the electric and magnetic dipole elements of the molecule, and Im is the imaginary part of the corresponding expression (the summation is carried out over the excited states of the molecule).

The quantity g_ν may be represented in the form[2]

$$g = g^{(0)} + g^{(1)} + \sum_i g^{(i)}. \qquad (3)$$

Such a representation underlies the assumption of the possibility of considering the molecule as a set of separate atomic groups and bonds in which the electronic transitions are localized. Here $g^{(0)}$ is determined by the inductive interaction of such groups,[2,3] $g^{(i)}$ are the "internal" gyrations of the separate groups, and $g^{(1)}$ is expressed in terms of the matrix elements of the electric dipole of one group and the magnetic dipole of another. This term is significantly less than $g^{(0)}$ and may be neglected;[2,4] the term $g^{(0)}$ may be evaluated by a classical method;[3] for the evaluation of $g^{(i)}$, a knowledge of the wave functions of the ground and excited states of the group i is necessary, since the expression for $g^{(i)}$ coincides in form with expression (2).

An estimate of the magnitude of $g^{(i)}$ has been carried out in a number of works on the basis of the so-called one-electron model proposed by Condon, Altar, and Eyring.[5] In these works, only the long wavelength absorption bands of the chromophoric groups (those bands lying closest to the visible region and giving the fundamental contribution) were taken into account. The absorption bands were described as arising in consequence of a one-electron transition in the chromophoric group. The value of $g^{(i)}$ was computed with the help of approximate wave functions perturbed by the asymmetric field of the neighboring atoms.

Calculations have been made for 3-methylcyclopentanone[6] and some other compounds.[7-9] In these works the terms $g^{(0)}$ and $g^{(1)}$ in formula (3) were not considered at all, and g was identified with a single term of the sum $\sum_i g^{(i)}$. Order-of-magnitude agreement was obtained between the theoretical and experimental values of g. However, as we shall show later, such agreement is obtained only for a special and insufficiently grounded choice of wave functions.

In ref. 6, during the calculation of the gyration of the carbonyl group of 3-methylcyclopentanone (Fig. 1), wave functions of the type of the Slater functions:

$$\left.\begin{aligned} \psi_{2p_x} &= N_{2p_x} z \exp\left(-\frac{1.5}{2}\frac{r}{a_0}\right), \\ \psi_{2p_y} &= N_{2p_y} y \exp\left(-\frac{1.8}{2}\frac{r}{a_0}\right), \\ \psi_{3d_{xy}} &= N_{3d_{xy}} xy \exp\left(-\frac{1.5}{3}\frac{r}{a_0}\right), \end{aligned}\right\} \qquad (4)$$

where a_0 is the Bohr radius, were chosen for the electron of the oxygen atom.

These functions differ from those ordinarily used by the reduced numerical coefficients in the exponents. As a result, the dimensions of the electron clouds are clearly overstated. Thus the maximum in the probability of finding a $2p_z$ electron of oxygen appears at a distance of 1.41 A from the nucleus of the atom, while the experimental value of the length of the C=O bond equals 1.21 A. An analogous distention of the electron clouds is also made in refs. 7, 8, and 9. At the same time, an incorrect set of excited levels of the chromophoric group is used in the above-cited works (especially in ref. 6, which is devoted to 3-methylcyclopentanone).

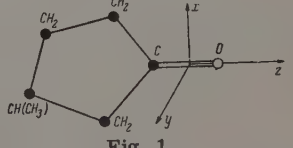

Fig. 1

The aim of the present work is the comparison of the terms $g^{(0)}$ and $g^{(1)}$ in the expression for the gyration of the molecule.

Let us carry out the corresponding calculations for 3-methylcyclopentanone. For the evaluation of $g^{(1)}$ we shall make use, as before, of the one-electron model, but instead of the functions (4) we shall use better functions originating from the work of Pople and Sidman.[10]

The chromophoric group C=O is characterized by its long wavelength absorption band at 2950 A. The transition of an electron of an unshared pair of the O atom to an antibonding orbital is responsible for this band.[10,11] In the symbols of ref. 10, this is an $n_p \mapsto \pi_2$ transition. For this transition

$$g^{(i)} = \frac{c}{3\pi h} \mathrm{Im}\, \frac{\mathbf{p}_{01}\mathbf{m}_{10}}{\nu_{01}^2 - \nu^2}, \qquad (5)$$

where 0 denotes the initial state of the electron in the unshared pair, 1 the excited π_2 state. The wave functions, with allowance for the perturbing action of the neighboring atoms, have the form

$$\left.\begin{aligned}\psi_0 &= \psi_{\pi_p} + K\psi_{\pi_1},\\ \psi_1 &= \psi_{\pi_2}.\end{aligned}\right\} \qquad (6)$$

Allowance for the perturbation of ψ_1 has an insignificant influence on the result of the calculation, which is not difficult to establish if one examines the set of perturbed states of the C=O group.[10,11]

In the coordinate system associated with the molecule (Fig. 1),

$$\left.\begin{aligned}\psi_{\pi_p} &= \psi^{O}_{2p_y},\\ \psi_{\pi_1} &= 0.6\psi^{C}_{2p_x} + 0.8\psi^{O}_{2p_z},\\ \psi_{\pi_2} &= 0.8\psi^{C}_{2p_z} - 0.6\psi^{O}_{2p_x},\end{aligned}\right\} \qquad (7)$$

where

$$\left.\begin{aligned}\psi^{O}_{2p_x} &= N^{O}x^{O}\exp(-\alpha^{O}r^{O}); \quad \left(N^{O}=\frac{4.1559}{a_0^{5/2}},\quad \alpha^{O}=\frac{2.2228}{a_0}\right);\\ \psi^{O}_{2p_y} &= N^{O}y^{O}\exp(-\alpha^{O}r^{O});\\ \psi^{C}_{2p_x} &= N^{C}x^{C}\exp(-\alpha^{C}r^{C}); \quad \left(N^{C}=\frac{1.6960}{a_0^{5/2}},\quad \alpha^{C}=\frac{1.5531}{a_0}\right);\end{aligned}\right\} \qquad (8)$$

The symbols "O" and "C" indicate that the expression refers to the oxygen and the carbon atom respectively.

We have neglected the overlap of the wave functions ψ^{O} and ψ^{C}. The calculation gives for the contribution to the molecular rotation for the D line of sodium ($\nu_D = 0.507\times10^{15}$ sec^{-1}, $\nu_{01} = 1.020\times10^{15}$ sec^{-1})

$$[M]_D = -5.55K\frac{n^2+2}{3}\cdot 10^3. \qquad (9)$$

The value of K is computed by first-order perturbation theory:

$$K = \frac{\int \psi_{\pi_1} w \psi_{\pi_p} d\tau}{\Delta E}; \qquad (10)$$

$$\Delta E = E_{\pi_p} - E_{\pi_1} = 5.9\cdot 10^{12}\ \text{ergs},$$

where w is the perturbation operator.

Since there are no charged groups or permanent electric dipoles in the 3-methylcyclopentanone molecule, we confine ourselves to the field of the hydrogen atom attached to the carbon atom C_δ. The H atoms attached to the remaining carbon atoms of the ring have no influence on the value of $g^{(1)}$, since they have a common plane of symmetry with the carbonyl group. The influence of the CH_3 group will be of the same order as the influence of the H atom under consideration.

According to ref. 6,

$$w = -\frac{e^2}{a_0}\left(1+\frac{a_0}{r^{H}}\right)\exp(-2\alpha^{H}r^{H}); \qquad \alpha^{H}=\frac{1}{a_0}, \qquad (11)$$

where e is the electronic charge and r^H the distance, reckoned from the center of the hydrogen atom.

For the evaluation of the integral in (10), it is convenient to go over to a new coordinate system ξ,η,ζ, with the ζ axis directed along the straight line joining the H and O atoms (Fig. 2).

Substituting (7-8) and (11) in (10), we obtain

$$K = -5.90\beta_{\zeta x}\beta_{\zeta y}\int r^{O3}(\cos^2\theta - \sin^2\theta\cos^2\varphi)\left(1+\frac{a_0}{r^{H}}\right)$$
$$\times\exp(-2\alpha^{O}r^{O})\exp(-2\alpha^{H}r^{H})\,d\tau, \qquad (12)$$

where $\beta_{\zeta x}$ and $\beta_{\zeta y}$ are the direction cosines of the ζ axis in the molecular coordinate system.

The integral in (12) is rewritten in the eliptical co-

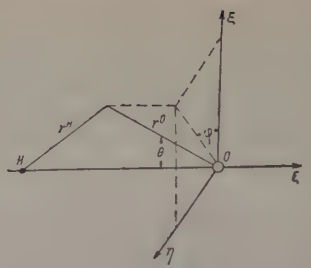

Fig. 2

ordinates μ, ν, φ:

$$\mu = \frac{r^{O}+r^{H}}{R_{OH}};\quad \nu = \frac{r^{O}-r^{H}}{R_{OH}};\quad d\tau = \left(\frac{R_{OH}}{2}\right)^3(\mu^2-\nu^2)\,d\mu d\nu d\varphi;$$
$$(1\leqslant\mu\leqslant\infty;\ -1\leqslant\nu\leqslant1;\ 0\leqslant\varphi\leqslant2\pi). \qquad (1$$

Expressing the quantity under the integral sign in terms of μ, ν, and φ we obtain, after integration with respect to φ,

$$K = -5.90\pi\beta_{\zeta x}\beta_{\zeta y}\left(\frac{R_{OH}}{2}\right)^5 N^{O2}\int_{-1}^{+1}\int_{1}^{\infty}(3+4\mu\nu+\mu\nu+3\mu^2\nu^2-\mu^2-\nu$$
$$\times\left[\mu^2-\nu^2+\frac{2a_0}{R_{OH}}(\mu+\nu)\right]\exp(-A\mu)\exp(-B\nu)\,d\mu d\nu, \quad (1$$

where

$$A = R_{OH}(\alpha^{O}+\alpha^{H}),\quad B = R_{OH}(\alpha^{O}-\alpha^{H}).$$

We take the values C—C = 1.54 A, C—H = 1.09 A, and C=O = 1.21 A for the bond lengths; we assume the valence angles to be tetrahedral except for the angles between the bonds forming the ring, and the ring to be planar. We obtain $R_{OH} = 4.21$ A, $\beta_{\zeta x} = 0.211$, $\beta_{\zeta y} = -0.271$, A = 25.6, B = 9.86.

The integral in (14) permits of separate integratio with respect to μ and ν and leads to the value K = 1.72 10^{-7}; correspondingly,

$$[M]_D = -9.55\frac{n_D^2+2}{3}\times10^{-4}\ \frac{\text{deg.}}{\text{dm.}}\cdot\text{cm}.$$

In ref. 6, the value $[M]_D = -15.7$(deg · cm^3/dm) was obtained for the contribution of the perturbation of this same atom; i.e., larger by approximately four orders o magnitude. Such a marked discrepancy is explained, as has already been indicated, by the unjustified choice of the wave functions (4) and the assumed set of levels

$$\psi_0 = \psi^{O}_{2p_z},$$

$$\psi_1 = \psi^{O}_{2p_x} + K\psi_{3d_{xy}}.$$

We shall show that this is actually the case. A rou estimate according to (14) gives

$$K \sim N^{O2}\frac{\exp[-|A-|B||}{A\cdot|B|},$$

where | B | is the absolute value of B.

For those parameters of the wave functions which were used in ref. 6, A = 12.62 and B = −2.53. This lea to the ratio K(6)/K = 2.20×10^3; here K(6) is the resul of ref. 6, K the result of our work.

Thus even a rough estimate which does not take ac count of a number of additional peculiarities of the com putation in ref. 6 confirms the extremely strong depend ence of the results of refs. 6-9 on the form of the wave

unctions. We see that in the better-grounded calculation $g^{(0)} \ll g$.

An expression for $g^{(0)}$ according to first-order polarizability theory has been obtained by Kirkwood[2] and by me of the present authors.[1,3] For groups which possess n axially symmetrical polarizability tensor, it has the orm

$$g^{(0)} = -\frac{2\pi}{3\lambda}\sum_{k>l}\frac{1}{R_{kl}^3}(\alpha_{k_\parallel}-\alpha_{k_\perp})(\alpha_{l_\parallel}-\alpha_{l_\perp})(\mathbf{R}_{kl}[\mathbf{lk}]) \times\left\{\frac{3}{R_{kl}^2}(\mathbf{R}_{kl}\mathbf{k})(\mathbf{R}_{kl}\mathbf{l})-(\mathbf{kl})\right\}, \quad (15)$$

where $\mathbf{R}_{kl} = \mathbf{R}_k - \mathbf{R}_l$. Here $\mathbf{R}_k$ and $\mathbf{R}_l$ are the radius ectors of the centers of the k-th and l-th bond or group $\alpha_{l_\parallel}$ and $\alpha_{l_\perp}$ are the polarizabilities of the l-th bond long and across its symmetry axis, and $\mathbf{l}$ and $\mathbf{k}$ are nit vectors along the symmetry axes of the groups l and ... The molecular rotation for the D line of Na is obtained rom (1) and (15),

$$[M]_D = 7.73\left(\frac{n^2+2}{n}\right)_D D_D^{(0)}\cdot 10^{29}.$$

In view of the low anisotropy of the C—H bond, the ndamental contribution to the value of $g^{(0)}$ is given by he interaction of the group $C_\delta H(CH_3)$ with the $C_\alpha{=}O$ nd. Only one term therefore remains in (15). We have sed the polarizability values computed by Buks,[12] $\alpha_{CH(CH_3)} = 1.21\times10^{-24}$ cm³ and $\Delta\alpha_{C=O} = 1.11\times10^{-24}$ cm³. aking the center of the $C_\delta H(CH_3)$ group as being situated t the middle of the C_δ—C bond, we obtain $g_D = 1.78\times 10^{-29}$, whence

$$[M]_D = 33.60\ \frac{\text{deg.}}{\text{dm.}}\cdot \text{cm}^3.$$

The experimentally observed value of $[M]_D$ is 130 deg · cm³/dm.[6] Thus, while the contribution of $g^{(1)}$ proves to be vanishingly small, the polarization term $g^{(0)}$ is close in order of magnitude to the observed value of g. Hence one may conclude that the polarization interaction of the groups plays the principal role in the optical activity of molecules of the type of 3-methylcyclopentanone, in which there is one chromophoric group and conjugated bonds are absent. The calculations carried out by us for the amino acids[13] testify to the same conclusion.

REFERENCES

1. M. V. Vol'kenshtein, "Molekulyarnaya optika" (Molecular Optics). Gosudarst. Izd. Tekh.-Teoret. Lit., Moscow, Leningrad, 1951.
2. J. Kirkwood, J. Chem. Phys. 5, 479 (1937).
3. M. V. Vol'kenshtein, Doklady Akad. Nauk SSSR 71, 447 (1950); Izvest. Akad. Nauk SSSR, Ser. Fiz. 17, 574 (1953).
4. H. Murakami, J. Chem. Phys. 27, 1231 (1957).
5. E. Condon, W. Altar, and H. Eyring, J. Chem. Phys. 5, 753 (1937).
6. W. Kauzmann, J. Walter, and H. Eyring, Chem. Revs. 26, 339 (1940).
7. E. Gorin, J. Walter, and J. Eyring, J. Chem. Phys. 6, 824 (1938).
8. E. Gorin, W. Kauzmann, and J. Walter, J. Chem. Phys. 7, 327 (1939).
9. T. Kwoh and H. Eyring, J. Chem. Phys. 18, 1186 (1950).
10. J. A. Pople and J. W. Sidman, J. Chem. Phys. 27, 1870 (1957).
11. J. W. Sidman, Chem. Revs. 58, 689 (1958).
12. M. F. Buks, Opt. i Spektr. 2, 494 (1957).
13. M. V. Vol'kenshtein and M. P. Kruchek, "Strukturnaya khimiya" (Structural Chemistry). (In press.)

USE OF ELECTRON PARAMAGNETIC RESONANCE FOR THE STUDY OF Eu-ACTIVATED SrS PHOSPHORS

V. G. Dubinin and Z. A. Trapeznikova

Received 11 February 1960

A comparison was made of the light sums stored during excitation and given off during de-excitation with the aim of determining the fraction of the quenching processes occurring in phosphors after ionization of the activator. It was found that in a phosphor without flux, only about half of the recombinations lead to emission, whereas in phosphors with flux, almost all the recombinations are accompanied by emission.

INTRODUCTION

In refs. 1-3 ionization of the activator Eu ($Eu^{++} \rightarrow Eu^{+++}$) in the phosphor SrS-Eu,Sm was detected by electron paramagnetic resonance.

In the present work this method was used for the investigation of SrS-Eu,Sm phosphors which differed in that one of them included a flux and the others did not. The same concentration of activator was added to all phosphors. The phosphors investigated differed sharply in the magnitude of the light sums emitted during heating or exposure to infrared light, and also in their ability to retain the light energy after termination of the excitation. At the same time, the character of the change in the paramagnetic absorption of Eu^{++} during excitation of the phosphors showed that the activator ionizes to the same extent (about 13-16%) in all of the phosphors.

As was shown in refs. 1-3, the paramagnetic resonance method makes possible the direct determination of the magnitude of the light sums stored by the phosphor. The magnitude of the emitted light sum, however, depends on the ratio of recombination events taking place with emission and without emission. Thus, a comparison of the magnitudes of the stored and emitted light sums allows one to determine the fraction of quenching processes taking place in the phosphor after ionization of the activator. The present work was directed toward this end. The values of the stored light sum were determined

from the change in paramagnetic resonance upon excitation of the phosphor, and values of the emitted light sum from the absolute number of quanta emitted by the phosphor during exposure to infrared light after excitation.

METHOD OF MEASUREMENT

A known quantity of a carefully de-excited phosphor in a quartz tube was inserted into the resonator and the paramagnetic resonance spectrum recorded. The phosphor was then excited in the resonator, after which the paramagnetic resonance spectrum of the excited phosphor was taken. From the difference in magnitude of the paramagnetic absorption of Eu^{++} the relative number of ionized centers was determined, and consequently, also the stored light sum. After this, the excited phosphor was spilled out of the resonator into a blackened cup. The surface area of the cup had been chosen so that the phosphor was scattered in a thin layer (one grain thick).*

*The phosphor had been preliminarily sifted to an almost uniform grain size.

This was done in order to eliminate errors associated with reabsorption. The magnitudes of the integrated intensity of emission of the phosphor situated on a black background and on white paper differed by a factor of almost two, which indicated the impossibility of disregarding reabsorption.

The release of the stored light was achieved by exposing the sample to the light of an incandescent lamp through an IKS-1 filter with a transmission band at 900-1100 mμ. (As was shown in ref. 4, infrared light of this spectral range is best for liberating stored light.) The intensity of emission from the phosphor was measured with the aid of an FEU-32 photomultiplier, which had been previously calibrated in energy units. Since the intensity of light from the phosphor is insufficient to be measured by a thermopile, a source of greater intensity was used to imitate the phosphor, the radiated energy of which was then determined with a thermopile. (An incandescent lamp was used to simulate the phosphor.) The spectra of the phosphor and the lamp could be made the same by means of appropriate light filters and a $CuCl_2$ solution of the proper concentration. The latter was used to absorb heat radiation from the incandescent lamp during the measurement of its radiation with the thermopile.

In this way, calibrating the FEU in absolute energy units according to the emission spectrum of the phosphor and knowing the energy of the quantum corresponding to the mean effective value of the frequency in the emission spectrum of the phosphor, it is possible to directly translate the energy given off by the phosphor during luminescence into the number of quanta. Repeated controlled measurements showed that the reproducibility of the results was about 10%.

If the number of quanta emitted is related to the number of activator ions in the phosphor, then it is possible to compare this number to the relative number of ionized luminescence centers as determined by the change in paramagnetic absorption.

It was established in this manner that the concentration of the Eu^{++} activator in the phosphor with flux (LiF) was approximately 1.5 times greater than that for the phosphor without flux.* In connection with this result a calculation of the relative number of quanta emitted wa also carried out. The results obtained are presented in Table 1.

*The difference in Eu^{++} concentration between phosphors with and without flux was found from the difference in the magnitude of paramagnetic absorption of Eu^{++}. This question, namely, the influence of the flux on the activator concentration in the phosphor, will be taken up in a later publication.

Table 1

Phosphor	k_c (%)	k_q (%)
SrS-Eu, Sm № 1	16	6
SrS-Eu, Sm № 2	16	7
SrS-Eu, Sm(LiF) № 3	13	11
SrS-Eu, Sm(LiF) № 4	14	12

k_c is the relative number of ionized centers measured by the method of paramagnetic resonance during steady-state excitation.

k_q is the relative number of quanta emitted by the phosphor under the action of infrared light. (The values of k_q are somewhat low, since the measurements of this quantity was carried out 3 to 5 min after the cessation of excitation.)

DISCUSSION OF THE RESULTS OBTAINED

As can be seen from Table 1, in spite of the almos identical values of the stored light sum, the different phosphors give it up differently during de-excitation. T stored light emitted by phosphors without flux is marke less than that emitted by phosphors with flux.

Usually, all losses associated with the transforma of light in phosphors is characterized by the quantum o put q, which is determined by the ratio of the number quanta given out by the phosphor in emission to the nur ber of quanta absorbed in excitation.

In ref. 5 the quantum output of the phosphor SrS-E Sm (without flux) was determined; under excitation in t absorption band of the Eu^{++} activator this yield turned to be 0.12. Starting from this, it is possible to determi the quantum output of the phosphor SrS-Eu,Sm (with flu from the values of the indicated intensities with the aid of the formula

$$q_2 = q_1 \frac{(I_{2\infty}/\varkappa_2)}{(I_{1\infty}/\varkappa_1)},$$

where I_∞ is the steady-state intensity, and $\varkappa$ is the ab sorptivity of the phosphor, corresponding to the minimum in the diffuse reflection versus wavelength curve The corresponding data for the two most different phos phors are presented in Table 2.

Table 2

Phosphor	I_∞ (rel. units)	x (rel. units)	q
SrS-Eu, Sm № 1	200	0.47	0.12
SrS-Eu, Sm(LiF) № 4 . .	580	0.68	0.24

The quantum output of recombination luminescenc can be expressed in the form of the product

$$q = \eta\rho,$$

where η is the efficiency of ionization (the ratio of the number of ionization events to the total number of quan absorbed), and ρ is the efficiency of emission of an Eu ion upon recombination with an electron, i.e., the ratio of the number of quanta emitted to the number of electrons (n_e) which are at the same time engaged in recombination with both the ionized centers (n_A) and with hol in the host lattice (n_s) ($n_e = n_A + n_s$).

Since ρ characterizes the losses taking place in t phosphor after ionization, one can write

$$\rho = \frac{n_\bullet}{n_e} = \frac{\alpha n_A}{n_A + n_s} = \frac{\alpha}{1 + \frac{n_s}{n_A}},$$

where α is the probability of radiative transitions in t luminescence center.

When the phosphor is excited by absorption in the osorption band of the activator, absorption in the host ttice can be neglected.* Hence if the exciting light does

*As is shown in ref. 5, the absorption of an unactivated hosphor in this region of the spectrum is very small, e., the quantity of holes being generated will also be ery small.

ot show a quenching action, i.e., if it does not liberate oles from the ionized centers, then

$$\frac{n_s}{n_A} \ll 1$$

nd so

$$\rho \approx \alpha.$$

Thus, in the case given, the losses which occur in ne phosphor after ionization will be essentially deter- ined by the probability of radiative transitions in the uminescence center.

Usually the magnitude of ρ, expressed as the ratio f the number of quanta emitted to the number of trapped lectrons, is difficult to calculate on account of the im- ossibility of making an accurate determination of the bsolute number of trapped electrons. Consequently, only he magnitude of q is determined in most cases. In our ase, however, it is possible to evaluate ρ, since the umber of localized electrons can be determined in the llowing fashion:

The absolute number of ionized centers of lumines- ence is found from the relation

$$n_A = k_c N,$$

here k_c is the relative number of ionized centers de- ermined by the method of paramagnetic resonance, and N is the total number of centers. Since excitation of the osphor is conducted in the absorption band of the ac- ivator, it is possible to say that the number of localized lectrons is equal to the number of ionized luminescence enters (i.e., $n_e = n_A$). The absolute number of quanta mitted by the phosphor can be calculated. Actually, ince the emission is produced by infrared light in the egion of the absorption maximum determined by the lo- alized electrons,[5] one can surmise that basically, the nfrared light liberates the localized electrons.

The number of quanta emitted by the phosphor is

$$n_q = k_q N,$$

where k_q is the relative number of quanta, determined by the method described above. The magnitude of ρ can now be determined from the formula

$$\rho = \frac{n_q}{n_e} = \frac{n_q}{n_A} = \frac{k_q N}{k_c N} = \frac{k_q}{k_c}.$$

Knowing ρ, one can also use Eq. (2) to determine the ther parameter that characterizes the losses in the phosphor, namely, η, the efficiency of ionization.

Data for the phosphors SrS-Eu,Sm No. 1 and SrS- Eu,Sm(LiF) No. 4 are given in Table 3.

Table 3

Phosphor	k_c' (%)	k_q (%)	ρ	η
SrS-Eu, Sm № 1 . . .	14	6	0.43	0.28
SrS-Eu, Sm(LiF) № 4 .	13	12	0.92	0.27

k_c' is the relative number of ionized centers at the moment of measurement of the number of quanta (the values of k_c' are smaller than those presented in Table 1 and pertain to the steady state).

From Table 3 it follows that in the indicated phos- phors, out of ten absorbed quanta, only approximately three ionize luminescence centers, and the remainder are dissipated as heat or are expanded in stimulating emission. At the same time, the ultimate fate of the energy absorbed by these phosphors is different. From the table it can also be seen that the phosphor SrS-Eu,Sm(LiF) No. 4 has practically no loss following ionization. This indicates that the exciting light does not liberate holes in this phosphor. Accordingly, one can surmise that the liberation of holes does not occur in the phosphor SrS-Eu, Sm No. 1, either. Thus, losses are possible only after recombination, and will be determined by the probability of radiative transitions in the luminescence center. According to Table 3, in the phosphor with flux, practically all of the transitions in the luminescence center (92%) occur with emission, whereas in the phosphor without flux, radiative transitions amount to at most about 43%.

The ratio of the probabilities of emission after recombination for these two phosphors is

$$\delta = \frac{\rho_1}{\rho_2} \approx 47\%.$$

The magnitude of δ can also be calculated in another way. Since in these phosphors the effectiveness of ionization is the same, then in the steady state the total number of recombination events should also be the same. Hence for equal absorptive abilities, their steady-state intensities should differ to the same extent that the emission probabilities after recombination differ. According to the data presented in Table 2, we obtain

$$\delta = \frac{(I_{1\infty}/\tau_1)}{(I_{2\infty}/\tau_2)} \approx 50\%.$$

Such agreement confirms the hypothesis about the losses after recombination. All of the above (namely, the fact that in SrS-Eu,Sm phosphors transitions both with and without emission are possible) can be explained if it is assumed that different kinds of centers exist in them, one of which emits a quantum of light on recombination, whereas the others dissipate this energy in heat. Introduction of a flux changes the ratio between the centers and increases the fraction of the centers which emit quanta upon recombination. During thermal de-excitation, the light sums emitted by the phosphors SrS-Eu,Sm and SrS-Eu,Sm(LiF) are also markedly different.

In addition to this, the dependence of the magnitude of the stored light sum on the storage time for phosphors with and without flux was measured by two methods (by the change in paramagnetic absorption of Eu^{++} and by the variation of the light sum emitted by the phosphor with time). The results of the study are presented in the Figure. As can be seen in the Figure, a faster decrease in the light sum with time is observed in the phosphor without flux. The latter fact indicates that in this phosphor, evidently, more of the electrons are located at

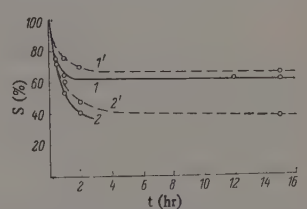

Dependence of magnitude of the stores light sum on the storage time of the phosphor. Curves 1 and 1′—phosphor SrS-Eu,Sm(LiF); Curves 2 and 2′—phosphor SrS-Eu,Sm. Method of measurement: curves 1 and 2— by the change in paramagnetic absorption; curves 1′ and 2′—by the change in emitted light sum.

shallow levels. Since the lifetime of electrons is a great deal shorter in shallow levels than in deep levels, they recombine at a faster rate; thus the stored light sum decreases at a faster rate by natural quenching.

In this fashion, it is possible by means of paramagnetic resonance to determine more accurately how losses occur in the transformation of light by phosphors and to establish the dependence of these losses on the method of preparation of the phosphors. However, the nature of these losses still remains unclear.

In conclusion, the authors wish to thank V. V. Antonov-Romanovskii and M. V. Fok for their constant interest in the work and their valuable advice concerning the results obtained.

REFERENCES

1. V. V. Antonov-Romanovskii, V. G. Dubinin, A. M. Prokhorov, Z. A. Trapezinokova, and M. V. Fok, Zhu Eksptl. i Teoret. Fiz. 11, 1466 (1959).
2. V. G. Dubinin and Z. A. Trapeznikova, Opt. i Spektr. (in press).
3. R. S. Title, Quantum Electronics—Resonance Phenomena Symposium, p. 14, New York, 1959.
4. I. B. Keirim-Markus, Opt. i Spektr. 7, 384 (1959), Optics and Spectroscopy 7, 250 (1959).
5. L. I. Anikina, Trudy Fiz. Inst., Akad. Nauk SSSR 7, 3 (1956).

THE VALENCE OF MANGANESE AS AN ACTIVATOR IN PHOSPHORS

V. V. Osiko and G. V. Maksimova

Received 15 January 1960

Kröger[1] and a number of authors after him have suggested that manganese can be found in phosphors in various valence states. They have stated that in phosphors with structureless, bell-shaped spectra, manganese appears to be divalent. However, phosphors whose spectra lie in the red region and have a clearly defined structure, even at room temperature, contain manganese in the quadrivalent state. Experimental evidence for activation by quadrivalent manganese is presented in refs. 1 and 2. Williams has proposed a theoretical basis for the observed differences in the luminescent spectra of di- and quadrivalent manganese.

Since the abovementioned investigations by Kröger, papers have appeared periodically in the literature, devoted to the study of luminors activated by manganese, their luminescence being ascribed to manganese present in one valence state or another. In most of these cases, the valence of the manganese has not been determined experimentally (most authors rely on Kröger's evidence). Chemical determinations of the valence of manganese were performed by Kröger for only one luminor (magnesium titanate with manganese), so that these results naturally cannot be applied to all luminors containing manganese. It is obviously necessary to undertake a systematic study of the relationship between luminescent properties and the valence of manganese, using as large a number of specimens as possible.

SPECIMENS AND METHOD OF INVESTIGATION

We determined the valence of the manganese activator in a large number of luminors. Phosphors activated by manganese were prepared by the methods described in the literature. Firing was carried out in both oxidizing (air) and reducing (ammonia) atmospheres. Some of the phosphors were kindly placed at our disposal by colleagues at the Luminescence Laboratory of the Physics Institute, Academy of Sciences, USSR.

The valence of the manganese activator in the phosphors was studied by chemical analytical methods. We determined the total manganese content and the amount of manganese with valence greater than two (oxidized manganese). These determinations were performed on two separately weighed samples. The total manganese content was determined by the persulfate method: the weighed samples were first dissolved by heating in concentrated sulfuric acid, and the concentration of the permanganate then determined colorimetrically in the final solution with the aid of an FM universal photometer. Oxidized manganese was determined iodometrically by the method described by Kroger[1] with the aid of a speci apparatus. First of all, we determined our limit of detection and average experimental error. The limit of de tection under our conditions (sample weights ≈ 0.1 gm) was 8×10^{-8} gram-equivalents of oxidized manganese. This guarantees a reliable determination of quadrivalen manganese when its concentration in a phosphor is 2×10^{-6} gm/gm (the corresponding content of trivalent man ganese is 4×10^{-6} gm/gm). The spread of results for r peated determinations does not exceed ±4 percent. The determination of oxidized manganese was performed three times in each of the phosphors.

From the values of the concentrations found, we ca culated the average valence of manganese in the lumino $V_{av} = 2 + 54.03\ e/a$. (V_{av} is the average valence of the manganese; e is the number of gram-equivalents per gram of oxidized manganese (the number of gram-equiv lents of thiosulfate consumed in titration); and a (gm/gr is the total manganese content.

Depending on the nature of the relationship of the luminescent spectra to the values of V_{av}, the phosphors tested were divided into three groups possessing the fo lowing properties.

Group I. (Table 1.) Under the ordinary conditions of preparation of the specimens, there is no oxidized manganese (all manganese is present in the divalent sta

Table 1. ($V_{av} = 2$)

Luminor	Conditions of preparation (°C)*	Color	Luminesce spectrun λ_{max} (mμ)
$MgF_2 \cdot 0.1Mn$	1100	White	590
$(Mg, Be)F_2 \cdot 0.1Mn$	1100	»	Yellow
$Mg_2PO_4F \cdot 1Mn$	1000	»	644, 676
$(Mg, Ca)_2PO_4F \cdot 1Mn$	1000	»	645
$(Mg, Sr)_2PO_4F \cdot 1Mn$	1000	»	650
$(Mg, Zn)_2PO_4F \cdot 1Mn$	1000	»	640
$Mg_2P_2O_7 \cdot 0.5Mn$	1100	»	Red
$2MgO \cdot Li_2OWO_3 \cdot 0.05Mn$	800	Pink	664, 680, 7
$Sr_2P_2O_7 \cdot 0.5Mn$	1100	White	Yellow
$ZnF_2 \cdot 1Mn$	750	»	587
$Zn_3(PO_4)_2 \cdot Mn$	1000	»	Red
$Zn_2SiO_4 \cdot 1Mn$	1350	»	523
$Zn_2GeO_4 \cdot 1Mn$	1100	Yellow	535
Zn, Sn—silicate · 0.5Mn	1200	White	523
Zn, Cd, Sn—silicate · 0.5Mn	1100	»	530
$ZnO \cdot B_2O_3 \cdot 1Mn$	850	»	542
$3ZnO \cdot B_2O_3 \cdot 1Mn$	1000	»	595
Zn, Ba—silicate · 1Mn	1100	»	664
Cd phosphate 0.4Mn	800	»	595
Cd phosphate NaF · 0.4Mn	700	»	630
$CdSO_4 \cdot 0.5Mn$	800	Cream	590
$3CdO \cdot 3Li_2O \cdot 3SiO_2 \cdot 0.15Mn$	1000	White	514, 62
$5.5CdO \cdot 0.5Li_2O \cdot 6SiO_2 \cdot 0.1Mn$	1000	»	600

*The prepared luminors were fired in ammonia.

Group II. (Table 2.) Under the ordinary conditions of preparation, $V_{av} > 2$, but the luminescent spectrum does not depend on V_{av} (after firing in a reducing atmosphere the luminescent spectra do not change, even when V_{av} becomes exactly 2).

Table 2. ($V_{av} > 2$; the Luminescent Spectrum Does Not Depend on the Atmosphere Used during Firing)

Luminor	Conditions of preparation (°C)*	Color	Luminescent spectrum λ_{max} (mμ)	V_{av}
$MgO \cdot SiO_2 \cdot 0.1Mn$	1200, air	Cream	642, 740	2.36
$MgO \cdot SiO_2 \cdot 0.1Mn$	1000, NH_3	White	642, 740	2
$MgO \cdot SiO_2 \cdot 0.03Mn$	1200, air	»	675, 740	2.44
$MgO \cdot SiO_2 \cdot 0.03Mn$	1000, NH_3	»	675, 740	2
$Mg_3(PO_4)_2 \cdot 1Mn$	1000, air	Gray	Red	2.01
$Mg_3(PO_4)_2 \cdot 1Mn$	1000, NH_3	White	White	2
$ZnO \cdot SiO_2 \cdot 0.5Mn$	1250, air	»	570	2.02
$ZnO \cdot SiO_2 \cdot 0.5Mn$	1000, NH_3	»	570	2
Ba, Sr, Li—silicate Ce · 1Mn	800, NH_3	Pink-gray	664	2.04
$2ZnO \cdot 80SiO_2 \cdot 0.25Mn$	1350, air	Gray	523	2.01
$2ZnO \cdot 80SiO_2 \cdot 0.25Mn$	1000, NH_3	White	523	2
$CdO \cdot SiO_2 \cdot 0.1Mn$	900, air	Gray	—	2.16
$3CdO \cdot 4.5Li_2O \cdot 3SiO_2 \cdot 0.1Mn$	900, air		—	2.45
$Al_2O_3 \cdot 0.25Mn$	1350, air	Brown	620	2.21
$Al_2O_3 \cdot 0.25Mn$	1000, NH_3	White	620	2

*The prepared luminors were fired in NH_3.

**Luminor was prepared in a reducing atmosphere. (Translator's note: This luminor is not identified in Russian original.)

Group III. (Table 3.) $V_{av} > 2$ (however, it does not become 4 in any instance). The luminescent spectrum depends on the valence of the manganese. (After firing in a reducing atmosphere and at sufficiently high temperature the luminescence either disappears entirely, or its spectrum changes in proportion to the extent of the reduction of manganese to the divalent state.)

Table 3. ($V_{av} > 2$; the Luminescent Spectrum Depends on the Atmosphere during Firing)

Luminor	Conditions of preparation (°C)*	Color	Luminescent spectrum λ_{max} (mμ)	V_{av}
$MgO \cdot Li \cdot 0.05Mn$	1200, air	Pink	653, 658, 662 665, 672, 677	2.92
$MgO \cdot Li \cdot 0.05Mn$	1000, NH_3	White	725	2
$Mg_2TiO_4 \cdot 0.5Mn$	1200, air	Pink	657, 664, 673	3.68
$Mg_2TiO_4 \cdot 0.5Mn$	1000, NH_3	Gray-green	—	2
$MgO \cdot GeO_2 \cdot 0.1Mn$	1100, O_2	Pink	624, 633, 641, 651	3.23
$MgO \cdot GeO_2 \cdot 0.1Mn$	1000, NH_3	Gray	—	2
Mg—arsenate · 0.4Mn	1100, air	Yellow	Narrow bands, red	3.56
Mg—arsenate · 0.4Mn	1000, NH_3	Gray	—	2
$Li_2TiO_3 \cdot 0.1Mn$	1200, air	Pink	Narrow bands, red	2.95
$Li_2TiO_3 \cdot 0.1Mn$	1000, NH_3	Gray	—	2

*The prepared luminors were fired in NH_3.

From a comparison of the data presented in the tables, it is possible to arrive at the following conclusions: (1) in all luminors with green and yellow luminescence $V_{av} = 2$; (2) among the luminors with orange-red and red luminescence, there are some with $V_{av} = 2$, and some with $V_{av} > 2$; (3) there is no simple relationship between V_{av} and the crystallochemical characteristics of luminors—ionic radii, structure, etc. (Therefore, although Group III contains only lithium- and magnesium-base luminors,* i.e., substances with small cations, the reverse is not true. Indeed, it can be seen from the data that magnesium-base luminors are found in all three groups.)

*No compounds of aluminum were investigated.

It is appropriate to ask what the valence of activator manganese depends upon in phosphors. It seems to us that the valence of manganese cannot be simply related to any one of the known factors, and that it is only determined by their over-all effect. These factors include: (1) the crystallochemical factors (the ratio of the ionic radius of the activator to that of the cation of the matrix; and also the crystallochemical structure of the luminor); (2) the physico-chemical factors (temperature, oxidation-reduction properties of the firing atmosphere, total concentration of mangense); (3) the properties of the manganese compound used to make the addition, and (4) the phase composition of the system. In addition, the degree of deviation of the luminor from thermodynamic equilibrium should also be taken into account.*

*We studied the role of each of the above-mentioned factors in detail in the case of the system ZnO-MnO-O_2, which is considered as a physico-chemical model of luminors. The corresponding article has been sent to one of the chemical journals, simultaneously with the present article.

In conclusion, the authors express their deep gratitude to M. A. Konstantinova-Shlezinger for the guidance in this work and also to H. A. Gorbacheva, Yu. S. Leonov, and E. Ya. Arapova for the phosphors put at our disposal for these investigations.

REFERENCES

1. F. A. Kröger, "Some Aspects of the Luminescence of Solids." Amsterdam, 1948.
2. F. A. Kröger, "Luminescence in Solids Containing Manganese." Amsterdam, 1940.

THE PROPERTIES OF THE LONGEST WAVELENGTH LINE IN THE INTRINSIC ABSORPTION OF Cu_2O

I. S. Gorban' and V. B. Timofeev

Received 8 January 1960

A method is suggested for measuring the contours of very narrow absorption lines, based on using a Fabry-Perot interferometer crossed with a spectrograph. The properties of the longest wavelength line in the intrinsic absorption of Cu_2O are studied over a wide range of low temperatures. It is shown that the line under study is associated with the intrinsic absorption of cuprous oxide. Features of the temperature dependence of the line are related to the mechanism of interaction between excitons and crystal lattice vibrations.

The longest wavelength line of the narrow band absorption of Cu_2O is superimposed on the first edge and is clearly observed in cooled crystals. Its origin is still obscure, chiefly because we have not sufficient experimental data to show unambiguously that this line arises from intrinsic absorption in the crystal. The solution of this problem requires quantitative measurements by means of which the stability of this line can be checked in specimens of different origin.

Several research workers have suggested that the line is related to the yellow series, and have treated it as the first term in this series, corresponding to transitions to the $n = 1$ exciton level.[1] Others consider that the line belongs to the longer wavelength red series and is related to transitions to the $n = 2$ exciton level.[2] They suppose that the red series itself is a satellite series and is the result of indirect transitions, accompanied by absorption of a ~0.13 ev phonon. According to a third point of view, this line is not related to any series, but corresponds to the formation of a Frenkel exciton.[3] Quantitative studies[4] have shown that this line can hardly be related to the yellow series, but that on the other hand it cannot be related to the satellite series in the sense in which this was understood previously.[2] The properties of the continuous absorption background against which the yellow and green series appear show that this line can be assigned the value $n = 2$ of the red series. Moreover the red series and its continuum beyond the limit of convergence are related to direct forbidden transitions,[5] in contrast to the point of view given previously.[2] It is not impossible that the failure to observe terms of the red series higher than $n = 2$ is caused by the existence of exciton states which are not related to borderline cases of the Wannier-Mott type.

The object of the present work was to obtain further experimental data on the properties of this line.

EXPERIMENTAL METHOD

Figure 1a shows a spectrogram of the transmission through a plate of Cu_2O, 0.72 mm thick, cooled to 36°K; it was obtained with an ISP-51 spectrograph with the UF-85 autocollimating camera. It is easily seen that the line in question is superimposed on the first edge,[1] the linewidth being close to that of atomic lines but the intensity being very low. It is therefore very difficult to measure the contour of this line by the usual spectrophotometric methods. Instead, we used a Fabry-Perot interferometer, crossed with the spectrograph mentioned above. The light source was a 300 watt projection lamp. With the aid of a condensing system, the light from this lamp was first passed through the specimen (located in a cryostat) and then through the interferometer, working with an externally converging beam.[6] The interferometer image was formed in the plane of the entrance slit of the spectrograph.

The study of the structure of narrow absorption lin with a Fabry-Perot interferometer crossed with a spec trograph has its own peculiarities. When using a source with a continuous spectral energy distribution, the combination of the interferometer with the spectrograph gives the spectral lines crossed by interference bands (Fig. 1b); this is called a channeled spectrum. If the width of the entrance slit is gradually increased, the interference maxima of the channeled spectrum gradually widen and (at a certain width) come into contact with on another, forming a quasi-continuous spectrum; this is similar to the behavior of the lines of an emission spectrum. Further widening of the slit leads to a correspon ing widening of the interference maxima and to the formation of new intensity maxima in the region where neighboring bands overlap; the positions of these new maxima coincide with the positions of the minima of the initial channeled spectrum (Fib. 1c). Obviously, the intensity of the minima will correspond to the intensity maxima of the initial spectrum. As the entrance slit of the spectrograph is further widened, the channels in the spectrum periodically appear and disappear. If there is

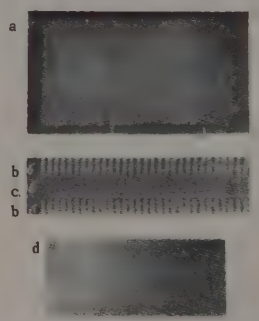

Fig. 1. Spectrograms. a—Transmission of Cu_2O in the region of the first absorption edge for a specimen with $\rho = 0.7 \times 10^3$ ohm-cm at 96°K; b—formation of a channeled spectrum by crossing a Fabry-Perot interferometer with a spectrograph; c—distribution of interference bands in a channeled spectrum as the width of the output slit varies; d—form of the absorption line under study with a Fabry-Perot interferometer crossed with a spectrograph (the dark bands correspond to different orders of interference).

an absorption line in the continuous spectrum, dark interference bands appear (Fig. 1d) at the places where the bright channels intersect the line at the slit width corresponding to the first disappearance of the channels. The spectrogram then obtained looks exactly like the negative of a spectrum with an emission line of the same wavelength as the absorption line.[7]

The distribution of darkening in the interference bands of the absorption line was measured with an MF-2 microphotometer. The conversion from optical densities to intensities was made with the aid of calibration exposures. The spectrogram was microphotometered both along the line and beside it, which yielded a curve showing the increase in absorption (in cm^{-1}) in the line over the background of the absorption edge. Results are given below. No allowance has been made for the distortion introduced by the apparatus into the absolute value of the absorption coefficients in the line. It has been estimated that the value of absorption coefficients obtained in this work are systematically low by not more than 30%. Since in what follows we will be interested in relative data, systematic errors have little importance.

RESULTS AND DISCUSSION

Figure 2 gives three curves showing the contrast between the line under study and the background of the absorption edge.* The circles represent the results of measurements at T = 96° K on a Cu_2O crystal with a resistivity $\rho = 0.7 \times 10^3$ ohm-cm; the crosses are for a specimen with $\rho = 6 \times 10^4$ ohm-cm and the dots for one with $\rho = 1.97 \times 10^6$ ohm-cm. The wave number in cm^{-1} is plotted on the x-axis and the absorption coefficient in decimal cm^{-1} is plotted on the x-axis and the absorption coefficient in decimal cm^{-1} on the y-axis. It is easily seen that the position of the line is different in the spectra of the specimens with different dark conductivities (in the Figure the maxima have been brought into line for all of the curves, but each curve has its own x-axis scale). In the specimens with the lower resistivity (which corresponds to a higher concentration of excess oxygen) the line is shifted toward the long wavelength region of the spectrum. At 96° K, the contour of the line is asymmetrical. In contrast to the shape of the impurity absorption band, however, the absorption falls off more slowly on the long wavelength side of the maximum than on the short wavelength side. The degree of asymmetry of the line is somewhat reduced as the saturation of the Cu_2O specimens with oxygen impurity increases. The integral absorption is almost unchanged, however.

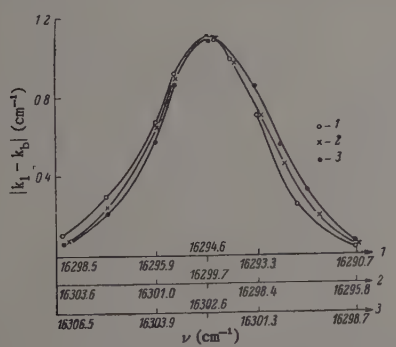

Fig. 2. Curve showing the contrast between the line under study and the absorption edge background at 96° K for crystals with different values of resistivity ρ. Values of ρ (in ohm-cm): 1—0.7×10^3; 2—6×10^4; 3—1.96×10^6. The maxima of the curve have been brought into line on the figure (each curve has its own x-axis scale).

The observed discrepancy in the positions of the line in the spectra of different specimens is accompanied by variations in crystal density. The lines remain shifted with respect to one another throughout the whole range of temperatures investigated. Figure 3 gives two curves showing the variation of the position of the line under study with temperature for two specimens with widely differing resistivities. In the spectrum of the crystal with $\rho = 1.96 \times 10^6$ ohm-cm, the line is shifted by about 8 cm^{-1} relative to its position for the specimen with $\rho = 0.7 \times 10^3$ ohm-cm. The integral absorption of the line remains constant for specimens of Cu_2O of very different technological histories. This supports the opinion that the line is the result of intrinsic absorption. The variation of its position in the spectra of the different specimens is apparently related to the variation of the macroscopic parameters of the crystal (density, refractive index, dielectric strength, etc.) with the impurity oxygen content.

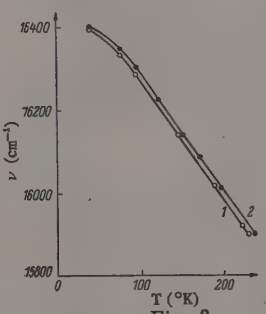

Fig. 3

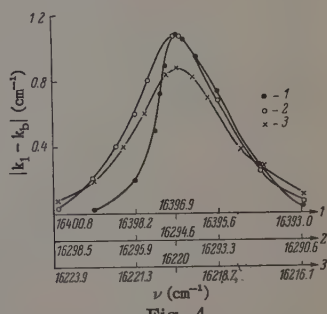

Fig. 4

Fig. 3. Temperature variation of the wave number of the line under study for crystals with (curve 1) $\rho = 0.7 \times 10^3$ ohm-cm and (curve 2) $\rho = 1.97 \times 10^6$ ohm-cm.
Fig. 4. Absorption curves for a specimen with $\rho = 0.7 \times 10^3$ ohm-cm at temperatures: 1—20° K; 2—96° K; 3—120° K. The curve maxima have been brought into line in the figure (each curve has its own x-axis scale).

Figure 4 shows absorption curves obtained at 20°, 90°, and 120° K for a specimen with $= 0.7 \times 10^3$ ohm-cm (here again, each curve has its own x-axis scale). At liquid hydrogen temperature (20° K) the line contour is very asymmetrical, the absorption dropping far more rapidly on the short wavelength side of the maximum than on the long wavelength side. No fine structure was observed in this case. As the temperature was raised to 96° K, the line shifted towards longer wavelengths and gradually broadened, chiefly due to reduction in the curvature of the short wavelength branch. The absorption coefficient which characterizes the contrast between the line maximum and the absorption edge background hardly changes, however. With further increase in temperature, the half-width continues to increase, but the intensity at the maximum begins to drop until the line disappears completely at temperatures close to 273° K. This variation of the line contour at various temperatures is in qualitative agreement with the theory[9] which treats interaction between excitons and lattice vibrations as a function of temperature.

*The measurements were made on very small crystal specimens in which the absorption line was not polarized.

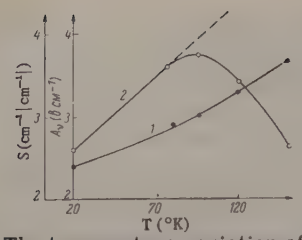

Fig. 5. The temperature variation of (curve 1) the half-width A_ν and (curve 2) the integral intensity S of the absorption line under study.

Figure 5 shows the temperature dependence of the half-width (A_ν) and the integral absorption (S) of the line under study. It is easy to see that the half-width increases according to a law that is close to linear, while the integral absorption begins by increasing almost linearly due to the widening of the line and then sharply decreases. The maximum value of the integral absorption was found to occur at a temperature close to 100°K.*

*Absorption measurements on this line, made with polarized light[12] on single crystal specimens,[11] have shown that the line contour does not depend on either the direction of propagation of light in the crystal or on the orientation of the plane of polarization. The temperature dependence of the contour and of the integral absorption in single crystals is qualitatively the same as in polycrystalline specimens. The line intensity in single crystals depends on the experimental conditions.

Over the whole temperature range in which the line can be measured, the temperature dependence of the integral absorption is described by the empirical formula:

$$S = S_0 + \alpha \cdot T - \frac{\beta}{e^{\frac{\theta}{T}} - 1}, \qquad (1)$$

where $S_0 = 0.9\ \text{cm}^{-1} \cdot \text{A}$; $\alpha = 6.6 \times 10^{-2}\ \text{cm}^{-1} \cdot \text{A} \cdot \text{deg}^{-1}$; $\beta = 4.5 \times 10^{-3}\ \text{cm}^{-1} \cdot \text{A}$ and $\theta = 151°\text{K}$. All the parameters of the formula are given for the case where the band area is measured in $\text{cm}^{-1} \cdot \text{A}$ (the absorption coefficient in decimal cm^{-1}, the wavelength in A).

The first term in Eq. (1) is interpreted as the integral absorption of the line close to T = 0°K. The second term introduces a component varying linearly with temperature. Apparently the line broadens with increasing temperature because of an interaction between excitons and low frequency lattice vibrations when the condition $h\nu_1$ is less than kT is satisfied, where ν_1 is the effective frequency of phonons belonging to the acoustic branch. Finally, the third term is apparently related to exciton-vibrational excitations, in which the optical branch of frequencies takes part.

It is interesting to note that an effective vibration frequency ν_2 can be defined from the relation $\theta = h\nu_2/k$ (k is Boltzmann's constant). It turns out that $\nu_2 = 105\ \text{cm}^{-1}$, which agrees well with the half-width of the edge, in the center of which the line is situated.

It is therefore not impossible that the edge is of vibrational origin, related to the exciton-vibrational excitations which occur with the participation of optical vibrations of the crystal lattice. It is also possible that th relative reduction in the intensity of the line under study by comparison with the adjoining exciton-vibrational background of the absorption edge is largely due to the increase in the absorption in the latter. This point of view makes the presence of the negative term in Eq. (1) understandable.*

*If the absorption edge is of exciton-vibrational origin, it must be supposed that the increase in its intensity wit increasing temperature occurs more rapidly beside the line than under it.

We note that the qualitative considerations introduc above are not to be construed as a negation of the views on the origin of the absorption edge put forward earlier. However it must be admitted that the earlier treatment ambiguous.

The authors take pleasure in expressing their grati tude to V. L. Brouda for making the work with liquid hydrogen possible.

REFERENCES

1. E. F. Gross, Uspekhi Fiz. Nauk 33, 595 (1957).
2. S. Nikitine, Helv. Phys. Acta 28, 247 (1954); J. phys radium 19, 170 (1958).
3. A. G. Zhilich and P. P. Pavinskii, Vestnik Leningra Gosudarst. Univ. No. 4, 50 (1957).
4. I. S. Gorban', Opt. i Spektr. (in press).
5. R. J. Elliot, Phys. Rev. 108, 1384 (1957).
6. S. Tolansky, "Spektroskopiya vysokoi razreshayush sily" (High Resolution Spectroscopy), Izd. Inostrann Lit., Moscow, 1955.
7. Ch. Fabry, Compt. rend. 140, 1136 (1905); Ch. Fabry and H. Buisson, J. Phys. 9, 197 (1910).
8. S. I. Pekar and M. Krivoglaz, Trudy Inst. Fiz. Akad Nauk Ukrain. SSR No. 4, 37 (1953); I. S. Gorban' and A. A. Shishlovskii, Doklady Akad. Nauk SSSR 108, 1 (1956).
9. Y. Toyodzawa, Progr. Theoret. Phys. (Kyoto) 20, 1 (1958).
10. E. F. Gross and I. Pastrnyak, Fiz. Tverd. Tela 1, 6 (1959).
11. I. S. Gorban' and V. B. Timoveef, Fiz. Tverd. Tela 2, 8 (1960).
12. E. F. Gross and A. A. Kaplyanskii, Fiz. Tverd. Tel 2, 379 (1960).

THE OPTICAL PROPERTIES OF BULK BISMUTH IN THE 3-36μ REGION

M. N. Markov and A. S. Khaikin

Received 25 January 1960

The optical constants n and κ of Bi were determined in the 3-36μ region by measuring its reflectance. An absorption band was found in the vicinity of 27μ. The concentration of conduction electrons was found to be 5×10^{19} cm^{-3}. The properties of Bi were treated from the band model viewpoint, with a forbidden band gap $\Delta E_0 = 0.04$ ev.

The electrical properties of bismuth have been studied in considerable detail.[1-3] The data on optical properties available thus far, however, have been insufficient, and could not be satisfactorily interpreted, since they contained contradictions and did not cover the necessary portion of the spectrum.[4-9] This paper describes an investigation of the optical properties of bulk bismuth in the 3-36μ region. In this study, measures were taken to produce a surface structure with the smallest possible number of defects.

METHOD OF MEASUREMENT

In order to determine the optical constants of bismuth, the method described by Šimon in 1951 was used.[10] The essence of the method consists of measuring the reflectance for two angles of incidence of natural light. From the observed values of the reflectance it is possible to calculate the optical constants n and κ, the absorption constant A, dielectric constant ε, etc.

The method of Šimon is simpler than the polarization methods currently used in metal optics (e.g. Avery,[11] Motulevich and Shubin[12]), since it does not require the use of such large samples or of polarizers, which are difficult to prepare and use in the 3-40μ region.

The reflection measurements were made with a single beam arrangement, and an illuminator unit of the type described by Šimon was constructed. In this unit, the source remains stationary while the angle of incidence is being varied, so that the measurements were free of positioning errors. The complete illumination system and the sample were mounted on two plates which could be rotated with respect to each other.

A globar and two mirrors, which formed a 1:1 image of the globar on the sample, were mounted on the movable plate. The stationary plate was fastened to the apparatus and included one mirror which projected a 2:1 image of the sample onto the entrance slit of a monochromator. For any angle of rotation of the movable plate, the image of the globar fell on the sample, which was located on the axis of rotation of this plate. The sample and the comparison mirror were attached to a carriage which permitted rapid interchange of the sample and the mirror in the beam. The system was constructed with a view toward its use with instruments of the IKS-14 type.

The samples were made from bismuth whose nominal purity was 99.97%. The samples were prepared by casting in a mold measuring 20×30 mm. The bottom of the mold consisted of a thick slab of glass polished to a mirror finish. Before the sample was cast, the glass was heated to a temperature somewhat above the melting point of bismuth (269°C), so that the structure of the samples would be as uniform as possible. The bismuth was also heated only a little above its melting point, in order to avoid oxidation. A thin polished mirror was introduced into the mold. It was 1.5 mm thick (for a mold 4 mm thick) and measured 10×30 mm. It served as the base of the comparison mirror. Thus, the comparison mirror was fused into the sample so that the surfaces of the mirror and the sample were parallel. An opaque coating of aluminum was evaporated onto the mirror under vacuum. The mirror surface of samples made in this fashion yielded a geometrically accurate reflection, although crystal grains in the form of occasional networks of fracture lines were visible on it.

The samples were then polished electrolytically in a saturated potassium iodide solution, acidified with hydrochloric acid by adding 20 ml of the latter to a liter of solution.[13] The polishing time was 2 to 5 min, using a current density of 60 ma/cm^2 at the end of the process. The polished surface had the same general appearance as the cast surface, except that the boundaries of the larger crystals had become visible.

RESULTS OF THE MEASUREMENTS

Each measurement consisted of 4 readings: u_a, the amount of reflection from the aluminum; u_o, the amount of reflection from the sample; u_{sa}, the amount of scattered light associated with reflection from aluminum; and u_{so}, the amount of scattered light associated with reflection from the sample. The intensity of the scattered light was measured in the usual way with the help of glass plates up to 27μ and of NaCl plates beyond 27μ. The reflectance R is calculated from the equation

$$R = k \frac{u_o - u_{so}}{u_a - u_{sa}},$$

where k is the reflection coefficient of aluminum taken (from Beattie[14]) to be 0.98 over the wavelength region in question. The mean square error in R (for 3 to 5 measurements on each sample) averaged about 2%. The magnitude of the errors was a function of the general behavior of the apparatus (noise, zero drift, etc).

From the magnitude of the reflectance at $\varphi = 20°$ (R_{20}) and at $\varphi = 70°$ (R_{70}) the optical constants, i.e., the refractive index n and the absorption index κ, were determined by graphical analysis. Special plots for R_{20} and R_{70} as a function of n with κ as parameter were constructed; from these plots the values of n and κ could be determined from the known values of R_{20} and R_{70}. In the calculations, the polarization of light by the apparatus was taken into account (by the method of Šimon). Calculation of the polarization of an IKS-14 monochromator gives a value of P = 45% for a NaCl prism and P = 55% for a KRS-5 prism. The experimentally observed polarization in our IKS-14 monochromator with a NaCl prism was P = 44%. Since the difference in corrections to R for P = 45% and P = 55% is small, the average value was used for these prisms, namely P = 50%.

The mean square errors, evaluated from the dispersion in n and κ values, amounted to about 10% for

n and about 15% for κ for every sample. The dispersion of measured parameters in three samples was about 5% for R, about 20% for n, and about 10% for κ. This variation is not caused by inaccuracies of the method, but by differences in the reflectances of the various samples. The reasons for such differences may be, first of all, certain imperfections in the sample surface which cause light scattering, and secondly, insufficient averaging of reflections from variously oriented crystals in the case of polycrystalline samples.

The results of the measurements are given in the Table.

Average Values of R_{20}, R_{70}, n, κ, and A obtained from Measurements on Three Samples of Electropolished Bi

λ (μ)	R_{20}	R_{70}	n	κ	A
3	0.68	0.58	2.6	4.5	0.32
7	0.66	0.54	4.6	4.5	0.33
11	0.66	0.54	4.8	4.3	0.34
14	0.63	0.52	5.2	4.2	0.36
16.7	0.60	0.47	5.6	3.7	0.39
20	0.56	0.44	4.9	3.1	0.44
25	0.49	0.40	3.8	2.7	0.50
27	0.45	0.39	2.9	2.5	0.54
30	0.53	0.49	2.2	3.0	0.47
32	0.63	0.58	1.8	3.5	0.40
34	0.76	0.69	1.4	4.2	0.25
36	0.78	0.73	1.3	4.5	0.21

The reflection spectrum of bulk Bi in the 3-36μ region is shown in Fig. 1. As is evident from this figure, the reflectivity passes through a minimum at 27μ. The location of this minimum is the same for polished and unpolished samples, even though the magnitude of R and the depth of the minimum are greater (by approximately 5%) in polished samples. The reflection rises sharply beyond this minimum. Since $\varphi = 20°$ corresponds to almost normal incidence, the quantity $1 - R_{20}$ is nearly equal to the absorption coefficient A. A, therefore, has a maximum in the vicinity of $\lambda = 27\mu$ (Fig. 2). This figure also shows the dependence of n and κ on wavelength for polished samples. Just as in the case of reflection, the differences between the values of these parameters for polished and unpolished samples is not very large, and their dependence on λ is similar, so that hereinafter we shall consider only polished samples. The value of the absorption coefficient A calculated from the measured values of n and κ coincided very closely with $1 - R_{20}$ (to within an accuracy of about 4%), which served as an indication that the derived values of n and κ were correct.

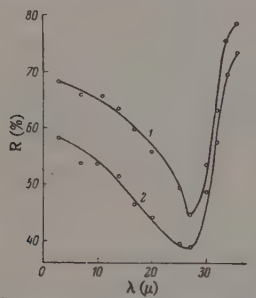

Fig. 1. Reflectance of cast electropolished bismuth in the 3-36μ region for different angles of incidence. Angles of incidence: curve 1—20°; curve 2—70°.

Figure 3 shows the real part of the dielectric constant as a function of λ^2 for three samples. As can be seen in the figure, Re $\varepsilon \sim$ const. – $k\lambda^2$ over a considerable range of wavelengths. Note also the substantial differences between the n, κ and Re ε values for the three samples for $\lambda < 20\mu$, and the improved agreement in the longer wavelength region.

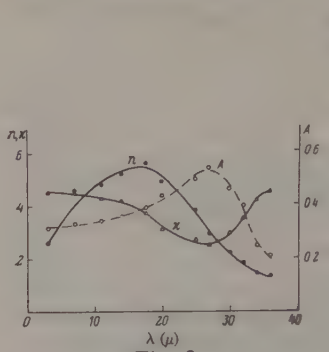

Fig. 2

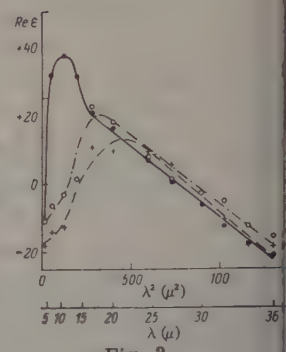

Fig. 3

Fig. 2. Indices of refraction n, and absorption κ, the absorption coefficient A of electropolished bismuth in the 3-36μ region.
Fig. 3. Real part of ε for three samples of electropolished bismuth in the region 3-36μ.

When our results are compared to those of other investigators, it must first be noted that the latter were limited to the spectral region $\lambda < 15\mu$. Figure 4 shows the values of n, κ, and A obtained from our data for electropolished bismuth, from Hodgson's data[4] for mechanically polished bismuth, and also from the data of Markov and Lindstrem[5] for an evaporated bismuth layer about 1μ thick. It is readily seen that the results of those authors differ considerably from ours. These large differences can be explained by differences in surface structure. It has been established that evaporated bismuth has a structure which differs greatly from the usual structure of bulk bismuth (the specific resistivity of evaporated bismuth is three times as great as that of the bulk metal,[15] etc.). Mechanical polishing of bismuth, because of this metal's extreme softness, produces a cold-worked surface layer of varying structure. Since it is assumed that electropolishing does not leave a surface layer of a different structure, it is clearly valid to conclude that our results are applicable to the structure which is characteristic of bulk bismuth (by the word "structure," we do not mean the lattice configuration, but rather the shape and dimensions of crystalline regions, the dimensions and numbers of defects in these regions, etc.).

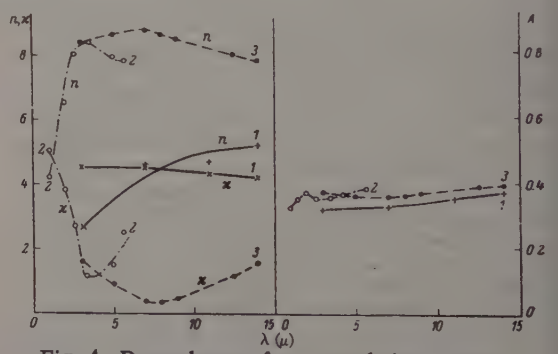

Fig. 4. Dependence of n, κ, and A on wavelength. Curves 1—our data; curves 2—data of ref. 4; curves 3—data of ref. 5.

It is interesting to note that the absorption coefficients A calculated from the data of refs. 4 and 5 agree quite well with ours. Clearly, in these cases the rhombo

hedral lattice of bismuth is preserved. The value of A depends principally on the existence of this lattice, whereas the values of n and κ are strongly affected by structure.

DISCUSSION OF THE RESULTS

The electronic theory of metals leads to the following expression for Re ε[16]

$$\mathrm{Re}\,\varepsilon \simeq \varepsilon_0 - \frac{4\pi Ne^2}{m(\omega^2+\nu_0^2)} \simeq \varepsilon_0 - \frac{\omega_0^2}{(\omega^2+\nu_0^2)},$$

where N is the concentration of conduction electrons (cm^{-3}); $e = 4.8 \times 10^{-10}$ cgs units is the electronic charge; $m = 9.1 \times 10^{-28}$ gm is the mass of a free electron; ω is the light frequency; ν_0 is the effective collision frequency of the electrons; and ω_0 is the plasma frequency. The calculation of N from this expression is easiest when $\nu_0 \ll \omega^2 \ll \omega_0^2$. This condition is satisfied in our case for $\lambda > 20\mu$, since in that region, there is a linear dependence of Re ε on λ^2 (Fig. 3). Consequently, in this spectral region, $\varepsilon_0 = \text{const}$, and Re $\varepsilon \cong$ const. $- (e^2N\lambda^2/\pi mc^2)$. From the slope of the linear portion of Re ε, we obtain

$$N = 5 \cdot 10^{19}\ \mathrm{cm}^{-3}$$

(to an accuracy of about 50%).

By taking account of the fact that the measured dc conductivity of our samples was $\sigma_0 = 0.85 \times 10^4$ ohm^{-1} cm^{-1}, we can calculate from the equation

$$\sigma_0 \cong \frac{e^2N}{m\nu_0}$$

that $\nu_0 \simeq 1.5 \times 10^{12}$ sec^{-1}. For $\lambda = 36\mu$ ($\omega = 5.2 \times 10^{13}$) $\omega^2/\nu_0^2 = 2 \times 10^3 \gg 1$. On the other hand,

$$\omega_0 = \left(4\pi e^2 \frac{N}{m}\right)^{1/2},$$

and in our case is equal to about 4×10^{14}, which corresponds to $\lambda \sim 5\mu$, that is, the short wavelength limit of the spectral region which we studied. Given the values of N and ν_0, it is possible to evaluate the contribution of conduction electrons to the absorption A_{el}. If we use the approximate expression[16]

$$A_{el} \approx \nu_0 \left(\frac{m}{\pi e^2 N}\right)^{1/2},$$

we obtain $A_{el} \approx 0.5\%$. Thus the contribution of conduction electrons to the absorption in bismuth in the wavelength region of interest here is clearly very small. Note that in order for the observed absorption (≈ 50% at its maximum) to be caused by conduction electrons, the quantity N would have to be increased by 4 orders of magnitude, i.e., the bismuth would have to become an ideal metal.

In the calculations presented above, it was assumed that the skin-effect is normal in bismuth. Knowing the values of N and ν_0, one can make the following evaluations. The velocity on the Fermi surface is $v_0 \sim 10^7$ cm/sec, and the free path length is $l \sim 0.05\mu$. The skin depth δ changes from 0.2 to 3μ as the wavelength varies from 3 to 36μ, as a result of which the condition for a normal skin effect ($l \ll \delta$) is well satisfied over the whole region under investigation.

As was shown by Jones,[17] it is possible to calculate the concentration of conduction electrons in pure bismuth from the concentration of tin in Bi-Sn, which corresponds to the transition of the temperature coefficient of resistivity of the alloy to a negative value[1-3] (this alloy has the same structure as Bi). In this way, it was shown[17] that it is less than or equal to 0.0013 electrons/atom, which leads to $N \approx 4 \times 10^{19}$ cm^{-3}. The agreement between our value and that measured by Jones should be noted, since the two results were obtained from investigations of entirely different properties of bismuth. Despite the fact that small concentrations of certain metal impurities (e.g., tin or lead in amounts of about 1%) affect the electrical properties of bismuth very strongly, it can be assumed that they do not change its absorption very much, since these impurities only change the number of conduction electrons, whose contribution to the absorption is very small.

This last result makes it possible to relate the observed absorption with possible transitions across the forbidden band. The width of this band (corresponding to the absorption maximum at $\lambda = 27\mu$) corresponds to $\Delta E_0 = 0.04$ ev. The existence of a forbidden band in bismuth had been assumed previously,[4,17] but Jones[17] was unable to determine the width of this band on the basis of theoretical considerations. Hodgson,[4] starting from the experimentally observed minimum of κ for $\lambda = 3.5\mu$, determined a forbidden bandwidth of 0.3 ev, which is in general quite doubtful, since there is no maximum observed in A in this region. On the other hand, if one analyses the dependence of A on λ (Fig. 4), calculated from the data of ref. 4, it can be assumed that the drop of A in the region $\lambda < 2\mu$ corresponds to the short wavelength edge of the absorption band.

The existence of a forbidden energy gap should lead to a negative temperature coefficient of resistance in pure bismuth. This has not, however, been observed experimentally (e.g., see ref. 3). In order to explain this fact one can calculate the concentration of electrons transferred into the conduction band of pure bismuth by thermal excitation.[18] At room temperature, (kT = 0.026 ev, $\Delta E_0 = 0.04$ ev) we have $N_0 = 5 \times 10^{18}$ cm^{-3}. Thus it is clear that the number of electrons thermally excited into the conduction band at room temperature amounts to only 10% of the total number of electrons in the band. This also explains the metallic behavior of the resistivity of pure bismuth as a function of temperature. A study of the photoconductivity and of the temperature dependence of the location of the absorption maximum should give additional information concerning the extent and structure of the band.

The authors take this occasion to express their deep gratitude to N. N. Sobolev for permitting the use of his KRS-5 prism spectrometer, and also to V. S. Silin for valuable advice and discussion of the results.

REFERENCES

1. W. Ufford, Proc. Am. Acad. Arts Sci. **63**, 309 (1928).
2. O. Thomas and O. Evans, Phil. Mag. **16**, 329 (1933).
3. N. Thompson, Proc. Roy. Soc. **A155**, 111 (1936).
4. J. N. Hodgson, Proc. Phys. Soc. **B67**, 269 (1954).
5. M. N. Markov and I. S. Lindstrem, Opt. i Spektr. **7**, 349 (1959), Optics and Spectroscopy **7**, 228 (1959).
6. C. V. Kent, Phys. Rev. **14**, 459 (1919).
7. W. Meier, Ann. Phys. **31**, 1017 (1910).
8. W. Woltevsdorff, Z. Physik **91**, 230 (1934).
9. N. E. Alekseevskii and E. V. Potapov, Zhur. Eksptl. i Teoret. Fiz. **33**, 283 (1957).
10. I. Šimon, J. Opt. Soc. Am. **41**, 336 (1951).
11. D. G. Avery, Proc. Phys. Soc. **B65**, 425 (1952).
12. G. P. Motulevich and A. A Shubin, Opt. i Spektr. **2**, 633 (1957).
13. W. I. McG. Tegart and R. G. Vines, Rev. met. **48**, 245 (1951).
14. O. Beattie, Phil. Mag. **46**, 235 (1955).

15. M. N. Markov and I. S. Lindstrem, Fiz. Tver. Tela 1, 827 (1959).
16. V. L. Ginzburg and G. P. Motulevich, Uspekhi Fiz. Nauk 55, 469 (1955).
17. H. Jones, Proc. Roy. Soc. A147, 396 (1934).
18. A. F. Ioffe, "Fizika Poluprovodknikov" (Physics of Semiconductors). Acad. Sci. USSR Press, 1957.

DETERMINATION OF THE OPTICAL CONSTANTS OF ABSORBING SUBSTANCES FROM THE MEASUREMENTS OF STOKES' PARAMETERS OF REFLECTED LIGHT

A. P. Prishivalko

Received 18 January 1960

A method of determination of the optical constants of absorbing substances is described which is based on the measurement of the Stokes' parameters of light which is reflected from the sample under investigation. The theoretical basis of this method and nomograms for its application are given.

In practice it is often necessary to obtain sufficiently complete and reliable information on the optical constants of a large number of substances, and this is the reason for the appearance of numerous works dedicated to this problem. Much attention has been paid to the determination of the optical constants of strongly absorbing substances, especially in the infrared part of the spectrum. A large number of methods for the determination of optical constants have been described in recent years. Many of them turn out to be modifications of the well-known Drude method. This method depends, firstly, on measurements at the principle angle of incidence, which for strongly absorbing substances (especially in the infrared region) approaches 90°, and secondly, on the application of compensating devices which do not exist for the infrared region.

In the proposed modifications these difficulties are circumvented in various ways. Thus, for instance, in place of a direct measurement of the relative phase difference of the p- and s-components ($\Delta = \delta_p - \delta_s$) in the reflected light using compensators, it is determined in an indirect way from measurements of the intensity at several positions of the polarizer.[1-3] Multiple reflections from surfaces of identical samples which are placed parallel to one another are employed in order to avoid measurements at the principle angle of incidence.[1,3-5] It is possible to carry out such measurements with arrangements in which a very precise parallelism of the reflecting surfaces is assured. The samples should be quite identical and should possess surfaces of considerable dimensions.

The second group of methods, based on the measurement of reflection coefficients or their ratios for light which is incident on the surface of the sample at an angle, is simpler in practice. The most complete method is that which is based not on absolute measurements, but on the determination of $\rho^2 = R_p R_s$ for two angles of incidence.[6-8] However, this method is primarily applicable to the determination of the optical constants of substances which are not very strongly absorbing. In ref. 9 it was shown that for very strongly absorbing substances the measurement of ρ^2 at relatively small angles of incidence does not give substantially new information in comparison with the measurement of the reflection coefficient of the s- component, and even compared to the measurement of the reflection coefficient at normal incidence. New information can be obtained if, when measuring ρ^2, one of the two angles of incidence is close to the principle angle.

For a reliable determination of the refractive index n and absorption coefficient χ measurements are necessary of two quantities which are related to n and χ in essentially different ways. Some of the published methods for the determination of the optical constants do not satisfy this important requirement. Others are too complicated for application under normal laboratory conditions. Requirements such as simplicity of the experimental apparatus and small time requirements for the execution of the necessary calculations, together with reliability of the obtained results, are essential and justify the search for new methods of determination of the optical constants of strongly absorbing substances.

In this work an attempt is made to apply measurements of the components of the Stokes' parameter vector to the determination of optical constants.

The Stokes' parameter vector is a four-dimensional vector whose components are statistical parameters which are additive for incoherent light fluxes. These parameters, usually called the Stokes' parameters, fully determine the state of a light flux both from the point of view of its intensity and of its polarization.[10] At present there exist experimental setups which make it possible to measure all four Stokes' parameters simultaneously.

Consider a plane electromagnetic wave $\mathbf{E} = (E_1\mathbf{e}_1 + E_2\mathbf{e}_2)e^{i\omega t}$ where E_1 and E_2 are two complex amplitudes which are either not dependent or only slightly dependent on the time t, and $\mathbf{e}_1$ and $\mathbf{e}_2$ are unit vectors perpendicular to the direction of propagation of the wave. In this case the Stokes' parameters are expressed in terms of the component field intensities (E_1 and E_2) of the light flux in the following way:

$$\left.\begin{aligned} S_1 &= E_1E_1^* + E_2E_2^*, \\ S_2 &= E_1E_1^* - E_2E_2^*, \\ S_3 &= E_1E_2^* + E_1^*E_2, \\ S_4 &= -i(E_1E_2^* - E_1^*E_2) \end{aligned}\right\} \qquad (1$$

or, in a more compact form, $S_i = \mathbf{E}\sigma_i\mathbf{E}^*$, (i = 1,2,3 4) where σ_1 is a unit matrix of the second rank and σ_2, σ_3, and σ_4 are Pauli matrices.

To determine the first three Stokes' parameters experimentally it is necessary to measure the intensity of the observed light beam for three different positions of the analyzer. To determine the fourth parameter it is necessary to insert into the beam, in addition to the analyzer, a compensator which will introduce a path differ-

ence τ between the two components E_1 and E_2. If the position of the analyzer is specified by the angle α between its plane of transmission and the reference plane,*

*The plane which contains the direction of propagation of the wave and the direction of the unit vector e_1 is called the reference plane.

hen the intensity of the light passing through the system will be a function of τ and α, that is, $I = I(\tau,\alpha)$. According to Rozenberg[10] we have:

$$\left.\begin{aligned} S_1 &= I(0,\ 0) + I\left(0,\ \frac{\pi}{2}\right), \\ S_2 &= I(0,\ 0) - I\left(0,\ \frac{\pi}{2}\right), \\ S_3 &= 2I\left(0,\ \frac{\pi}{4}\right) - S_1, \\ S_4 &= 2I\left(\frac{\pi}{2},\ \frac{\pi}{4}\right) - S_1. \end{aligned}\right\} \qquad (2)$$

From the determination of the components of the vector parameter it follows that

$$S_1 = I,\ S_2 = IP_1,\ S_3 = IP_2,\ S_4 = IP_3, \qquad (3)$$

where P_i does not depend on the intensity of the beam I. The quantities P_i can be looked upon as the components of some three-dimensional vector P. This vector fully determines the state of polarization of the beam and is called the polarization vector. Its components can be obtained from measurements.

Having established the relationship between the experimentally determined quantities P_1, P_2, and P_3 and the values of the refractive index n, the absorption coefficient χ, and the angle of incidence φ, one can use it for the determination of the optical constants. The application of the quantities P_1, P_2, and P_3 for this purpose is convenient because to determine them one requires not absolute, but relative measurements, and these can be carried out more reliably.

Writing the expressions for the amplitudes r_p and r_s of light reflected from the surface of a specimen in the form*

*The minus sign for the coefficient of reflection of the p-component has been chosen for reasons given in refs. 4, 9, and 11.

$$r_s = -a_s \frac{\sin(\varphi - \varkappa)}{\sin(\varphi + \varkappa)} = -a_s \frac{a + bi - \cos\varphi}{a + bi + \cos\varphi}, \qquad (4a)$$

$$r_p = -a_p \frac{\tan(\varphi - \varkappa)}{\tan(\varphi + \varkappa)} = r_s \frac{a_p}{a_s} \frac{a + bi - \sin\varphi\tan\varphi}{a + bi + \sin\varphi\tan\varphi} \qquad (4b)$$

where

$$a + bi = \sqrt{n^2 - \varkappa^2 - \sin^2\varphi - 2in\varkappa}, \qquad (4c)$$

we obtain

$$P_1 = \frac{a_p a_p^* [(a - \sin\varphi\tan\varphi)^2 + b^2] - a_s a_s^* [(a + \sin\varphi\tan\varphi)^2 + b^2]}{a_p a_p^* [(a - \sin\varphi\tan\varphi)^2 + b^2] + a_s a_s^* [(a + \sin\varphi\tan\varphi)^2 + b^2]}, \qquad (5a)$$

$$P_2 = \frac{\begin{aligned} &a_p a_s^* [a^2 + b^2 - \sin^2\varphi\ \tan^2\varphi + 2ib\sin\varphi\ \tan\varphi] \\ &+ a_p^* a_s [a^2 + b^2 - \sin^2\varphi\tan^2\varphi - 2ib\sin\varphi\tan] \end{aligned}}{a_p a_p^* [(a - \sin\varphi\tan\varphi)^2 + b^2] + a_s a_s^* [(a + \sin\varphi\tan\varphi)^2 + b^2]}, \qquad (5b)$$

$$P_3 = -i \frac{\begin{aligned} &a_p a_s^* [a^2 + b^2 - \sin^2\varphi\tan^2\varphi + 2ib\sin\varphi\tan\varphi] \\ &- a_p^* a_s [a^2 + b^2 - \sin^2\varphi\ \tan^2\varphi - 2ib\sin\varphi\ \tan\varphi] \end{aligned}}{a_p a_p^* [(a - \sin\varphi\tan\varphi)^2 + b^2] + a_s a_s^* [(a + \sin\varphi\ \tan\varphi)^2 + b^2]} \qquad (5c)$$

If we assume for simplicity that the incident light is linearly polarized at an angle of 45° to the plane of incidence ($a_p = a_s$), we can show that the determination of each of the components of the polarization vector of the reflected light yields essentially new information, so that they appear as quite different functions of the unknown quantities n and χ.

After suitable rearrangements and putting $a_p = a_s$ expressions (5) take the form

$$P_1 = -\frac{2a\sin\varphi\tan\varphi}{a^2 + b^2 + \sin^2\varphi\tan^2\varphi}, \qquad (6a)$$

$$P_2 = \frac{a^2 + b^2 - \sin^2\varphi\tan^2\varphi}{a^2 + b^2 + \sin^2\varphi\tan^2\varphi}, \qquad (6b)$$

$$P_3 = \frac{2b\sin\varphi\tan\varphi}{a^2 + b^2 + \sin^2\varphi\tan^2\varphi}, \qquad (6c)$$

where

$$a = \sqrt{\frac{1}{2}[\sqrt{(n^2 - \varkappa^2 - \sin^2\varphi)^2 + 4n^2\varkappa^2} + (n^2 - \varkappa^2 - \sin^2\varphi)]}, \qquad (6d)$$

$$b = \sqrt{\frac{1}{2}[\sqrt{(n^2 - \varkappa^2 - \sin^2\varphi)^2 + 4n^2\varkappa^2} - (n^2 - \varkappa^2 - \sin^2\varphi)]}. \qquad (6e)$$

If

$$\sin^2\varphi \ll |(n - i\varkappa)^2| \qquad (7)$$

Eqs. (6a), (6b), (6c) can be replaced by the approximations

$$P_1 \cong -\frac{2n\sin\varphi\tan\varphi}{n^2 + \varkappa^2 + \sin^2\varphi\tan^2\varphi}, \qquad (8a)$$

$$P_2 \cong \frac{n^2 + \varkappa^2 - \sin^2\varphi\tan^2\varphi}{n^2 + \varkappa^2 + \sin^2\varphi\tan^2\varphi}, \qquad (8b)$$

$$P_3 \cong \frac{2\varkappa\sin\varphi\tan\varphi}{n^2 + \varkappa^2 + \sin^2\varphi\tan^2\varphi}. \qquad (8c)$$

The expressions (8) show clearly the essentially different dependence of P_1, P_2, and P_3 on n and χ. In the case of metals, when the inequality (7) is satisfied, these relationships can be used for the determination of the optical constants. It is also clear from (8) that the measurements necessary for this purpose can be carried out at angles of incidence which are smaller than the principal angle. This is very important for the arrangement of the experiment.

Two equations are necessary for the determination of the two unknown quantities n and χ. Since the use of a compensator is not necessary for the determination of P_1 and P_2, it is natural to select for this purpose Eqs. (6a) and (6b) or the corresponding approximations (8a) and (8b). The determination of P_3 in the visible and ultraviolet regions can serve as a supplementary measurement for obtaining more precise results.

After rearrangement we obtain from Eqs. (6a) and (6b)

$$n^2 - \varkappa^2 = \frac{2P_1^2 + P_2^2 - 1}{(1 - P_2)^2}\sin^2\varphi\tan^2\varphi + \sin^2\varphi, \qquad (9a)$$

$$2n\varkappa = \frac{2P_1\sqrt{1 - P_1^2 - P_2^2}}{(1 - P_2)^2}\sin^2\varphi\tan^2\varphi. \qquad (9b)$$

These expressions determine the value of the real $(n^2 - \chi^2)$ and imaginary $(2n\chi)$ parts of the dielectric permeability which in a number of cases are important in themselves. They can also be used for the determination of n and χ through the solution of a bi-quadratic equation obtained by the substitution of (9b) in (9a).

If the condition (7) is satisfied, we obtain from the approximate equations (8a) and (8b)

$$n \cong -\frac{P_1}{1 - P_2}\sin\varphi\tan\varphi, \qquad (10)$$

$$\varkappa \cong \frac{\sqrt{1-P_1^2-P_2^2}}{1-P_2}\sin\varphi\tan\varphi. \qquad (11)$$

These relationships are quite simple and can be used for a direct determination of n and χ.*

*With suitable assumptions expressions (10) and (11) reduce to the well-known formulas of Drude which are utilized in the optics of metals.

In the case when it is necessary to employ the exact expressions (9) the work of finding numerical values of $(n^2-\chi^2)$ and $2n\chi$ can be considerably reduced if previously constructed nomograms are available.

In order that the nomogram may be used for any angle of incidence, it is necessary to construct it not for $(n^2-\chi^2)$ and $2n\chi$ but for the quantities

$$X=\frac{n^2-\varkappa^2-\sin^2\varphi}{\sin^2\varphi\tan^2\varphi}, \qquad (12a)$$

$$Y=\frac{2n\varkappa}{\sin^2\varphi\tan^2\varphi}. \qquad (12b)$$

The appearance of such a nomogram is shown in Fig. 1. The values of P_1 and P_2 are plotted along the coordinate axes (the nomogram is constructed only for positive values of P_2).

The family of curves which correspond to constant values of Y and which are loop-shaped, converges in the upper left corner of the diagram. The curves corresponding to constant values of X emerge from the same point and are approximately orthogonal to the first family of curves.

Simple expressions, obtained from (9) and (12), are used for the construction of the nomograms.

$$P_1=-\sqrt{\frac{1}{2}\left[X(1-P_2)^2+(1-P_2^2)\right]}, \qquad (13a)$$

$$P_1=-\sqrt{\frac{1}{2}\left[(1-P_2^2)\pm\sqrt{(1-P_2^2)^2-Y^2(1-P_2)^4}\right]}. \qquad (13b)$$

The values of X and Y corresponding to the experimentally determined values of P_1 and P_2 are found, and then a simple calculation yields $(n^2-\chi^2)$ and $2n\chi$.

It can be seen from Fig. 1 that not all the areas of the nomogram are equally adequate in the precision of the provided results. However, if we consider that for strongly absorbing substances, and in particular, for metals the quantity X assumes normally negative values, it can be seen that for such cases this corresponds to the most favorable part of the nomogram.

A similar method for the graphical determination of $(n^2-\chi^2)$ and $2n\chi$ is developed in ref. 9. The quantities measured there are $\rho^2=R_p/R_s$ and Δ, the relative phase difference of the p- and s-components for linearly polarized light reflected from the surface of the sample. The advantages and disadvantages of the two methods, the question of accuracy, and a comparison with some other methods will be considered in detail in a future publication. Preliminary calculations have shown that the accuracies of the method presented here and of the method described in ref. 9 are of the same order.

One more stage of calculations is necessary in order to obtain n and χ from $(n^2-\chi^2)$ and $2n\chi$. One can avoid this by constructing special nomograms expressing directly the relationship between the quantities P_1, P_2, and P^3 and the optical constants n and χ for some definite angle of incidence. For this purpose the real and imaginary parts of the amplitude reflection coefficients were computed on the electronic computer "Ural" for a large number of values of n, χ, and φ. From the data obtained tables of P_1, P_2 and P_3 were compiled, and from these the nomograms shown in Figs. 2-4 were constructed.

A nomogram for the determination of the quantities n and χ from the measured values of P_1 and P_2 for a fixed angle of incidence of $\varphi = 45°$ is shown in Fig. 2. The full lines are drawn through points with a constant value of the absorption coefficient χ; the broken lines pass through points with equal values of the refractive index n. The nomogram shown in Fig. 3 serves for the determination of n and χ from measured values of P_1 and P_3 for the same angle of $\varphi = 45°$ (it can be applied when working in the visible and ultraviolet regions).

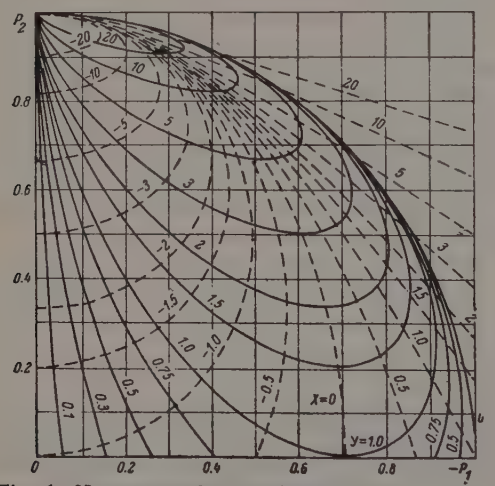

Fig. 1. Nomogram for the determination of the parameters X and Y. The broken curves pass through points corresponding to constant values of X; the full curves correspond to constant values of Y. The numbers next to the curves are the values of X and Y.

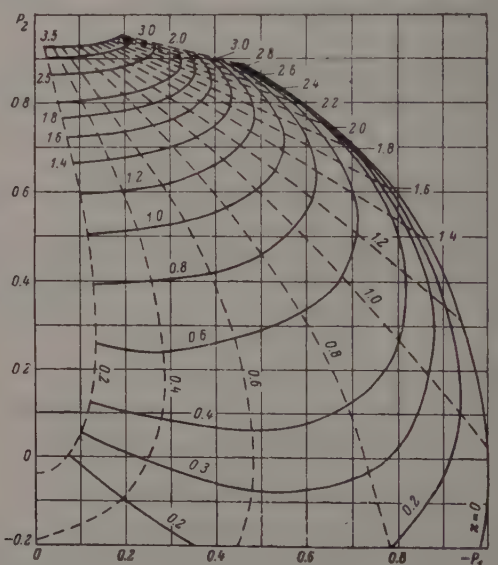

Fig. 2. Nomogram for the determination of the refractive index n and the absorption coefficient χ from the measurements of the values of P_1 and P_2 for $\varphi = 45°$. The broken curves connect points with the same values of n, the full curves connect points with equal χ. The numbers next to the curves are the values of n and χ.

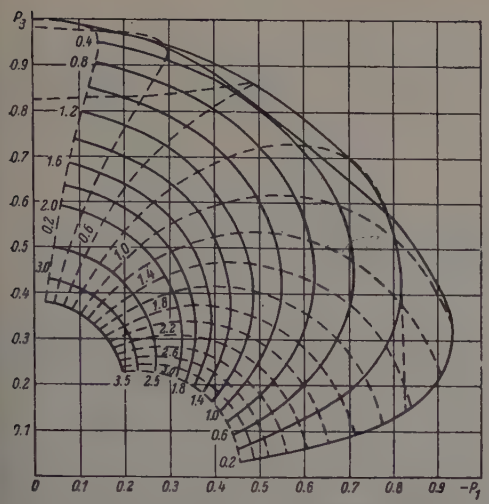

Fig. 3. Nomogram for the determination of n and χ from measurements of the values of P_1 and P_3 for $\varphi_2 = 45°$.

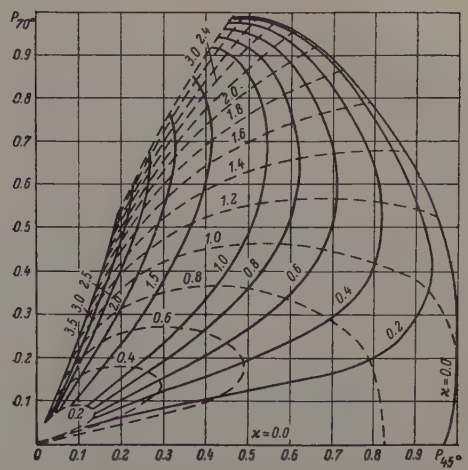

Fig. 4. Nomogram for the determination of n and χ from measurements of the values of P_1 for $\varphi_1 = 70°$ and $\varphi_2 = 45°$.

Figure 4 represents a diagram for the determination of the optical constants from the measurements of P_1 for two different angles of incidence ($\varphi_1 = 70°$ and $\varphi_2 = 45°$). If we choose the plane of reference in such a way that it coincides with the plane of incidence, then $P_1 = (I_p - I_s)/(I_p + I_s)$. From this it is seen that the last variation is a practical application of polarization measurements at two different angles of incidence. It can be successfully applied when the values of the absorption are not very large.

In conclusion I would like to express my gratitude to B. I. Stepanov for his interest in this work and his valuable advice.

REFERENCES

1. J. R. Beattie, Phil. Mag. **46** 235 (1955).
2. N. G. Bakhshiev, Opt. i Spektr. **2**, 818 (1957).
3. M. M. Noskov and B. A. Charikov, Opt. i Spektr. **1**, 1007 (1956).
4. I. N. Shklyarevskii and V. K. Miloslavskii, Opt. i Spektr. **3**, 361 (1957).
5. G. P. Motulevich and A. A. Shubin, Opt. i Spektr. **2**, 633 (1957).
6. D. G. Avery, Proc. Phys. Soc. (London). **B65**, 425 (1952).
7. L. A. Afanas'eva, M. M. Noskov, and V. I. Cherepanov, Fiz. Metal. i Metalloved. **1**, 566 (1955).
8. A. P. Prishivalko, Inzh.-Fiz. Zhur. **3**, 83 (1960).
9. J. R. Beattie and G. K. T. Conn, Phil. Mag. **46**, 222 (1955).
10. V. G. Rozenberg, Uspekhi Fiz. Nauk **56**, 77 (1955).
11. I. V. Grebenshchikov, A. G. Vlasov, B. S. Neporent, and N. V. Suikovskaya, "Prosvetlenie optiki" (Shedding Light on Optics). Gosudarst. Izd. Tekh.-Teoret. Lit., 1946.

AMPLITUDE AND PHASE CHARACTERISTICS OF AN INTERFERENCE LIGHT MODULATOR

I. I. Adrianova, Yu. V. Popov and A. V. Lapina

Received 8 January 1960

The results of a theoretical and experimental study of modulation of light flux with an interference modulator are described. A good agreement of the experimental and theoretical amplitude characteristics was obtained. The phase characteristics of the interference modulator were more uniform than in other types of modulators.

An interference light modulator based on the principle of a Michelson interferometer has advantages over the more common high frequency Kerr cell and diffraction modulators. The above-mentioned modulator is characterized by small light losses (not more than 45%), large numerical aperture, and economy.[1-3] The special feature of the interference modulator is the possibility of working at the fundamental and the harmonics of a strictly fixed frequency which is determined by the properties of a piezo-electric mirror (its resonance frequency).

A schematic drawing of the interference modulator is shown in Fig. 1. One of the interferometer mirrors Q is made out of a piezo-electric crystal plate. When this mirror is made to vibrate, the interference pattern changes and the light leaving the interferometer is modulated. The instantaneous value of the light intensity I leaving the interferometer (not taking into account the absorption within it) is given by the expression:[4]

$$I = \frac{I_0}{2}\{1 + \cos(2kz_0)\,J_0(2kZ) + 2\sin(2kz_0)\,J_1(2kZ)\sin(\Omega t + \varphi) + 2\cos(2kz_0)\,J_2(2kZ)\sin 2(\Omega t + \varphi) + \ldots\}, \quad (1)$$

where I_0 is the light intensity entering the interferometer, J_0, J_1, J_2 are Bessel functions of the zero, first, second order etc., $2kz_0$ is the initial phase difference, Z is the amplitude of vibration of the piezo-electric mirror in the direction perpendicular to its plane, Ω is the angular frequency of vibration of the piezo-electric mirror, and $k = 2\pi/\lambda$ (λ is the wavelength of light).

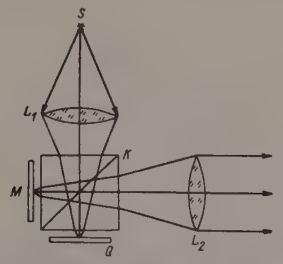

Fig. 1. Schematic drawing of interferometric light modulator. S—light source; L_1, L_2—lenses; M—mirror; Q—piezo-electric crystal plate; K—beam-splitting cube.

From this it follows that the light modulation takes place according to a complicated law and that the expression for the intensity contains a constant component, a primary-frequency component, and components of higher harmonics.

For strictly monochromatic light and initial adjustments such that

$$2kz_0 = (2n+1)\frac{\pi}{2} \qquad (n = 0, 1, 2\ldots), \quad (2)$$

corresponding to a light intensity equal to half the maximum value, the modulation takes place with a frequency equal to the frequency of vibration of the piezo-electric mirror, with the addition of odd harmonics.

When the initial adjustments are such that

$$2kz_0 = n\pi \qquad (n = 0, 1, 2\ldots),$$

which corresponds to an adjustment for maximum or minimum intensity of the light passing through the interferometer, the modulation takes place with double the frequency of vibration of the piezo-electric mirror, with the addition of higher even harmonics.

The amplitudes of the individual harmonic components depend on the initial adjustment z_0 of the interferometer as well as on the amplitude of vibration Z of the mirror. For some specific values of z_0 and Z the amplitudes of the individual harmonics can be made equal to zero. When the amplitudes are changed, the phases of the individual harmonic components do not change smoothly; when the amplitude passes through a zero value the phase changes abruptly by 180°.

The experimental harmonic analysis of the light modulated by an interference modulator, which had a piezo-electric mirror made out of a tourmaline plate with a resonance frequency of 5 Mc, was carried out with the aid of an FEU-19 photomultiplier and a four-channel resonance amplifier, the frequencies of the channels being 5, 10, 15, and 20 Mc. The measurements were carried out for different initial adjustments of the interferometer and constant amplitude of vibration of the piezo-electric mirror, as well as for different amplitudes of vibration of the piezo-electric mirror and constant initial adjustments of the interferometer. As the amplitudes of vibration of the piezo-electric mirror are determined by the magnitude of the high frequency voltage applied to the mirror, and as for small amplitudes this dependence can be assumed to be linear to a first approximation, the amplitude of vibration was not determined directly during the experiment and only the magnitude of the voltage applied to the piezo-electric mirror was measured.

The experimental and theoretical dependence of the amplitudes of the first, second, and third harmonics of the signal on the initial adjustment of the interferometer is shown in Fig. 2. The initial location of the reflecting surface of the piezo-electric mirror is plotted along the abscissa, the zero location being that for which the intensity of the light in the absence of vibrations has a minimum value (n = 1 in formula (3)). Along the ordinate axis are plotted the magnitudes of the harmonic components expressed as a percentage of the maximum value of the first harmonic, the latter being obtained when the interferometer is initially adjusted in the absence of vibrations for the mean value of the light leaving the interferometer (n = 0 in formula (2)). It is readily seen that the maximum value of the amplitude of the second harmonic in the total modulated light has a magnitude of the order of 35% of the maximum value of the amplitude of

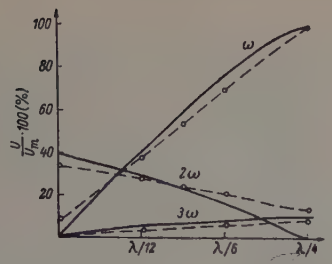

Fig. 2. The magnitudes of the signals of the first, second, and third harmonics expressed as a function of the initial adjustment of the interferometer. The full lines represent the theory; the broken lines represent experimental results.

the first harmonic when the voltage applied to the piezo-electric mirror is such as to yield the maximum value of the first harmonic. In this case the content of the third harmonic does not exceed 7%. In these as in all further measurements the presence of the fourth harmonic could not be detected.

During the study of the harmonic composition of the modulated light as a function of the amplitude of vibration of the piezo-electric mirror, the initial adjustment remained unchanged and the voltage applied to the piezo-electric mirror was varied from zero to the maximum permitted value for which a breakup of the crystal did not occur.

Theoretical and experimental curves are shown in Fig. 3 which correspond to an initial adjustment of the interferometer for the mean intensity of light for the first and third harmonics, and to an adjustment for minimum light intensity for the second harmonic, these adjustments corresponding to maximum signals of the first and second harmonics respectively. The magnitudes of the signals of the corresponding harmonics, expressed as a percentage of the maximum value of the signal of the first harmonic for an initial adjustment of the interferometer for mean light intensity, are plotted along the ordinate axis in Fig. 3. Along the abscissa are plotted, for the experimental curves, the values of the voltage applied to the piezo-electric mirror (expressed in volts) and, for the theoretical curves, the argument of the Bessel function 2kZ from formula (1). The scale used for the voltage applied to the piezo-electric mirror was chosen in such a way as to make the positions of the maxima of the theoretical and experimental curves for

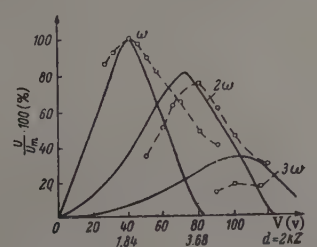

Fig. 3. The magnitudes of the signals of the first and third harmonic for an initial adjustment of the interferometer for mean intensity of the light, and of the second harmonic for an initial adjustment of the interferometer for minimum light intensity, expressed as a function of the voltage applied to the piezo-electric mirror. The full lines represent the theory, the broken lines represent experimental values.

the first harmonic coincide on the abscissa axis.

From a comparison of the results of the calculation and the experiment it is seen that the theoretical treatment of the modulation of light by the interferometer gives a good description of the nature of the phenomenon. The small deviation of the experimental curves from the theoretical values should apparently be explained by the insufficient monochromaticity of the light source and the nonlinear dependence of the amplitude of vibration of the piezo-electric mirror on the magnitude of the exciting voltage. The fact is verified that to obtain a maximum value of the amplitude of the second harmonic in the modulated light a voltage is necessary which is approximately twice as high as that needed for the maximum value of the amplitude of the first harmonic, the adjustments of the interferometer being optimum in the respective cases. The maximum value of the amplitude of the second harmonic is then 80% of that of the first harmonic.

The expression "phase characteristics of the modulator" is applied to the distribution of the phase of modulation along the cross section of the modulated light beam. A study of the phase characteristics was carried out with the aid of the phase-measuring system of a geodesic light rangefinder.[3] This method enables phase angles to be measured with an accuracy of ±1°. All measurements of the phase characteristics were carried out for the second harmonic because the examination of the surface of the oscillating piezo-electric mirror is carried out most conveniently when the interferometer is adjusted for minimum light intensity.

It is well-known that piezo-electric plates vibrate not over the whole surface in the manner of a piston, but in separate zones, and consequently it is rational to divide the study of the phase characteristics of the interference modulator into two stages: an investigation of the distribution of the phase of modulation along the cross section of the light beam obtained from an individual zone of vibration, and subsequently the comparison of the phases of modulation of light beams modulated by different zones.

The experimentally measured distribution of the phase of modulation along the cross section of the light beam is shown in Fig. 4. The experimental points are plotted along the abscissa, and the deviations of the phase of modulation from the mean value are plotted along the ordinate axis. The different curves correspond to different zones of vibration. From the given results it follows that within the limits of accuracy of the experiment (not less than ±2°) the light is modulated with the same phase by different zones of the piezo-electric mirror. Hence all points on the surface of the piezo-electric plate vibrate strictly in phase or in antiphase and differ from

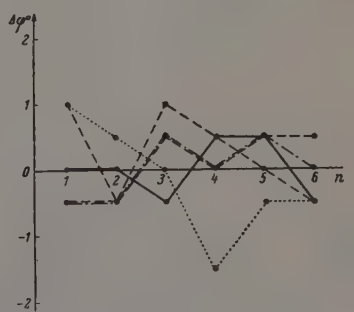

Fig. 4. The distribution of the phase of modulation along the cross section of a light beam modulated by different zones of the piezo-electric mirror in the interferometric light modulator.

one another only by the amplitude of vibration.

It can be concluded from the above investigation that the phase of the modulation of light from an interferometric modulator retains a practically constant value along the cross section of a beam of light obtained by reflection from one vibration zone of the piezo-electric mirror. This property of the interferometric modulator must be considered as an important advantage over the Kerr cell and diffraction modulators.

REFERENCES

1. A. A. Lebedev, V. V. Balakov and V. G. Vafiadi, Doklady Akad. Nauk SSSR 108, 458 (1956).
2. Yu. V. Popov, Kand. diss. Leningrad (Candidate's Dissertation, Leningrad State Univ.), 1955.
3. Yu. V. Popov, Izvest. Vysshikh Ucheb. Zavedenii, Geodez. i Aerofotos''emka (Reports of Higher Educational Institutions, Geodesy and Aerial Photograph No. 2, 57 (1957).
4. Yu. V. Popov and I. I. Adrianova, Izvest. Vysshikh Ucheb. Zavedenii, Geodez. i Aerofotos''emka No. 1, 49 (1959).

X-RAY MONOCHROMATOR FOR ULTRASOFT RADIATION WITH THE RECORDING OF THE ABSOLUTE NUMBER OF QUANTA

A. P. Lukirskii, M. A. Rumsh, and L. A. Smirnov

Received 26 January 1960

The construction of a diffraction-grating, vacuum, x-ray monochromator for the spectral region from 15 to 120 A is described. Methods of adjusting the monochromator and methods of obtaining electronic regulation of the monochromatic radiation are presented. A method for the absolute counting of the number of quanta with the aid of a Geiger counter is developed.

THE MONOCHROMATOR

The monochromator to be described is designed for the study of the efficiency of various radiation detectors. A focusing diffraction grating* is used as the dispersive element in the apparatus. The source of radiation is a demountable x-ray tube which makes it possible to obtain a series of characteristic lines without breaking the vacuum. A drawing of the monochromator is shown in Fig. 1,a. The entrance slit S_e is placed on the Rowland circle between the x-ray tube and the diffraction gratin and the diaphragm D is set near the grating. The mono chromatic radiation is selected by the detector slit S_d, behind which the radiation detector is located. The Gei ger counter is placed between the detector slit and the detector to be studied and with the aid of special acces sories can be removed from the beam without breaking the vacuum, thus allowing the radiation to fall on the other detector. The detector slit and the detectors are mounted on the platform P, which can be translated, without breaking the vacuum, in two mutually perpendic lar directions, thus making it possible to place the detector slit at different points of the Rowland circle. Th platform with the radiation detectors can be rotated about an axis coincident with the detector slit, also wit

*The grating, made in GOI (State Optical Institute) and ruled on glass, has 600 lines/mm and a radius of curvature of 1 meter. The grazing angle of incidence of rays on the grating is equal to 2.5°.

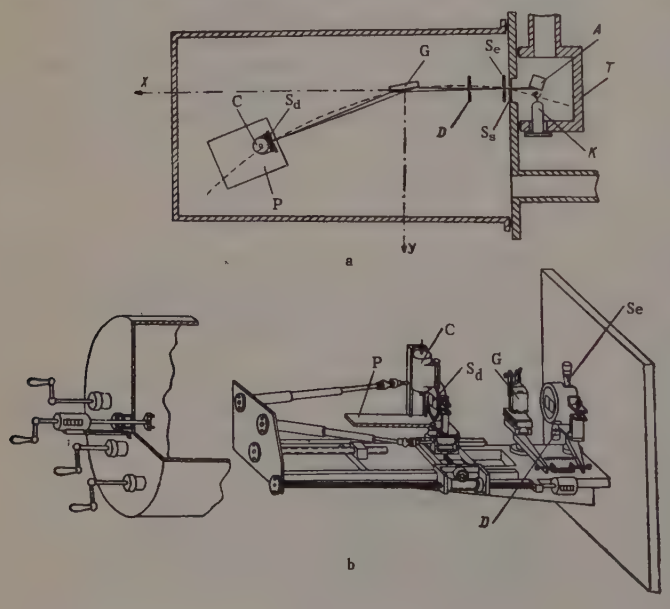

Fig. 1. Construction of the x-ray monochromator. S_e—entrance slit; D—diaphragm; G—grating; S_d—detector slit; C—Geiger counter; P—platform; S_s—separator slit; T—x-ray tube; A—anode; K—cathode.

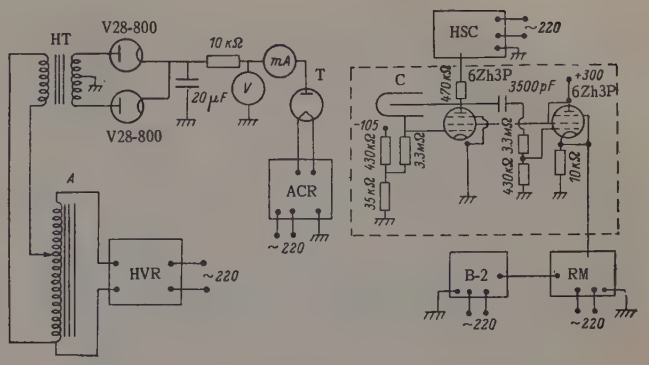

Fig. 2. Block diagram of the x-ray tube supply and Geiger counter recording circuit. HVR—high-voltage regulator; A—autotransformer; HT—high-voltage transformer; V28-800—kenotron; V—electrostatic kilovoltmeter; mA—milliammeter; T—x-ray tube; ACR—anode current regulator; C—Geiger counter; HSC—high-voltage supply for counter; RM—counting-rate meter; B-2—scaling circuit of a B-2 radiometer. The section within the dotted outline is located in the vacuum chamber of the monochromator.

out breaking the vacuum. Such motion is necessary to point the detectors toward the diffraction grating. The monochromator is enclosed in a vacuum chamber. Between the x-ray tube and the vacuum chamber of the monochromator is placed the separator slit S_s of area 5 mm², through which radiation from the tube passes into the monochromator. The volumes of the x-ray tube and the monochromator are pumped out by separate diffusion pumps, which are equipped with stainless steel oil baffles and liquid-oxygen traps. This pumping system permits vacuums of 5×10^{-7} and 2×10^{-5} mm Hg in the x-ray tube and monochromator chamber, respectively. Such a high vacuum in the x-ray tube is necessary to obtain characteristic lines in the ultrasoft radiation region that are stable in time. The vacuum chamber of the monochromator is connected with apparatus for filling the Geiger counter. Construction details of the monochromator are shown in Fig. 1,b.

X-RAY TUBE SUPPLY CIRCUIT AND RECORDING CIRCUIT

Circuits for electronic stabilization of the anode current of the x-ray tube and of the high voltage were used in order to stabilize the radiation intensity with time. A block diagram of the x-ray tube supply is presented in Fig. 2. Regulation of the anode current was carried out by means of a regulator analogous to the one in the URS-501 instrument[1] except that in our regulator the range of emission currents was considerably wider (from 20 μa to 150 ma). Regulation of the high voltage was accomplished using a magnetic-amplifier stabilizer which was controlled by the rectified voltage from a separate rectifier. This rectifier was fed by the same alternating potential as was the transformer of the high-voltage apparatus. The high-voltage regulator had a stabilization coefficient of about 30. The remaining parts of the supply circuit are seen in the block diagram.

The recording and supply circuit for the Geiger counter is also presented in Fig. 2. In order to obtain a good "plateau" a forced-quenching circuit of the Neher-Harper type[2] was used. Impulses from the quenching circuit proceeded to the counting-rate meter, in the first stage of which they changed sign, and then to the scaling circuit of a B-2 radiometer.

ADJUSTMENT OF MONOCHROMATOR

In adjusting the apparatus with the curved grating operating at grazing incidence it is necessary to establish strict parallelism between the entrance and detector slits and the rulings of the grating. Deviation of the slits from the required position in planes perpendicular to the direction of the beam is particularly inadmissable. The entrance slit, diffraction grating, and detector slit were mounted on cones, which were inserted in conical sockets. The conditions of manufacture were such that the axes of the conical sockets were strictly parallel to one another. All three cones were made to be interchangeable, and, in addition, a fourth socket was placed on the table of an autocollimator. The slits and the grating were mounted in turn in this socket. By clamping a small plane-parallel glass plate to the jaws of a slit (or by holding it between the jaws), parallelism of the slit and its axis of rotation was established. Precise setting of the distances between slits and grating (the distances between axes of the cones were precisely measured) was insured by coincidence of the slits with the axes of the conical bearings; this coincidence was set with the aid of a microscope. Each slit was placed in such a way that its position did not change as a result of rotation in its conical socket.

In the adjustment of the slits the autocollimator was set up such that its optic axis was perpendicular to the axis of rotation of the conical bearing. After this the adjustable stage with the grating was placed in the conical socket on the autocollimator. The diffraction grating was made so that its rulings were parallel to the boundary surfaces of the glass block. By fastening plane-parallel plates to these end surfaces and to the rule surface of the grating, strict parallelism was established between the rulings and the axis of rotation of the cone by means of the autocollimator. The remaining steps of the adjustment (coincidence of the ruled surface and the axis of rotation of the cone, setting of the necessary angle of incidence of rays on the grating, adjustment of the separator slit, and adjustment of the x-ray tube) were carried out in the monochromator with the use of a light beam.

In order to illustrate the operation of the monochromator, Fig. 3 presents the characteristic K-series lines of fluorine, oxygen, carbon, boron, and beryllium, which have wavelengths of 18.3, 23.6, 44, 67, and 113 A, respectively. These lines were obtained using LiF, MgO, aquadag, boron, and beryllium applied to the surface of the anode in the form of fine powder suspended in alcohol (with the exception of MgO, which was obtained by the combustion of Mg). The use of powders insures stability of the radiation with time because of the poor heat contact between the powder and the anode and the low heat conductivity, which leads to heating of the powder by the electron beam. Hot surfaces are coated to a considerably smaller degree with carbon which results from the decomposition of residual organic vapors (diffusion pump oil, etc.) in the electron beam.

The characteristic lines are obtained by measuring the intensity during translation of the counter along the y-coordinate for fixed values of the x-coordinate corresponding to calculated values for the wavelength at the "center of gravity" of the lines (see Fig. 1,a). As can

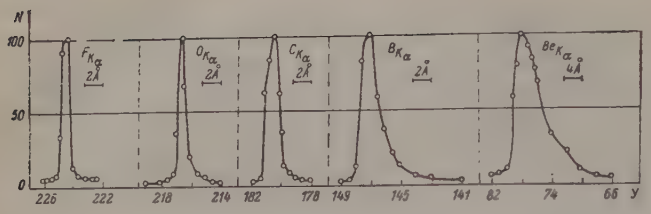

Fig. 3. Characteristic K-series lines of fluorine, oxygen, carbon, boron, and beryllium. N—intensity in relative units; y—translation of detector in y-direction (1 division equals 0.1 mm).

be seen from Fig. 3, the characteristic lines have background. The considerable excess in intensity of the lines over the magnitude of the background attests to the favorable operation of the grating and correct adjustment.

DETERMINATION OF THE ABSOLUTE NUMBER OF QUANTA IN THE MONOCHROMATIC BEAM

The use of the Geiger counter for recording ultrasoft x-radiation is known in the literature.[3,4] With special recording circuits it is possible to exclude the main deficiencies in the operation of counters which there are in the cited works and to use counters for absolute measurements of intensity. Two drawbacks which have been met in previously used counters are poor counting characteristics ("plateau"), which, moreover, shift with time along the voltage scale ("plateau drift"), and absorption in the "dead region" of the counter which cannot be taken into account.

In order to determine the absolute number of quanta with a counter it is necessary to satisfy the following conditions: (1) the counter must have a good "plateau" (i.e., a relatively small number of spurious counts); (2) there must be no "dead region;" (3) it is necessary to know the amount of absorption in the counter window, the absorption coefficient of the counter gas, and also the "dead time" of the counter is needed in order to introduce corrections for "missed counts."

The construction of the counter used by us is shown in Fig. 4. As can be seen from the diagram, the window 9 was glued over the slit in the frame 7. This frame was connected to the casing of the counter 1 through the rubber gasket 8. The possibility of removing the frame with the window made it easy to glue on the window and to determine its transmissivity. In order to do this the frame and window were mounted in the vertical slider of the monochromator in place of the Geiger counter and could then be moved into and out of the beam. Another radiation detector (e.g., photomultiplier of the Allen type[5]) was attached to the platform, and with it measurements were made of the transmissivity for the characteristic lines O_k, C_k, B_k, and Be_k. Results of the measurements are given in the Table.

Transmissivity of Window

Spectral line (A)	Transmissivity (%)
O_k (23.3)	88
C_k (44)	92
B_k (67)	80.5
Be_k (113)	55

A double sheet of celluloid with a total thickness of about 0.1μ was used as a window. This thin sheet is very weak, and even when glued on a slit of width 0.3 mm it can withstand a pressure difference of only about 150 mm Hg. Therefore we used a special gas filling system allowing the counter to be pumped out together with the monochromator chamber; also the air could be let into both simultaneously. The gas mixture was prepared in a separate tank, from which it was fed into the counter each time after pumping out the apparatus. In the operation of the counter its "plateau" shifted as a result of a cha in the composition of the gas. Forced circulation of the mixture was used to speed up the establishment of a "plateau." Experiment showed that forced circulation o the gas stabilizes the operation of the counter, practical eliminating "plateau drift" with time. The copper casin of the counter 1 has two hose connections 6 for filling a forced circulation. The diameter of the cylindrical bore of the casing equals 18 mm.

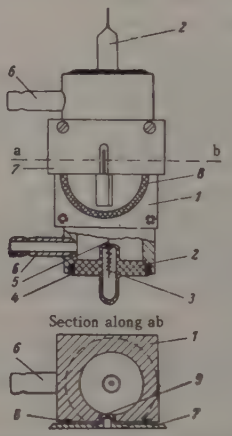

Fig. 4. Construction of Geiger counter. 1—casing (copper); 2—glass insulator; 3—spring; 4—picein; 5—tungsten wire (diameter 0.05 mm); 6—hose connections for filling; 7—frame; 8—rubber gasket; 9—celluloid window.

As the counter gas we used either a mixture of arg and methane (80% A and 20% CH_4) or a mixture of argon and absolute ethyl alcohol (90% A and 10% C_2H_5OH). The use of forced quenching provides an extension of the "plateau" to 250 volts with a slope of about 2% per 100 volts. Consequently, "spurious impulses" could be disregarded.

A study of counter efficiency was carried out by measuring the intensity for different gas pressures. Figure 5 gives curves of counting rate as a function of gas pressure (80% A and 20% CH_4) for K-radiation of Be, B, C, and O. From the graph it is evident that for pressures greater than 80 mm Hg all curves approach "saturation." This attests to the fact that under these conditions total absorption of radiation occurs within th gas of the counter. The absence of a falling off for high pressures indicates that there is no "dead region" in t counter. Extrapolation of the curves into the region of small pressures (anticipating a dependence according t the law $1 - e^{-kp}$, where p is the pressure and k the ab sorption coefficient) shows that the curves pass through the origin. This indicates that photoelectrons from the window have only a second-order role, which is in agre ment with a small absorption and, apparently, a low va of the photoelectric yield in the window. Therefore, the

photoeffect in the window was not taken into consideration. Thus in our case many phenomena (the effect of "spurious impulses," the effect of a "dead region") have been reduced to negligibly small quantities. The pressure in the counter is chosen such that practically total absorption of the radiation occurs within the gas. If under these conditions account is taken of absorption in the window and of "missed counts," then the reading of the counter will lead to the absolute number of quanta incident on the window.

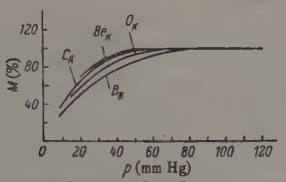

Fig. 5. Dependence of relative counting rate M of Geiger counter on gas pressure p for constant intensity of radiation.

Absorption in the window was determined experimentally.

Correction for "missed counts" was introduced using the equation[2]

$$N_i = \frac{N}{1 - \tau N},$$

where N_i is the actual counting rate, N the measured counting rate, and τ the "dead time." The "dead time" was determined experimentally by the method of two sources[6] (as sources we used two radioactive preparations of Co^{60}) and for our counter amounted to about 2.5×10^{-4} sec. It is evident that the maximum counting rate for such a counter is about 500 impulses/sec. For counting a larger number of quanta an attenuator consisting of a series of raster screens with about 30-μ mesh laid one on top of another was placed before the counter. Such an attenuator produces the same attenuation for all wavelengths. A special investigation of the dependence of the counting rate on the point of incidence of the beam in different parts of the attenuator showed that the attenuation was the same in different spots. Calibration of the attenuator was accomplished in the same way that the transmissivity of the counter window was determined. A selection of raster attenuators made it possible to increase the counting rate to 3×10^5 quanta of monochromatic radiation per second. The possible error in determining the absolute number of quanta is estimated to be no more than 10%.

In conclusion we wish to express our thanks to A. A. Lebedev for discussions and his interest in this work.

REFERENCES

1. I. B. Borovskii, "Fizicheskie Osnovy Rentgenospektral'nykh Issledovanii" (Physical Principles of X-ray Spectral Analysis). Izd. Moskovsk. Univ., Moscow, 1956.
2. S. Korff, "Schetchiki Elektronov i Yadernykh Chastits" (Electron and Nuclear Counters). Izd. Inostrannoi Lit., Moscow, 1947.
3. I. L. Rogers and F. C. Chalklin, Proc. Phys. Soc. (London) B67, 348, 412 (1954).
4. A. P. Lukirskii, Radiotekh. i Elektron. 2, 328 (1957).
5. E. R. Piore, G. G. Harvey, E. M. Gyorgy, and R. H. Kingston, Rev. Sci. Instr. 23, 8 (1952).
6. M. A. Blokhin, "Metody Rentgenospektral'nykh Issledovanii" (Methods of X-ray Spectral Analysis). Moscow, 1959.

MEASUREMENT OF THE PHOTOELECTRIC YIELD FOR ULTRASOFT X-RADIATION

A. P. Lukirskii, M. A. Rumsh, and L. A. Smirnov

Received 26 January 1960

A method for measuring the photoelectric yield for ultrasoft x-radiation is described. The method is based on a system devised for absolute counting of very small numbers of photoelectrons using an electron multiplier and for absolute counting of quanta using a Geiger counter. Results of measurement of the photoelectric yield for a series of metals and nonmetals are presented.

INTRODUCTION

Study of the photoelectric yield under the action of short wavelength ultraviolet light and ultrasoft x-radiation is of interest from the point of view of both theory and application. Some works[1,2] have indicated the possibility of using photomultipliers of the Allen type for the absolute measurement of intensity in these spectral regions.

The external photoeffect for short wavelength ultraviolet light has been investigated many times.[3-8] In the contiguous, ultrasoft x-ray region this problem has until now been discussed in only a few works.[9-12] In these works only the relative photoelectric efficiency of a series of metals for polychromatic radiation was determined. The lack of detailed quantitative studies of the photoelectric yield is explained by the experimental difficulties connected with (1) the necessity of either obtaining powerful monochromatic beams or else measuring very weak photocurrents, and (2) the determination of the absolute intensity of beams causing the photoemission. These difficulties are relatively easy to overcome when working in the short wavelength ultraviolet part of the spectrum since discharge in a capillary (Lyman source[13]) is sufficiently stable and provides the necessary intensity of the monochromatized beam to allow measurement of the photocurrent by the usual electrometric methods. In this case measurement of the absolute intensity is made using sensitive detectors which have been calibrated relative to an intense source of thermal radiation.

In this work a photomultiplier of the Allen type[1] operating in a system for counting separate photoelectrons was used for the measurement of the photocurrents. The possibility of counting separate electrons enabled us to use a special x-ray tube of relatively low power as a radiation source. We used the characteristic K-series

radiations of the elements oxygen, carbon, boron, and beryllium, which have wavelengths of 23.6, 44, 67, and 113 A, respectively.

A monochromator with a curved diffraction grating was used for monochromatization of the radiation. Measurements of the intensity of the monochromatic radiation were made with a specially constructed Geiger counter, for which the operating conditions that make it possible to determine the absolute number of quanta passing through the detector slit were found experimentally. The construction of the monochromator* made the following operations possible without breaking the vacuum: isolation of different monochromatic lines by the detector slit; placing of either the Geiger counter or the photomultiplier behind the detector slit; and small shifts of the counter or photomultiplier relative to the selected monochromatic beam.

*The construction and operation of the monochromator and also the technique of measuring the absolute number of quanta are described in the preceding article.

The x-ray tube supplies (i.e., high-voltage and filament supplies) were regulated by special electronic stabilizers, which in combination with the high vacuum in the x-ray tube (5×10^{-7} mm Hg) kept the monochromatic radiation sufficiently constant during the measurement time. The width of the monochromator slit was chosen such that the isolated spectral interval amounted to 1 A.

MEASUREMENT OF THE PHOTOCURRENT

An Allen-type multiplier was used to record the photoelectrons. These multipliers possess a comparatively stable amplification factor, very low background, and also permit air to be let into the apparatus. Electron multipliers with dynodes of a Cu-Be alloy[14] were used in this work.

The photocathode was mounted in the first dynode in such a way that it practically duplicated the form of the plane middle part of the dynode. The angle of incidence of the beam on the photocathode was equal to about 60°.

The power supply and recording circuits are shown in Fig. 1. Voltage was supplied to the dynodes through a divider which was connected to a source of regulated voltage, the magnitude of which could be varied between 4100 and 5400 volts

The first resistor of the voltage divider was variable and was placed outside the monochromator so that the voltage between the photocathode and the second dynode could be varied. From the collector of the photomultiplier an impulse passed to a preamplifier, which was placed in the vacuum chamber of the monochromator in the immediate vicinity of the multiplier. The preamplifier consisted of a single stage amplifier and cathode follower. The gain of the preamplifier was equal to 6 for impulses no shorter than 5 μsec. In addition, the preamplifier produced an approximately 4-5 μsec lengthening of impulses arriving from the multiplier. This lengthening was necessary for triggering of the scaling circuit. From the preamplifier an impulse was fed to a wide-band, two-stage amplifier with variable gain (from 0.5 to 50), after which it proceeded to a B-2-radiometer scaling circuit. The "threshold of operation" of the recording apparatus for 5-μsec rectangular impulses fed into the preamplifier and for maximum gain of the wide-band amplifier was equal to 2 mv.

A multiplier with the above described recording circuit registers all photoelectrons under the conditions that (1) all impulses of the multiplier are greater than the "threshold of operation" of the circuit, and (2) all

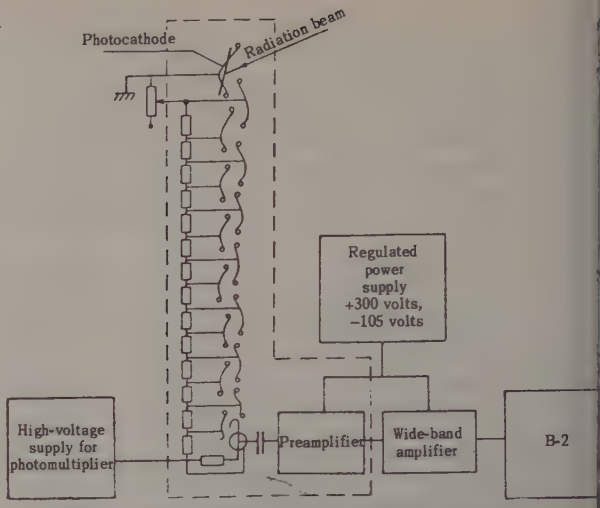

Fig. 1. Block diagram of recording circuit using electron multiplier (part in dotted outline is located within the vacuum chamber of the monochromator).

photoelectrons fall on the second dynode of the multiplie In order to find the conditions under which these requir ments are fulfilled the following dependences were investigated:

1. The dependence of the number N of registered impulses on the gain G of the wide-band amplifier was studied for a sufficiently large voltage between the phot cathode and the second dynode for x-rays incident on th middle of the photocathode. This dependence is present in Fig. 2. From the graph it is seen that beginning with certain value G_0 of the gain, the number of registered i pulses ceases to increase (saturation), which verifies t practically all impulses are being counted. Thus, for $G > G_0$ practically all impulses are recorded by the described apparatus.

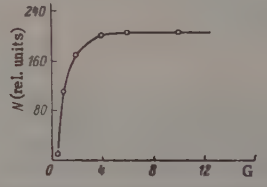

Fig. 2. Dependence of the number of impulses registered by the multiplier on the gain of the wide-band amplifier.

2. The dependence of the number N of registered impulses on the voltage U applied between the photocathode and the second dynode was studied for values o $G > G_0$ and for rays incident on the middle of the photo cathode. This dependence was investigated with regard to different wavelengths and for all photocathodes. Figu 3 presents curves corresponding to a Ni photocathode f the extreme wavelengths K_α of O (λ = 23 A) and K_α of Be (λ = 113 A).* From the graphs it can be seen that be

*According to the data of Rudberg,[15] 80% of the photoelectrons arising under the action of carbon K-radiatio have energies of 20-30 ev. Such an energy distribution of photoelectrons explains the shape of the curves of Fi 3, which exhibit a sharp rise as the magnitude of U approaches a value that insures the collection of photoele trons at the second dynode.

inning with $U = U_0 = 240$ volts, all photoelectrons fall n the second dynode and lead to the appearance of photo- urrent impulses. In order to make more precise the

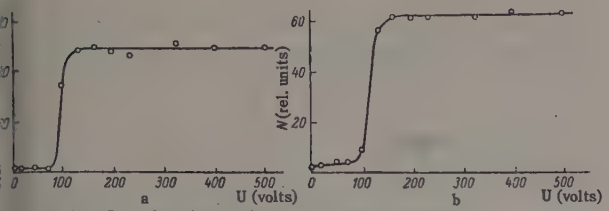

Fig. 3. The dependence of the number of electrons registered by the multiplier on the magnitude of the voltage between the photocathode and the second dynode. a—for Be K-radiation; b—for O K-radiation.

onditions under which all photoelectrons are collected t the second dynode, the dependence of the number of mpulses N on the point of incidence of rays on the photo- athode was studied. This dependence is presented in ig. 4. From the graph it can be seen that there are re- ions on the photocathode, considerably larger than the idth of the x-ray beam, from which photoelectrons are mpletely collected by the second dynode. Thus, if the ain of the wide-band amplifier $G > G_0$, the voltage be- ween cathode and second dynode $U > U_0$, and the beam alls at a spot on the photocathode corresponding to the iddle of the horizontal part of the curve in Fig. 4, then ll electrons will be registered. Possible sources of er- or may be "miscounts," which depend on the finite ength of the impulses, and the natural background of the ultiplier. If, however, counting rates of less than 1000 mpulses/sec are used, then for impulses 10^{-5} sec long issed counts amount to a fraction of a percent. The na- ural background of the multiplier, although negligibly small, can easily be measured and taken into account in he final results.

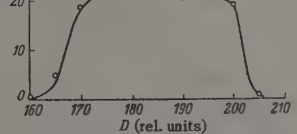

Fig. 4. Dependence of the number of registered electrons N on the point D of incidence of the monochromatic beam on the photocathode. One division corresponds to a translation along the cathode of 0.18 mm; the width of the beam is no more than 1 mm.

Thus, in general, the number of registered impulses equals the number of photoelectrons if we neglect the probability of the appearance of two electrons as a result of the action of a single quantum.

MEASUREMENT OF THE PHOTOELECTRIC YIELD

In the light of the above, measurement of the photoelectric yield in our case amounted to counting with the multiplier the number of photoelectrons arising each second and determining the intensity of the x-ray beam in number of quanta per second using the Geiger counter. Since measurements of photoemission and x-ray intensity were conducted successively in time, they were repeated many times, and average values were used in the calculation of the photoelectric yield. The ratio of the number of impulses recorded by the multiplier in some interval of time to the number of quanta incident on the photocathode for the same interval was taken as the magnitude of the photoelectric yield. The value thus obtained represents the fraction of quanta leading to photoemission from the cathode. This quantity is equal to the photoelectric yield with a precision set by the probability of the appearance of several electrons under the action of a single quantum. For large photoelectric yields this probability is, apparently, considerably different from zero, and the actual value of the quantum yield may prove to be higher than the values determined by us.

Results of measurements for various photocathodes are presented in the Table. It should be noted that the metallic photocathodes which we used were not subjected to outgassing (their surfaces were cleaned with a fine abrasive). The nonmetallic photocathodes were made by vacuum evaporation on a nickel substrate.

Values of Photoelectric Yields of Various Cathodes (%)

Photocathode material	Wavelength of characteristic line (A)			
	O_k (23.6)	C_k (44)	B_k (67)	Be_k (113)
Be	0.7	1.1	2.35	2
Ni	2.1	2.3	3.7	4.9
W	3.6	4.0	2.2	0.94
LiF	—	6.0	17.0	61.0
NaF	3.2	12.5	26.0	85.0
CaF_2	15.9	7.1	14.2	25.0
SrF_2	22.0	31.0	27.0	24.0
NaCl	13.5	19.5	13.5	27.0

We must also note that the results obtained should be considered as preliminary since, according to the data of ref. 15 for ultrasoft x-radiation and ref. 9 for short wavelength ultraviolet radiation, a strong dependence of the photoelectric yield on the degree of outgassing of the photocathode surface should be expected. It is very probable that for sputtered layers a dependence of the photoelectric yield on the thickness of the layer should also be observed.

In conclusion, we wish to express our gratitude to A. A. Lebedev for discussions and for his constant interest in this work.

REFERENCES

1. E. R. Piore, G. G. Harvey, E. M. Gyorgy, and R. H. Kingston, Rev. Sci. Instr. **23**, 8 (1952).
2. N. O. Chechik, S. M. Fainshtein, and T. M. Lifshits, "Elektronnye umnozhiteli" (Electron Multipliers). Gosudarst. Izd. Tekh.-Teoret. Lit., Moscow, 1957.
3. C. Kenty, Phys. Rev. **44**, 891 (1933).
4. R. Baker, J. Opt. Soc. Am. **28**, 55 (1938).
5. H. E. Hinteregger and K. Watanabe, J. Opt. Soc. Am. **43**, 604 (1953).
6. H. E. Hinteregger, Phys. Rev. **96**, 538 (1954).
7. N. Wainfan, W. C. Walker, and G. L. Weissler, J. Appl. Phys. **24**, 1318 (1953).
8. W. C. Walker, C. Wainfan, and G. L. Weissler, J. Appl. Phys. **26**, 1366 (1955).
9. L. Davies, Proc. Roy. Soc. **A119**, 543 (1928).
10. G. B. Bandopadhynyu, Proc. Roy. Soc. **A120**, 784 (1928).
11. S. R. Rao and K. S. S. Jyer, Proc. Indian Acad. Sci. **A13**, 411 (1941).
12. S. R. Rao and Ramsmurti, Current Sci. (India) **11**, No. 12 (1942).
13. T. Lyman, "The Spectroscopy of the Extreme Ultraviolet." London, 1928.
14. A. M. Tyutikov and A. I. Efremov, Doklady Akad. Nauk SSSR **118**, 286 (1958).
15. E. Rudberg, Proc. Roy. Soc. **A120**, 385 (1928).

THE CONNECTION BETWEEN F-BAND HALF-WIDTHS AND DEFECTS IN SOLID SOLUTIONS OF ALKALI HALIDE CRYSTALS

I. Ya. Melik-Gaikazyan and E. K. Zavadovskaya

Received 29 February 1960

The position and shape of F-bands generated by X-rays in certain solid solutions of alkali halides have been studied most fully by Gnaedinger and Miessner for the KCl-RbCl and KCl-KBr systems.[1,2] These authors found similar relationships between the position of the F-band maximum and the composition of the solid solution. They also showed that the half-width (γ) of the F-band is not an additive quantity. Its deviation from the additive value ($\Delta\gamma$) also depends on the composition of the solid solution.

An attempt is made in Gnaedinger's paper to ascertain the nature of isostructural F-bands, starting from well known characteristics of F-bands in pure crystals. According to his model for an F-center in a solid solution, F-bands in mixed crystals are complex and consist of seven "components."

To check the validity of the assumptions, the experimental values of the F-band half-width were compared with the calculated values. As shown in the Figure, there is a marked disparity between the theoretical and experimental values of γ.

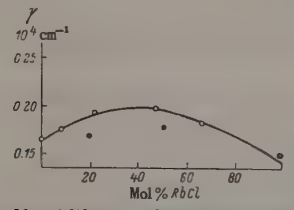

F-band half-width as a function of the composition of the KCl-RbCl solid solution (according to Gnaedinger's data[1]). Circles—experimental values of γ; dots—calculated theoretical values of γ.

We believe that the reason for this discrepancy is that the crystals used by Gnaedinger contain an appreciable number of Schottky defects; greater, in fact, than the equilibrium number of thermal defects. This fact is not taken into account in the theoretical calculations of γ. The problem of defects in single crystals is considered in a number of papers,[3-5] whose authors estimate the number of Schottky defects by comparing the x-ray and true densities of the sample. As a measure of imperfection, we can use the departure of n, the average number of particles per unit cell, from 8 (the value for an ideal crystal). Ufimtsev[6] noted that the degree of imperfection depends strongly on the stability of the solid solution. This, in turn, is determined by the ratio of the lattice energies U of the components of the solid solution. When the difference of lattice energies ΔU is small, the system is stable, and the imperfection of the mixed crystals is relatively small. When ΔU is appreciable, the solid solutions are characterized by weak bonding between constituent particles. This appreciably decreases the work of forming Schottky defects and results in a highly imperfect and unstable crystal. The presence of a large number of vacancies in an equimolar KCl-KBr solid solution is confirmed by the formation of pores after prolonged high temperature annealing of this crys

Data on the correspondence between ΔU, n, and γ values are given in the Table. The U data for the pure crystals KCl, KBr, NaCl, RbCl, and NaBr are computed from the formula of Kapustinskii.[8] The deviations $\Delta\gamma$ of the F-band half-width from the additive value are taken from Gnaedinger's[1] paper. The numbers for the equimolar composition of solid solutions for single crystals obtained by the Kiropoulos method were determined by M. S. Ivankina.[4]

The Relationship Between $\Delta\gamma$ (the Deviation from Additivity of the F-Band Half-Width) for Certain Solid Solutions,[1] ΔU (the Difference Between the Crystal Lattice Energies[8] of the Components of the Solid Solution), and Their Degree of Imperfection[4]

Composition of solid solution	ΔU kcal/mole	$\Delta\gamma$ (10^4 cm^{-1})	n	Stability of solution of molar compos
53% KCl — 47% RbCl	7.4	0.02	7.8	Stable
50% KCl — 50% KBr	7.9	0.02	7.7	"
17% NaCl — 83% NaBr	9.0	0.063	7.3	Unstable
90% KCl — 10% NaCl	20.5	0.08	—	Very unstab

Our theory of the effect of crystal imperfections on the F-band half-widths is also confirmed by the following: For the systems of solid solutions investigated, th maximum deviation $\Delta\gamma$ and the maximum degree of im perfection occur for the same composition of the solid solution. Thus it is known that the maximum degree of imperfection in the KCl-RbCl system occurs[5] at the composition 60% KCl-40% RbCl. According to Gnaedinger's data, this composition also shows the maximu value of $\Delta\gamma$. For KCl-KBr crystals, the maximum of $\Delta\gamma$ occurs at the composition 75% KBr-25% KCl which, according to our data obtained for crystals grown from aqueous solution, show the greatest degree of imperfection.

The following fact, observed by Gnaedinger, is mos interesting: A solid solution of KBr-RbCl acquires muc less coloration under the action of x-rays than the pure KBr and RbCl crystals. This may be due to the fact tha the KBr-RbCl crystals have few defects, since for this system ΔU is only 0.5 kcal/mole. On the other hand, a mixed crystal usually shows a greater density of dislocations than a pure crystal. The latter may lead to a de crease in the rate of formation of F-centers. This assumption requires careful experimental verification.

REFERENCES

1. R. Gnaedinger, J. Chem. Phys. 21, 323 (1953).
2. G. Miessner, Z. Physik 134, 576 (1953).
3. N. Wallace and P. Flin, Nature 172, 4380, 681 (1953

4. M. S. Ivankina, Thesis, Tomsk, 1959.
5. L. L. Makarov, B. G. Lur'e, and V. N. Malyshev, Fiz. Tverkogo Tel 2, 1 (1960).
6. A. A. Vorob'ev, P. A. Savintsev, and B. F. Ufimtsev, Tez. dokl. na Konf. po dielectrikam i poluprovodnikam (Thesis Report at the Conference on Dielectrics and Semiconductors), Leningrad, 1960.
7. M. S. Ivankina, E. K. Zavadovskaya, and I. Ya. Melik-Gaikazyan, Fiz. Tverkogo Tel 2, 4 (1960).
8. G. M. Unzhakov, Doklady Akad. Nauk SSSR 90, 1, 63 (1953).

QUANTUM-MECHANICAL TREATMENT OF THE NONLINEARITY OF A MOLECULE

S. M. Yazykova

Received 29 February 1960

In most of the works which have appeared in recent years on the refinement of the metallic model of the molecule, the nonequivalence of the single and multiple bonds in conjugated molecules and the interaction of the electrons of the molecule have largely been taken into account. However, a very important property of a large class of organic compounds—the nonlinearity of the molecules—has not been taken into account in the quantum-mechanical calculations. A method of treating the nonlinearity of a molecule is set forth below, using the butadiene molecule as an example.

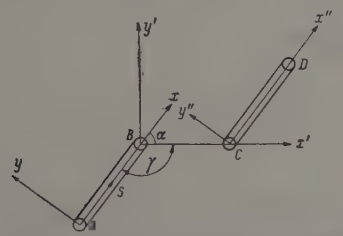

Sketch of the butadiene molecule. AB = CD = b = 3.35 atomic units; BC = l = 2.76 atomic units; $\angle ABC = \gamma = 124°$.

Let us consider the Schrödinger equation in the following form:

$$\frac{d^2\psi}{ds^2} + 2(E-U)\psi = 0, \tag{1}$$

s is the coordinate along the molecule (see figure), and the potential energy is given as follows:*

*All computations are carried out in atomic units.

$$\begin{aligned} U &= 0 \quad \text{for} \quad \left.\begin{matrix} 0 \leqslant s \leqslant b \\ l+b \leqslant s \leqslant 2b+l, \end{matrix}\right\} \\ U &= U_0 \quad \text{for} \quad b \leqslant s \leqslant b+l. \end{aligned} \tag{2}$$

Instead of solving Eq. (1) with a potential of the form (2), let us take advantage of the familiar solution of Eq. (1) for the separate segments AB, BC, and CD, after we have associated with each of these segments its own coordinate system: xy, x'y', x''y''.

$$\left.\begin{aligned} \psi_1 &= A_1 e^{ikx} + B_1 e^{-ikx}, \quad 0 \leqslant x \leqslant b; \\ \psi_2 &= A_2 e^{i\beta x'} + B_2 e^{-i\beta x'}, \quad b \leqslant x' \leqslant b+l; \\ \psi_3 &= A_3 e^{i\alpha x''} + B_3 e^{-i\alpha x''}, \quad b+l \leqslant x'' \leqslant 2b+l. \end{aligned}\right\} \tag{3}$$

By rotation and parallel translation of the coordinate axes, we reduce the systems x'y' and x''y'' to the system xy:

$$\begin{aligned} x' &= -x\cos\gamma - y\sin\gamma - b, \\ y' &= x - (b - l\cos\gamma). \end{aligned} \tag{4}$$

Taking account, furthermore, of the equation

$$y = \tan\gamma\,(x-b),$$

for the segment BC, we obtain a set of equations:

$$\left.\begin{aligned} \psi_1 &= A_1 e^{ikx} + B_1 e^{-ikx}, \\ \psi_2 &= A_2 e^{-i\beta[x\cos\gamma + \tan\gamma\cdot\sin\gamma(x-b)+b]} \\ &\quad + B_2 e^{i\beta[x\cos\gamma+\tan\gamma\cdot\sin\gamma(x-b)+b]} \end{aligned}\right\}, \; b \leqslant x \leqslant b - l\cos\gamma,$$

$$\psi_3 = A_3 e^{i\alpha(x-b+l\cos\gamma)} + B_3 e^{-i\alpha(x-b+l\cos\gamma)}, \tag{5}$$

$$b - l\cos\gamma \leqslant x \leqslant 2b - l\cos\gamma.$$

By matching the eigenfunctions and their derivatives with respect to x at points B and C, and making use of the boundary and symmetry conditions, we obtain a set of three algebraic equations. From the requirement that the set of these equations be compatible, we obtain, for states which are even with respect to the inversion operations, a transcendental equation for the determination of the energy levels:

$$\frac{\beta}{\alpha}\tan\alpha b + \cos\gamma\cdot\cot\frac{\beta l}{2} = 0. \tag{6}$$

Analogously, for odd states, we obtain the transcendental equation

$$\frac{\beta}{\alpha}\tan\alpha b - \cos\gamma\cdot\tan\frac{\beta l}{2} = 0. \tag{7}$$

Here

$$\alpha = \sqrt{2E}, \quad \beta = \sqrt{2(E-U_0)}.$$

In the limiting case where $\gamma = \pi$, we obtain the familiar transcendental equation of the linear model,[1,2] and for $\alpha = \beta$ we obtain the equation of the linear model without energy barrier.

Let us find the frequency of the long-wavelength transition ν_{23} of the butadiene molecule, considering the energy levels according to formulas (6) and (7). For the quantitative calculation, we shall make use at first of the parameters of the linear model as proposed by Veselov and Rekasheva:[1,2]

$u_0 = 0.04$ atomic units; L = 2b + l = 10.77 atomic units, where l is the length of a single bond, which is known to equal 2.76 atomic units; $b = l_1 + r_0/2$; $l_1 = 2.55$ atomic units, the length of a double bond; $r_0 = 2.910$, the homeopolar radius of hydrogen. The calculation performed gives, according to (6) and (7), $\nu_{23} = 33{,}300$ cm^{-1}; for the linear model, according to refs. 1 and 2, $\nu_{23} = 48{,}900$ cm^{-1}; the experimental value of $\nu_{23} = 47{,}700$ cm^{-1}.

According to a principle generally accepted in the

metallic model,[3] the size of the potential box—its width, L—is selected with the aim of making the calculated frequency of the long-wavelength transition coincide with the experimental. In our case, such a calculation gives L = 9.46 atomic units, which we represent in the form

$$L = 2b + l = (2 \cdot 3.35 + 2.76) \text{ atomic units}$$

To obtain the analytical form of the eigenfunctions, we make use of the symmetry conditions. Then all the coefficients may be expressed in terms of A_1.

We have:

$$\Psi^{(+)} = A^* \begin{cases} \sin \alpha x, & 0 \leqslant x \leqslant b \\ \dfrac{\sin \alpha b}{\cos \dfrac{\beta l}{2}} \cdot \cos\left[\dfrac{\beta (x-b)}{\cos \gamma} + \dfrac{\beta l}{2}\right], & b \leqslant x \leqslant b - l\cos\gamma. \\ \sin[\alpha (L_x - x)], & b - l\cos\gamma \leqslant x \leqslant 2b - l\cos\gamma. \end{cases} \quad (8)$$

$$\Psi^{(-)} = A^* \begin{cases} \sin \alpha x, & 0 \leqslant x \leqslant b \\ \dfrac{\sin \alpha b}{\sin \dfrac{\beta l}{2}} \cdot \sin\left[\dfrac{\beta (x-b)}{\cos \gamma} + \dfrac{\beta l}{2}\right], & b \leqslant x \leqslant b - l\cos\gamma \\ -\sin[\alpha (L_x - x)], & b - l\cos\gamma \leqslant x \leqslant 2b - l\cos\gamma, \end{cases} \quad (9)$$

$$A^* = 2iA_1, \quad L_x = 2b - l\cos\gamma,$$

where $\Psi^{(+)}$ are the functions of the even states of butadiene and $\Psi^{(-)}$ those of the odd states. In the limiting case where $\gamma = \pi$, $\Psi^{(+)}$ and $\Psi^{(-)}$ coincide with the corresponding expressions of the linear model.[1,2] With the help of the eigenfunctions (8) and (9), the oscillator strengths have been calculated for the long-wavelength transition $\Psi_2^{(-)} \rightarrow \Psi_3^{(+)}$. The calculation with L = 9.46 atomic units gives the too-large value f = 1.1 (according to the linear model, f = 0.98; according to Mulliken, f = 1.29)[4] in place of the experimental f = 0.53. The proposed method for treating the nonlinearity of molecules may be used in calculating any nonlinear molecules within the framework of the metallic model.

REFERENCES

1. M. G. Veselov and T. N. Rekasheva, Izvest. Akad. Nauk SSSR, Ser. Fiz. 18, 711 (1954).
2. T. N. Rekasheva, Kand. diss. (Thesis), Leningrad State Univ., 1953.
3. N. Bayliss, Australian J. Sci. Research 3A, 109 (1950).
4. R. S. Mulliken and C. A Rieke, Repts. Progr. in Phy 8, 231 (1941).

THE AGING OF ZnS PHOSPHORS

I. K. Vereshchagin

Received 21 March 1960

As noted by Riel[1,2] and Rusanova,[3] the prolonged storage of phosphors causes changes in the intensity and color of their photoluminescence. The results given below were obtained by comparing electroluminescent and photoluminescent spectra measured immediately after the phosphors were prepared and after storage in air for 1 to 3 years.

The powdered ZnS and Zn,CdS phosphors which we investigated were prepared in open and closed crucibles in air at 500-1000°C, and contained Ag and a large amount of Cu. After storage, most of the samples exhibited a marked enhancement of the short wavelength band in the photoluminescent spectra. This band is present in both nonactivated and Ag-activated phosphors. The luminescence band connected with the presence of copper is either weakened or keeps its original intensity, while the electroluminescent spectrum remains practically unchanged. In the course of storage, the photoluminescent spectrum gradually approached the electroluminescent one.

It has been found that these changes are eliminated by baking the phosphors in air for 20-30 min at a temperature above 200°C. The Figure shows typical cases of changes in the luminescent spectra of phosphors which were stored for a long period and were then baked. It is easily seen that the photoluminescent spectra obtained directly after the preparation of the sample practically coincide with those obtained after several years' storage followed by baking. The color of the powdered phosphors also changes. Immediately after being prepared, the samples were yellowish in color with a light gray tinge. They darken during storage, while the yellowness disappears. Baking at 220°C brings the phosphor powders back to their original color. Thus all of the effects of storage are fully reversible.

Since the changes observed in the spectra of the ph phors could have been due to surface effects, the sampl were etched with various acids (other than KCN) [sic] which to some extent would affect any possible surface compounds. However, the etching of old samples, or of

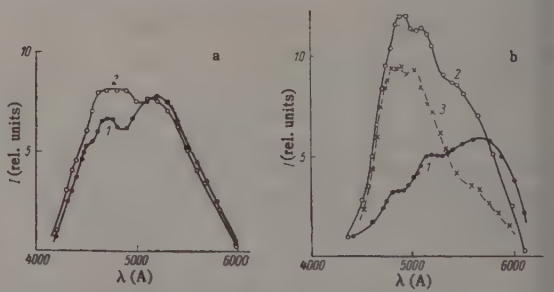

Luminescence spectra of two phosphors after preparation and after storage followed by baking. a—Zns:Ag:Cu (10^{-4} g atom Ag and 4×10^{-3} g atom Cu/gm ZnS), prepared at 950°C with NH_4Cl and NaCl, stored for 1 year. b—ZnS (90%), CdS (10%), Ag and Cu activated (10^{-4} g atom Ag and 10^{-3} g atom Cu/gm ZnS), prepared at 815°C with $BaCl_2$, stored for 3 years. Curve 1—photoluminescence after preparation and after baking (250°C, 25 minutes) at the end of storage; curve 2—photoluminescence at the end of the storage period; curve 3—electroluminescence of freshly prepared and baked samples: The spectra were obtained using a UM-2 monochromator and an FEU-19M photomultiplier.

those reconstituted by baking, did not modify their luminescence. The baking conditions were also varied. The samples were heated to 200-250°C in vacuo, under a layer of or mixed with a number of substances (ZnO, copper salts, S, and other). In all cases, baking the old sample gave the same results, while the luminescence of the sample already baked did not change. Hence these changes occur primarily throughout the volume of the crystals. This is also indicated by the coincidence of the spectra of x-ray-induced luminescence and photoluminescence of old and reconstituted samples, and by the insignificant changes in the electroluminescent spectra, whose properties, according to other observations, depend strongly on the state of the surface layers.

Although these low temperatures and short heat treatments were sufficient to restore the samples to their original condition, they could not have caused any appreciable diffusion of the activator within the crystals. The baking of ZnS:Ag moistened with a $Cu(NO_3)_2$ solution under the same conditions, which was done as a control experiment, did not result in any change of the photoluminescence or electroluminescence spectra. However, the latter increased several fold in brightness; i.e., the state of the crystal surfaces changed. The green copper band appeared only at 300°C and above, for heating periods of 45-60 min. Thus the changes occurring during storage must be ascribed to a change in constitution or structure within the crystals.

The processes described may be caused by a gradual disintegration of mixed ZnS and activator crystals.[3] It is difficult, however, to reconcile this idea with the low value of the baking temperature which is sufficient to restore the original properties of these phosphors. Riel assumes that one of the following may hold: in the course of time there is either a transition of Cu from one saturated state to another, accompanied by the appearance of blue radiation, or there is a diffusion of Cu to the surface of the crystals, prolonged storage being equivalent in its results to baking for several hours at 450°C.[2] In our case, however, baking results in the inverse process of restoration of the properties of the phosphor.

We can only make assumptions concerning the probable nature of the phenomena observed, since all processes are probably very complicated in phosphors which contain several activators, the remnants of fluxes, and a number of by products. The change in powder color during storage and baking may be connected with a variation in the amount of free sulfur in the phosphors. A similar yellow shade is characteristic of precipitated ZnS containing excess sulfur. In this case we can explain the gradual darkening of the powders by the formation of CuS or Ag_2S, which proceeds slowly at room temperature. The temperature of decomposition of CuS is 200-220°C, so that the baking treatment used would have been capable of destroying this compound and returning the phosphor to its initial state. It is assumed in several papers[4-6] that the blue band of nonactivated ZnS or of ZnS:Ag is connected with S vacancies. If this is the case, then a decrease in the amount of S in the lattice during aging will lead to the development of this band.

Furthermore, the formation of sulfides of activators changes the conditions of absorption of ultraviolet, while the phosphors studied show a dependence of the relative heights of the bands in the spectra on the intensity of excitation. The luminescence of ZnS:Cu, Ag becomes bluer with an increase in the intensity of photoexcitation or in the frequency of the electric field. This was also observed in refs. 2 and 7. We note that the presence of sulfur in the melt accentuates this effect.[2] The same effect apparently explains the fact that electroluminescence is usually bluer than photoluminescence. Identical brightness values for the electroluminescence and photoluminescence of the same sample correspond to different densities of excitation, since in the first case a much smaller crystal volume takes part in the luminescence.

Further study of these effects in general will at the same time help to ascertain the true nature of the aging processes of various classes of phosphors. This is also of immediate practical value.

REFERENCES

1. N. Riel, Ann. Phys. **24**, 536 (1935).
2. N. Riel and H. Ortman, Doklady Akad. Nauk SSSR **66**, 841 (1949).
3. A. I. Rusanova, Izvest. Akad. Nauk SSSR, Ser. Fiz. **15**, 754 (1951).
4. J. S. Prener and F. E. Williams, J. Chem. Phys. **25**, 361 (1956).
5. N. Riel and H. Ortman, J. phys. Radium **17**, 620 (1956).
6. W. Reichardt and G. Tappe, Z. Naturforsch. **13a**, 57 (1958).
7. I. Soudek, Ceskoslov. Fiz. Zhur. **8**, 336 (1958).

THE RELATIONSHIP BETWEEN ELECTRONIC-VIBRATIONAL ABSORPTION AND EMISSION BANDS

K. K. Rebane and O. I. Sil'd

Received 30 March 1960

Formulas relating absorption bands $\chi(\nu)$ to emission bands $I(\nu)$ now play an important part in the theoretical and experimental aspects of electronic-vibrational transitions in crystalline phosphors and complex molecules. Among these formulas are the mirror-symmetry law of Levshin[1] and Stepanov's[2] ratio (the relationship between $\chi(\nu)$ and $I(\nu)$ at the same frequency). The object of this note is to establish a relation analogous to the Levshin mirror symmetry law for the case of a luminescence center in a crystal (or molecule) whose vibration frequencies change as a result of an electronic transition. We shall apply the method of moments used by Lax.*[3]

*As far as we know, Kubarev[4] was the first to use the Lax method of moments in a study of the problem of mirror symmetry.

It follows from our new derivation of the formulas for the moments,[5,6] however, that the results are also applicable to bands which consist partially or entirely of lines. We start from the formulas in ref. 6.

Large Stokes losses are characteristic of luminescence centers in crystals. The shift of the spectral bands (the change of the first moment of the band S_1) with a change in temperature is of the order of kT. The principal change in bandwidth consists of a growth with temperature which is proportional to $\sqrt{T}$ (the second moment of the band $S_2 \sim T$). For such centers, the first moments of the absorption band taken relative to the electronic transition energy E have approximately the following form: (Terms of the higher order in kT/p^{χ} have been neglected.[6])

$$\left.\begin{aligned} S_0(E) &= 1, \\ S_1(E) &= p^{\chi} + \sum_i \frac{k\tau_{1i}}{2}\left(\frac{a'_{2i}}{a_{1i}} - 1\right), \\ S_2(E) &\cong (p^{\chi})^2 + \sum_i \frac{k\tau_{1i}}{2}\left[\frac{2}{a_{1i}}\left(\sum_k a'_{2ik}x'_{k0}\right)^2 + 2p^{\chi}\left(\frac{a'_{2i}}{a_{1i}} - 1\right)\right], \\ S_3(E) &\cong (p^{\chi})^3 \\ &+ 3p^{\chi}\sum_i \frac{k\tau_{1i}}{2}\left[\frac{2}{a_{1i}}\left(\sum_k a'_{2ik}x'_{k0}\right)^2 + p^{\chi}\left(\frac{a'_{2i}}{a_{1i}} - 1\right)\right]. \end{aligned}\right\} \quad (1)$$

We have introduced the following notations: The adiabatic potential of the electronic ground state is

$$U_I = \frac{1}{2}\sum_i a_{1i}x_{1i}^2;$$

and the adiabatic potential of the excited electronic state is

$$U_{II} = E + \frac{1}{2}\sum_{i,k} a'_{2ik}(x_{1i} - x'_{i0})(x_{1k} - x'_{k0});$$

where x_{1i} are the normal coordinates in the electronic ground state, the Stokes losses during absorption are

$$p^{\chi} = \frac{1}{2}\sum_{i,k} a'_{2ik}x'_{i0}x'_{k0}; \quad \tau_{1i} = \frac{\hbar\omega_{1i}}{2k\,\mathrm{th}(\hbar\omega_{1i}/2kT)};$$

ω_{1i} is the frequency of the i-th oscillator in the electronic ground state and T is the absolute temperature. At low temperatures ($kT \ll \hbar\omega_{1i}$) $\tau_{1i} = \hbar\omega_{1i}/2k$; at high temperatures ($kT \gg \hbar\omega_{1i}$) $\tau_{1i} = T$.

In terms of the coordinates x_{2i} (the normal coordinates in the excited electronic state) the adiabatic potentials have the form

$$U_I = \frac{1}{2}\sum_{i,k} a'_{1ik}(x_{2i} - x_{i0})(x_{2k} - x_{k0});$$

$$U_{II} = E + \frac{1}{2}\sum_i a_{2i}x_{2i}^2.$$

The coefficients a'_{1ik}, a_{2i}, and x_{i0} can be expressed in terms of a_{1i}, a'_{2ik}, and x'_{i0}. If we denote the matrices with the elements a_{1i}, a'_{1ik}, a_{2i}, a'_{2ik}, by A_1, A'_1, A_2, and A'_2, respectively, then the following relations will hold:

$$A'_1 = B^{-1}A_1B; \quad A_2 = B^{-1}A'_2B; \quad \|x'_{i0}\| = -B\|x_{i0}\|.$$

B is the transformation matrix which transforms the quadratic form

$$\sum_{i,k} a'_{2ik}(x_{1i} - x'_{i0})(x_{1k} - x'_{k0})$$

to the sum of squares

$$\sum_i a_{2i}x_{2i}^2,$$

if we change from the coordinates x_{1i} to the coordinates x_{2i}:

$$\|x_{1i} - x'_{i0}\| = B\|x_{2i}\|.$$

In order to obtain the moments of the emission band from Eq. (1), we must multiply the moments of odd order by −1, transpose the subscripts 1 and 2, and go from x'_{i0} to x_{i0}.

If a change in electronic state only results in a change in the frequencies and equilibrium positions of the normal vibrations, while the normal vibrations themselves are not "scrambled up," then $a'_{1i} = a_{1i}$ and $a'_{2i} = a_{2i}$ ($B = I$, where I is the unit matrix).

Equations (1), along with the rules for writing the corresponding formulas in the case of emission, in essence establish a connection between absorption and emission bands.

The first terms in Eqs. (1), which define the Stokes losses, are the basic ones. We may restrict ourselves to them in the zero order approximation, whereupon the relationship between the moments of the bands takes the exceptionally simple form:

$$\frac{S_1^{\chi}(E)}{S_1^{I}(E)} \cong -\frac{p^{\chi}}{p^{I}}; \quad \frac{S_2^{\chi}(E)}{S_2^{I}(E)} \cong \left(\frac{p^{\chi}}{p^{I}}\right)^2; \qquad \frac{S_3^{\chi}(E)}{S_3^{I}(E)} \cong -\left(\frac{p^{\chi}}{p^{I}}\right)^3,$$

where the superscripts χ and I refer to absorption and emission, respectively.

Several comments must be made with regard to an comparison of Eqs. (1) with experiment.

1. The formulas refer to the intensity distribution which are obtained when the experimental emission band is multiplied by ν^{-4} and the absorption band by ν^{-1}, where ν is the frequency of the light quantum. (Cf., for example, ref. 7.)

2. In general, the electronic energy E does not coincide with the abscissa of the intersection of band contours. It has to be determined separately, either as the minimum energy of absorption (the maximum energy of emission) at temperatures considerably below the Debye temperature, or from a joint consideration of several first moments (1).

3. The probabilities for transition between discrete vibrational levels 0—0 are the same for absorption and emission. However, the ordinates in continuous bands corresponding to 0—0 transitions are no longer equal. We shall explain this in terms of the example of a single oscillator and limiting low temperatures.

In this case the spacing between vibrational lines is $\hbar\omega_2$ in the absorption band and $\hbar\omega_1$ in the emission band (ω_1 and ω_2 are the vibration frequencies in the ground and excited electronic states, respectively). When we try to describe the probability distribution by means of a continuous function, we must take account of the difference in the densities of the vibrational lines and increase the ordinates of the absorption band by a factor of ω_1/ω_2. (See Figure.) In particular, the ordinates for the electronic energy E (0—0 transitions) of bands normalized in area to unity must be in the ratio of ω_1/ω_2. If we can determine this ratio from experiment, then we have determined the ratio of the vibration frequencies in the one-oscillator approximation.

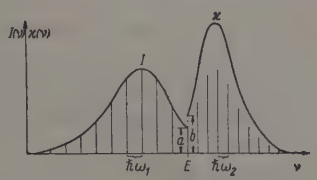

Diagram of absorption and emission bands of a one-oscillator model at extremely low temperatures ($\hbar\omega_2 \gg kT$). When passing from a discrete distribution of probabilities normalized to unity (the total length of the segments representing the probabilities in each of the bands is equal to unity) to continuous bands normalized in area to unity, we must multiply the ordinates of the absorption band by ω_1/ω_2 ($b/a = \omega_1/\omega_2$).

REFERENCES

1. V. L. Levshin, "Fotolyuminestsentsiya zhidkikh i tverdykh veshchestv" (Phosoluminescence of Liquid and Solid Substances), p. 96. Gosudarst. Izd. Tekh.-Teoret. Lit., Moscow, Leningrad, 1951.
2. B. I. Stepanov, Doklady Akad. Nauk SSSR 112, 839 (1957).
3. M. Lax, J. Chem. Phys. 20, 1752 (1952). (See translation (into Russian) in the collection, "Problemy fiziki poluprovodnikov" (Problems of Semiconductor Physics). Izd. Inostrannoi Lit., Moscow, 1957).
4. S. I. Kubarev, Report given at Eighth Conference on Luminescence, Minsk, 1959; Mater. VIII soveshch. po lyuminestsentsii (Proc. 8th Conf. Luminescence), Minsk, 1960.
5. K. K. Rebane, Opt. i Spektr. (in press) (1960).
6. K. K. Rebane and O. I. Sil'd, Izvest. Akad. Nauk Eston. SSR, Ser. Tekh. i Fiz.-Mat. Nauk (in press) (1960).
7. L. P. Kasachenko and B. I. Stepanov, Opt. i Spektr. 2, 339 (1957).

ANNULAR LOW PRESSURE MERCURY LAMP

I. I. Kondilenko and G. A. Vorob'eva

Received 1 April 1960

Various types of low pressure mercury lamps have been widely used of late for exciting Raman spectra. Their numerous advantages over high pressure lamps have been mentioned repeatedly in the literature.[1-4] In accordance with their construction, the lamps in the literature have been called straight, U-shaped, or helical.[5-11] Sources of novel design have been described by Czechoslovakian authors.[12]

With the purpose of obtaining a uniform and stable discharge surrounding the cuvette containing the material under investigation, we constructed a horizontal annular low pressure lamp with two liquid-mercury electrodes separated from the active discharge region. A general view of our annular mercury lamp is shown in the Figure. The lamp consists of two coaxial cylinders made of molybdenum glass with diameters of 30 and 70 mm respectively. The clearance between the walls is 20 mm. Tubular outlets are fused onto the opposite ends of the lamp for the electrodes (diameter 25 mm) which are cooled internally with running water. The total length of the working part of the lamp is 200 mm; the distance from the cylinders to the electrodes is 80 mm. Our source was prepared by the usual methods.[13,14] A supplemental mercury electrode was provided near the cathode to facilitate ignition. After the ignition arc has burned for two to three seconds and the cooling of the electrodes (to about 10°C) has begun, the lamp is ignited readily by

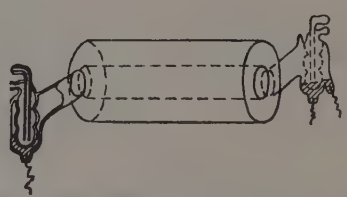

touching the glass surface of the electrode vessel with the discharge from a light (0.5 kg), compact (12 × 15 cm) high frequency generator (80 kc). This generator is particularly convenient for this work because of its small size.* The lamp is fed from a 110 volt dc power supply.

*We express thanks to V. P. Zakharov and A. A. Shishlovskyi for permission to use the generator.

The lamp operated quite stably from 6 to 25 amp; a rather intense and uniform light filled the space between the walls, at currents of 16 amp and higher. The voltage drop between the electrodes was 34 volts at 16 amp.

In order to increase the amount of useful light, the outer wall of the central part of the lamp was covered with magnesium oxide. The ends were blackened to decrease the illumination of instrument components by scattered light.

To obtain the Raman spectra, the cuvette with the substance being investigated and the cooler were inserted

into the inner cylinder of the lamp. Photographic spectra were obtained with the help of an ISP-51 spectrograph with a fast camera (f/2.5) and a dispersion of 65 A/mm near 4400 A. The minimum exposure required for a completely satisfactory Raman spectrum of CCl_4 is 15 sec. In addition to the Stokes components, the anti-Stokes components are also obtained at 217, 313, and 459 cm^{-1}.

An investigation of the dependence of radiation intensity on discharge current was also conducted. For this purpose, a series of Raman spectra of CCl_4 was photographed under otherwise constant experimental conditions, with the current varying from 7 to 23 amp. The photographic photometry data showed that the intensity of the 459 cm^{-1} line of CCl_4 increased fivefold when the current increased from 16 to 23 amp, while the continuous background in the spectrum of the source was extremely low, and increased no more than 70%. For this estimate, separate photographs were made of the direct radiation of the lamp at different exposures. This favorable an increase in the spectral brightness of the exciting mercury lines in comparison with the background is explained by the fact that in this lamp, the current density in the region of the annular discharge remains substantially lower than it is under identical conditions in the tubular mercury low pressure lamp. The high contrast properties of this light source are proven by the accuracy and sensitivity with which Raman analyses of mixtures can be carried out. From the data in the literature, the minimum concentration of an impurity which can now be determined in a mixture is 0.7%, or, exceptionally, 0.5%.[14] Without the use of a light filter, we succeeded in obtaining a Raman spectrum of 0.1% C_6H_6 in CCl_4 with an exposure of only 3 min and an excitation current of 18 amp. The benzene lines 992 and 3059 cm^{-1} can be clearly seen in the spectrogram. The lowest concentration of CCl_4 detectable in C_6H_6 in our experiments was 0.07%. The useful life of our lamp has not yet been established, since after 100 hr of use, the cylinders remained perfectly transparent.

In conclusion we note that this lamp is very simple manufacture, has a high light output, good spectral properties, and can be successfully used in numerous areas of research, in particular for the qualitative and quantitative analysis of mixtures by means of their Raman spectra.

REFERENCES

1. D. H. Rank and M. Gartney, J. Opt. Soc. Am. 38, 27 (1948).
2. J. W. Kemp and J. L. Jones, J. Opt. Soc. Am. 42, 8 (1952).
3. M. L. Sosinskii, Izvest. Akad. Nauk., SSSR, Ser. Fi 17, 621 (1953).
4. H. Moser, Proc. Intern. Colloq. Spectroscopy (London) VI, 490 (1957).
5. M. L. Sosinskii, Izvest. Akad. Nauk SSSR, Ser. Fiz 18, 709 (1954).
6. R. C. Kelting and L. J. Buttolph, Trans. Illum. Eng Soc. N.Y. 33, 643 (1938).
7. D. H. Rank and R. E. Kagarise, J. Opt. Soc. Am. 40 89 (1950).
8. J. J. Heigl, B. F. Dudenbostel, H. F. Black, and J. Wilson, Anal. Chem. 22, 154 (1950).
9. H. L. Welsh, M. F. Crawford, and T. Love, Can. J. Phys. 30, 577 (1952).
10. D. C. Schreiber, Optik 15, 12 (1958).
11. V. M. Pivovarov and Ya. S. Bobovich, Zhur. Tekh. Fiz. 26, 649 (1956).
12. J. Pliva, B. Schneider, J. Stokr, and K. Ulbert, J. Mechanika and Optika 2, 44 (1957); Proc. Intern. Colloq. Spectroscopy (London) VI 499 (1957).
13. V. P. Cheremisinov, Pribory i Tekh. Ekspt. 2, 122 (1956).
14. M. L. Sosinskii, Opt. i Spektr. 6, 405 (1959), Optics and Spectroscopy 6, 254 (1959).

THE EFFECT OF TEMPERATURE ON THE DECAY OF PHOSPHORESCENCE IN BORON PHOSPHORS

M. D. Khalupovskii

Received 12 April 1960

It is known that for many phosphors the nature of the decay depends on the spectral location of the phosphorescence band.[1-4] It was therefore of interest to study the effect of temperature on the decay laws of individual regions of the phosphorescence spectrum isolated by a monochromator. For this purpose we used an arrangement consisting of a single-disc phosphoroscope, a monochromator, and an FEU-17 photomultiplier. The phosphoroscope disc, about 32 cm in diameter and 15 kg in weight, was heated by an internally mounted spiral. The regulated voltage was applied to the spiral by means of sliding contacts. Since the phosphoroscope disc was fairly massive and the rate of rotation was low, the temperature of the phosphor investigated was practically the same when the disc was at rest as when it was rotating.

We used the following as activators of the boron phosphors: phthalic, salicylic, sulfosalicylic, and gallic acids; phthalic anhydride, phthalimide, phenanthrene, fluorescein, and uranin.

The effect of temperature on the decay law and its changes depends on the wavelength of the region of the phosphorescent spectrum observed. One can distinguish three types of dependence between the phosphor temperature and the indicated changes in the nature of the decay.

The boro-phthalic phosphor can serve as an example of the first type of dependence. As shown in ref. 3, at room temperature, all parts of its phosphorescent spectrum decay according to the same exponential law. This situation persists up to about 50°C, the rate of decay varying only inappreciably. Temperature quenching of phosphorescence arises at higher temperatures, and the decay law is no longer exponential. At the same time, the rate of decay remains the same in all regions of the spectrum.

The boro-fluorescein and boro-phenanthrene phosphors are representative of the second and third kinds of dependence, respectively.

At room temperature, the rate of decay of the boro fluorescein phosphorescence depends on the wavelength of the spectral region observed; the decay is nonexpon

tial. As the temperature rises, the difference in the rates of decay of different spectral regions decreases. (See Fig. 1.) The rates become approximately equal when the temperature reaches 30-40°C. The decay law remains nonexponential.

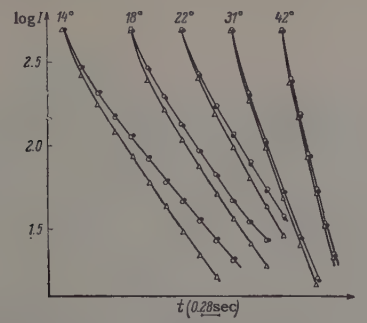

Fig. 1. Phosphorescence decay of the boro-fluorescein phosphor at different temperatures. Circles, triangles, and squares mark the decay curves near 450, 485, and 560 mμ, respectively.

Figure 2 shows the temperature variation of the decay laws of a phenanthrene-activated boron phosphor. The data given in the literature on the decay of phosphorescence of this phosphor are contradictory. According to the measurements of Vinokurov and Levshin,[5] the decay law is a simple exponential, while according to Tomaschek's data,[6] the decay law may be represented as the sum of four exponentials. To explain these disagreements, we measured the decay at room temperature of 12 different spectral regions of the boro-phenanthrene phosphor. Four characteristic curves are shown in Fig. 2. They indicate that the decay law of each spectral region may be approximated by an exponential (at room temperature) while the rate of decay of different spectral regions depends on the spectral location of the region.

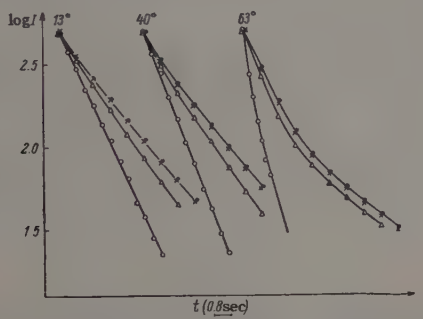

Fig. 2. Phosphorescence decay of a phenanthrene-activated boron phosphor at different temperatures. Circles, triangles, squares, and crosses mark the decay curves near 430, 465, 500, and 530 mμ, respectively.

The Table shows the dependence of the average duration of phorphorescence on the spectral location of the region studied. The values are given for one of the samples of the boro-phenanthrene phosphor at room temperature. It is interesting to note that the average duration of phosphorescence depends strongly on spectral location in the neighborhood of the bluer bands, but is practically constant in the green. (The bands have maxima at 465 and 496 mμ, respectively.)

The Average Duration of Phosphorescence of a Boro-Phenanthrene Phosphor as a Function of the Spectral Location of the Region Observed

Average wavelength of spectral region (mμ)	417	437	446	456	465	475	485	497	510	526	546	564
Average duration of phosphorescence	1.04	1.08	1.08	1.40	1.64	1.68	1.80	2.00	2.00	1.96	1.96	2.00

In the region of temperature quenching, the phosphorescence decay law of the boro-phenanthrene phosphor deviates considerably from a simple exponential law. At the same time, in contrast to the boro-fluorescein phosphor, the rate of decay remains different for different spectral regions.

REFERENCES

1. P. Pringsheim and H. Vogel, J. chim. phys. **33**, 345 (1936).
2. V. V. Bredel', Dissertation, 1953.
3. M. D. Khalupovskii, Opt. i Spektr. **3**, 385 (1957).
4. V. A. Pilipovich and B. Ya. Sveshnikov, Opt. i Spektr. **5**, 290 (1958), Optics and Spectroscopy **5**, 290 (1958).
5. L. A. Vinokurov and V. L. Levshin, Zhur. Fiz. Khim. **8**, 181 (1936).
6. R. Tomaschek, Ann. Phys. **67**, 612 (1922).

APPROXIMATE WAVE FUNCTIONS OF FREE IONS AND OF IONS IN A CRYSTAL

M. I. Petrashen', I. V. Abarenkov, and N. N. Kristofel'

Received 16 April 1960

In quantum-mechanical calculations of the properties of alkali halide crystals, it has been customary to use appropriate free ion functions as the one-electron (nonorthogonal) functions of ions in a crystal. It has been repeatedly shown[1] that such an approach is unsatisfactory.

We have suggested a simple method for calculating approximate one-electron functions of the "central ion" (CI) in an ionic crystal (i.e., an isolated electronic subsystem in a crystal). This method assumes that the one-electron functions of the free CI are known. If the free CI has not been calculated by the Hartree-Fock method, we can construct one-electron functions of the external layers of a free ion by a less laborious semiempirical method.[2,3] (These functions play a leading role in determining crystal properties.) In this method, the optical electrons are considered to exist in an effective field selected so as to make a certain calculated energetic characteristic of the atom coincide with its experimental value.

In the case of a single optical electron, the first ionization potential of the atom in the state considered is chosen as this energetic characteristic.[2] In the case of two optical electrons, the sum of the first and second ionization potentials of the atom in the state considered is used for this characteristic. We consider this quantity as the energy of a system of two optical electrons (neglecting the polarization of the shell by optical electrons). The equations for one-electron functions are then written in the form

$$\left.\begin{aligned}(H_0+H_q+E_q)\,\psi_p&=E\psi_p,\\(H_0+H_p+E_q)\,\psi_q&=E\psi_q.\end{aligned}\right\}\qquad(1)$$

Where

$$H_0=-\frac{1}{2}\Delta-\frac{Z}{r}+V(\mathbf{r}),$$

$V(\mathbf{r})$ is the potential of the effective field,

$$\left.\begin{aligned}H_i\psi&=\int\frac{|\psi_i(\mathbf{r}')|^2}{|\mathbf{r}-\mathbf{r}'|}\,d\tau'\psi\pm\int\frac{\bar{\psi}_i(\mathbf{r}')\psi_i(\mathbf{r})\,\psi(\mathbf{r}')}{|\mathbf{r}-\mathbf{r}'|}\,d\tau'\\E_i&=\int\bar{\psi}_iH_0\psi_i d\tau\quad i=p,\,q\end{aligned}\right\}\qquad(2)$$

and $E=-(I_1+I_2)$, where I_1 and I_2 are the experimental values of the first and second ionization potentials of the atom.

System (1) is written so that the calculated sum of the first and second ionization potentials equals $-E$.

In our approximation, the potential $V(\mathbf{r})$ of the effective field differs little from the field of the doubly ionized atom. The Hartree-Fock field is therefore a good approximation to $V(\mathbf{r})$ at large distances from the nucleus. At small distances, $V(\mathbf{r})$ must differ from the Hartree-Fock field to insure that the boundary conditions at $r=0$ are satisfied. However, the determination of the effective field in this region will always be somewhat arbitrary. System (1) must therefore be solved so that the values of $V(\mathbf{r})$ for small r will also be substantial only for values of ψ_p and ψ_q for small r. Then the solution of the equations of the system obtained by integration starting with large values of r can, near $r=0$, be simply extrapolated to 0 in suitable fashion.

The semiempirical method can obviously be generalized to atoms with a large number of electrons, but the computational difficulties increase rapidly. Let us note that the semiempirical functions corresponding to the components of a multiplet are obtained differently (due to the difference in the experimental values of the ionization potentials); i.e., the semiempirical method to some extent takes account of the spin-orbital interactio

Having obtained some kind of functions for the free ion, we can now turn to the construction of one-electron functions in an ionic crystal. We need not change the functions of the internal layers, where the field of the crystal is practically constant.

For the one-electron function of the periphery of th central ion in a crystal we have the equation

$$(H_0-U)\,\psi_k=E\psi_k,$$

where H_0 is the corresponding operator of the "free" CI, while U is the operator for the interaction energy between the CI electron and the rest of the crystal; U involves the coordinates of the ions and certain parameters. If we consider the ions surrounding the central ion to be points, we find that $U=U(\mathbf{r})$ is the potential*

*We use atomic units.

of the electrostatic field of a point lattice. It has been investigated in detail in ref. 4.

To the first approximation of perturbation theory,

$$E=E_0+A,$$

where E_0 is the eigenvalue in the equation for the function of the free CI. In the point lattice approximation,

$$A=-\int|\psi_k^0(\mathbf{r})|^2U(\mathbf{r})\,d\tau=\pm\frac{M}{a}+\eta,$$

where a is a lattice parameter and M is the Madelung constant. The upper and lower signs refer to a CI in cation and anion lattice sites, respectively, while $|\eta|\ll M/a$. Taking account of the fact that the CI is not actua surrounded by points gives a small correction to A.

An approximate solution φ_k of Eq. (3) can be constructed by the following simple method: We take as φ a function which satisfies the same boundary conditions as ψ_k and which is a solution of

$$\left.\begin{aligned}H_0\varphi_k(\mathbf{r})&=E_0\varphi_k(\mathbf{r})&&0\leqslant r<r_1\\[H_0+g(\mathbf{r})]\,\varphi_k(\mathbf{r})&=E_0\varphi_k(\mathbf{r})&&r_1\leqslant r\leqslant r_2\\H_0\varphi_k(\mathbf{r})&=(E_0+A)\,\varphi_k(\mathbf{r})&&r\geqslant r_2\end{aligned}\right\}$$

Equation (4) may obviously be considered as the Hartree-Fock equation for a one-electron function of a CI if we replace the potential of the crystal in it by the following effective potential

$$U_{\text{eff}}(\mathbf{r})=\begin{cases}-A & 0<r\leqslant r_1\\-A-g(\mathbf{r}) & r_1\leqslant r\leqslant r_2\\0 & r\geqslant r_2.\end{cases}$$

The quantities r_1, r_2, and $g(\mathbf{r})$ must be chosen so that

$$\int U_{\text{eff}}\,|\psi_k^0|^2\,d\tau=\int U(\mathbf{r})\,|\psi_k^0|^2\,d\tau=-A,$$

i.e., so that

$$\int_{r_1}^{r_2} g(\mathbf{r}) |\psi_k^0|^2 d\tau = 0,$$

and r_2 must be large enough so that

$$\int_0^{2\pi}\int_0^{\pi}\int_0^{r_2} |\psi_k^0|^2 d\tau = 1.$$

Thus the value of U_{eff} is such that an electron from a negative ion in the crystal is in a deeper potential well, and an electron from a positive ion in a shallower well, than a free ion.

In the region $r < r_1$ where the field of the ion itself predominates, we set $\varphi_k(\mathbf{r}) = C_1\psi_k^0(\mathbf{r})$, r_1 being chosen between the points corresponding to the last extreme value and the inflection of the function ψ_k^0. Experience has shown that the remaining arbitrariness in the choice of r_1 has little effect on φ_k. To solve Eq. (4) for $r > r_2$ with the condition $\varphi_k = (\infty)$, we use first an asymptotic series expansion and then a numerical integration up to $r = r_2$. (It is often possible to use the asymptotic expansion up to $r = r_2$). In the region $r_1 < r < r_2$, since we do not know the exact form of $g(\mathbf{r})$, we replace φ_k by an interpolation function of the type

$$W(r) = \begin{cases} C_2 r \dfrac{2}{\sqrt{-2(E_0+A)}} \exp\left\{-\sqrt{-2(E_0+A)}\, r + \dfrac{b}{r} + \dfrac{c}{r^2}\right\} & \text{positive CI} \\ C_3 \exp\left\{-\sqrt{-2(E_0+A)}\, r + \dfrac{b}{r} + \dfrac{c}{r^2}\right\} & \text{negative CI} \end{cases}$$

Such a function corresponds to the character of $g(\mathbf{r})$. The parameters C_1, C_2, C_3, b, and c are determined from the conditions of normalization and continuity of the function φ_k and its derivative at the points r_1 and r_2.

We have computed the approximate radial functions for a series of ions in alkali halide crystals by this method. The results of this computation will be published in the "Vestnik LGU" (Bulletin of Leningrad State University).

It turns out that taking account of the field of the point lattice of the crystal results in a compression of the electron clouds of anions and a (relatively smaller) spreading of the electron clouds of cations as compared with free ions. The degree of deformation is almost equal for different alkali halide crystals. This effect has been observed experimentally.[5]

A calculation of the diamagnetic susceptibility of the crystal serves as a check on the quality of the functions obtained. The results of calculations with crystalline functions agree better with experiment than those using the functions for free ions.

The crystalline functions obtained by the method described above may be used as the zeroth approximation functions in a perturbation calculation which can take into account the corrections necessary because of the departure from point structure in various problems of crystal physics. An example is the study of luminescence centers in crystalline phosphors.[6]

REFERENCES

1. R. Knox, Phys. Rev. 115, 1095 (1959).
2. M. I. Petrashen' and I. V. Abarenkov, Vestnik Leningrad Univ. No. 5, 141 (1954).
3. M. I. Petrashen' and I. V. Abarenkov, Fiz. Sbornik Lvovsk. Univ. (Physics Collection of Lvov University), No. 4, 9 (1958).
4. I. V. Abarenkov, Vestnik Leningrad Univ. No. 16, 5 (1958).
5. G. Schoknecht, Z. Naturforsch. 12a, 983 (1957).
6. N. N. Kristofel', Trudy Inst. Fiz. i Astron., Akad. Nauk Eston. SSR. No. 7, 85 (1958); Ibid. No. 7, 112 (1958); Ibid. No. 10, 3 (1959).

LOW TEMPERATURE THERMAL RADIATION DETECTOR

A. F. Mal'nev and L. S. Kremenchugskii

Received 27 April 1960

Reducing the working temperature of metallic bolometers improves their characteristics. This is due to the fact that at low temperatures there is a decrease in their heat capacity and thermal noise, and an increase in their temperature coefficient of resistance within the temperature interval $\theta_D/3 > T > \theta_D/10$ (θ_D is the Debye temperature). In ref. 1 the possibility was mentioned of lowering the threshold of sensitivity of a nickel bolometer approximately ten times by going from room temperature to liquid oxygen temperature.

We have prepared a highly sensitive and stable low temperature nickel bolometer which uses liquid nitrogen as the coolant. The design which we developed (cf. figure) provides for cooling of the working element of the bolometer—a nickel foil—by means of a thermal contact which is adequately insulated electrically from the body of the cryostat. When the nickel bolometer was cooled down to the boiling point of liquid nitrogen we observed a twofold increase in its temperature coefficient and a threefold decrease in its ohmic resistance, compared to values at room temperature. The temperature coefficient α was determined from the bolometer resistance vs temperature curve in the range 60°-77°K. The temperature was determined from the value of the vapor pressure of nitrogen in the closed copper cylinder in which the bolometer was placed.

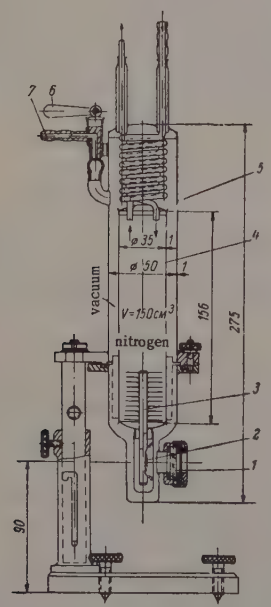

1—Cryostat window; 2—bolometer; 3—thermal conduction rod; 4—inner wall; 5—outer wall; 6—handle; 7—hose connector.

Bolometer number	1		2	
Temperature of medium (°K)	300	77*	300	77
Working current (ma)	12	8	30	12
Resistance at the working current (ohms)	22	10.5	24.4	7
Detector area (10^{-2}cm^{-2})	0.5	0.5	0.8	0
Volt/watt response at the modulating frequency of 8 cps (volts/watt)	1.45	15	0.96	6
Mean square value of noise (10^{-10} volts)	6.5	3	7	2
Threshold sensitivity at the modulating frequency of 8 cps (10^{-11} watts)	45	2	73	3
Threshold sensitivity at zero modulating frequency (10^{-11} watts)	43	1.6	70	2
Time constant (meter/sec)	5	15	6	19
Jones figure of merit	0.14	2.3	0.1	1

*The temperature of the bolometer was not measured accurately.

The value of α(77°K) was found to be 8×10^{-3} deg^{-1}. The determination of the basic parameters of the bolometers was carried out with equipment developed at the Physics Institute, Academy of Sciences, USSR, and by methods described in ref. 2. Mean square noise values were determined by a circuit with a large load resistan The Table shows the parameters of two nickel bolometers (Nos. 1 and 2), measured in a cryostat at room tem perature after filling the cryostat with liquid nitrogen. It is evident from the Table that the threhold sensitivity is more than 20 times that of bolometers working at room temperature and situated in air-filled cryostats.

Comparison of the present detector with superconducting and low temperature bolometers working at the temperature of liquid hydrogen-helium shows that this instrument is inferior to the best superconducting bolometers, but is fully comparable with many of them. Since liquid nitrogen is the coolant in our detector, it is possible to construct a relatively small and economic low temperature bolometer. A test of the stability of th volt/watt response of the detector shows that within 15 to 20 minutes after filling the cryostat with nitrogen, it attained its working sensitivity, and maintained this sen tivity for a day. This bolometer can be used in infrared spectrometers, for the study of emission characteristic of low temperature sources and for other purposes.

REFERENCES

1. K. Bischoff, E. Justi, M. Kohler, and G. Lautz, Z. Naturforsch. 10a, 401 (1955).
2. A. F. Mal'nev and L. S. Kremenchugskii, Izmeritel- naya Tekh. (in press).

THE EFFECT OF THE FLUX ON THE STATE OF THE ACTIVATOR IN A PHOSPHOR: AN INVESTIGATION BY THE PARAMAGNETIC RESONANCE METHOD

V. G. Dubinin

Received 1 April 1960

In refs. 1 and 2, the electron paramagnetic resonance ethod was used to investigate the state of the Eu^{++} ac- ator in unexcited and excited SrS-Eu,Sm phosphors. as found in these investigations that the intensity of lines in the paramagnetic absorption spectrum of Eu^{++} greater in phosphors prepared with a flux.* This

his fact was noted in ref. 3, where it was reported that the magnitude of paramagnetic absorption was ater in a phosphor containing a flux (LiF); however, e was no further investigation in this direction.

nomenon (the influence of the flux on the concentration Eu^{++} in the phosphor) appeared interesting, and it was ided to make a detailed investigation of it, using the rementioned method. To this end, the following phos- rs* were prepared: SrS-Eu,Sm(no flux), and SrS-Eu,

e author expresses thanks to R. M. Medvedevaya for paring the phosphors indicated.

(LiF) and SrS-Eu,Sm($SrCl_2$)(with flux), in which the ne concentration of Eu (10^{-4} gm atom per gm atom of and Sm (10^{-5} gm atom per gm atom of Sr) was intro- ed into the mixture before firing. The flux was intro- ed into the mixture in the form of LiF or $SrCl_2$ in h quantity that F and Cl amounted to 15% of the ght of the Sr.

The intensity of the paramagnetic absorption lines determined in the same manner as in ref. 2, namely, lative to the paramagnetic absorption line of a crys- of copper sulfate placed on the end plate of a resonant ity.

Usually, it was not possible to completely establish chemical composition of the phosphor after firing. erefore, in order to determine the weight of phosphor responding to a given quantity of Eu, crucibles of the ture without flux and with the $SrCl_2$ flux were weighed ore and after firing. In this way, it was established the weight of phosphor with flux corresponding to a en quantity of Eu was approximately 20% greater after ing. This difference is due both to the presence of the x itself, and to the fact that the $SrCl_2$, combining with forms an additional amount of SrS. Because of this, amount of the SrS-Eu,Sm($SrCl_2$) phosphor used in the amagnetic resonance experiments was increased by %. Unfortunately, this method was not applied in the e of the LiF flux, since the latter reacted with the cible. Hence, equal amounts of the phosphors SrS-Eu, (LiF) and SrS-Eu, Sm(no flux) were taken. Since the sphors with flux were more dense as a result of sin- ring, the quantity of phosphor containing a given quan- of Eu took up less space in the case of the phosphor th flux. In order to maintain approximately the same tribution of paramagnetic Eu^{++} ions in the magnetic d of the resonator, sufficient powdered SrS was added the phosphors containing flux to equalize the volume upied by the phosphors in the sample tubes.

The results of the experiment showed that the mag- tude of paramagnetic absorption of Eu^{++} was 1.5 times eater in phosphors with fluxes (LiF or $SrCl_2$) than in se without any flux, which indicates that after firing the concentration of the Eu^{++} activator is 30-40% greater in phosphors with the indicated fluxes than in the phosphor without flux,* in spite of the fact that before firing, the amount of Eu introduced into the mixture was the same for all phosphors.

*Nothing can be said about the state of Sm^{+++}, the other activator in the phosphor, since the paramagnetic resonance spectrum of Sm^{+++} is not observed at room temperature.

In a number of papers[4-6] the actual concentration of the activator in the phosphor was determined by studying the distribution of activators between matrix and flux using radioactive isotopes. In ref. 4, it was established that for the phosphor SrS-Eu,Sm with $SrCl_2$ or LiF flux, the concentration of the activator Eu in the $SrCl_2$ is about one-third of its concentration in the host substance, and in the LiF it is practically zero. This means that in an actual phosphor, where these fluxes constitute 10-20% of the total weight one should find about 90-100% of the activator in the host substance.

Eu was added to the mixture in the form of $Eu(NO_3)_3$, i.e., in the trivalent state. During firing, it enters into the phosphor as an activator, creating luminescence centers in the form of Eu^{++} ions located at cation sites of the SrS lattice (NaCl type).[7] Therefore, if it is assumed that the Eu does not vaporize, then according to ref. 4 about 90-100% of the Eu introduced will be in the Eu^{++} state in phosphors containing a flux, whereas in phosphors without flux, judging from the paramagnetic absorption, the quantity of Eu in this state is about 1.5 times less, i.e., at most 60%. The state of the remaining 40% of the Eu introduced into the mixture is still not clear at present.

It was natural to assume that the flux remaining in the host lattice would deform it, and also that any flux situated near some of the activator ions would react chemically with them. It was decided to verify this from the paramagnetic resonance line widths. It is known that the intrinsic width of a paramagnetic resonance absorption line is very small in comparison to the widening caused by other factors. In particular, a marked widening of the line is caused by the so-called spin-lattice interaction. (Other causes are possible; for example, chemical interaction between flux and activator or any disturbance to the symmetry of the lattice. Direct measurements of the absorption lines of Eu^{++} phosphors with and without flux showed the existence of some difference (5-8%), which is not outside the limits of error of our measurements.

Differences in paramagnetic resonance line width can also be determined by measurements of the relaxation time, since $\Delta\nu \sim 1/\tau$, where $\Delta\nu$ is the line width and τ is the relaxation time. At our request, the relaxation times of phosphors with and without fluxes were measured in the oscillator laboratory; here again, no marked differences were detected.*

*The measurements were undertaken by A. A. Manenkov, to whom the author conveys his sincere appreciation.

It must also be reported that neither the flash spectra nor the emission spectra of these phosphors showed any difference under excitation in the optical absorption band of Eu^{++}. This was also noted in ref. 4. This absence of any direct influence of the flux on the Eu centers can be explained by the fact that Eu^{++} is in an $^8S_{7/2}$ state, which is characterized by a generally weak interaction between the paramagnetic ion and the host lattice, and by the fact that the flash and emission spectra consist of broad bands, in which differences are not noticeable.

No.	Phosphor[a]	Flux	Concentration[b] of Eu^{++} %	Light sum[b] emitted under infrared light, %	Intensity during excitation (rel. units)	Phosphorescence immediately after excitation (rel. un.)
1	SrS-Eu, Sm	b. n . . .	100	100	47	~6
2	SrS-Eu, Sm	$SrCl_2$ . . .	140	40	85	~9
3	SrS-Eu, Sm	LiF . . .	150	170	66	~8
4	SrS-Eu, Sm	b. n . . .	100	100	19	~2
5	SrS-Eu, Sm	LiF . . .	140	300	58	~14

[a]Nos. 1–3 are specially prepared phosphors with the same concentration of activator. Nos. 4 and 5 are phosphors of an old preparation with approximately the same concentration of activator introduced.

[b]The Eu^{++} concentration and the magnitude of the light sum for the phosphor without flux has been taken as 100%.

On the other hand, there is an indirect influence of the flux in the phosphors (see Table). This is manifested, as can be seem from the Table, in the change of activator concentration in firing, in the differences in phosphorescence and emission during excitation, and also in the difference of the light sums emitted by the phosphors during de-excitation.

In conclusion, I wish to express my thanks to V. V. Antonov-Romanovskii and M. V. Vok for guidance in this work, and to V. L. Levshin for discussing the results.

REFERENCES

1. V. V. Antonov-Romanovskii, V. G. Dubinin, A. M. Prokhorov, Z. A. Trapeznikova, and M. V. Fok; Zhu Exsptl. i Teoret. Fiz. 37, 1465 (1959).
2. V. G. Dubinin and Z. A. Trapeznikova, Opt. i Spektr 9, 472 (1960), Optics and Spectroscopy 9, 187 (1960)
3. W. Low, Phys. Rev. 98, 426 (1955).
4. R. W. Mason, C. F. Hiskey, and R. J. Ward, J. Am. Chem. Soc. 71, 509 (1949).
5. J. Prener, R. W. Mason, and R. Ward, J. Am. Chem Soc. 71, 1803 (1949).
6. A. Drecben and R. Ward, J. Am. Chem. Soc. 73, 467 (1951).
7. S. P. Keller, J. E. Mapes, and G. Cheroff, Phys. Re 108, 663 (1957).

THE SPECTRUM OF THE NEGATIVE MOLECULAR ION OF PHTHALOCYANIN

A. V. Shablya and A. N. Terenin

Received 20 May 1960

At the present time the absorption spectra of negatively charged molecules of naphthalene, anthracene, phenanthrene, tetracene, perylene, diphenyl, and others which consist of the bands in the visible region are known.[1,2] The ion radicals of this type are prepared by bringing solutions of the above-mentioned hydrocarbons in dimethoxyethane into contact with metallic sodium under vacuum conditions.[3] Intense coloration appears in parallel with the increasing electrical conductance of the solution. The paramagnetism of such solutions has been determined using EPR methods and the existence of an unpaired electron in these molecular ions has been demonstrated.[4,5] Doubly-charged ions have also been discovered, and their spectra measured.[2] The theoretical calculations made on these spectra, using the molecular orbital method, were in good agreement with experiment.[6]

In this work the same technique was applied to magnesium phthalocyanin and chlorophyll with the aim of obtaining the spectra of their ion radicals. This problem arose in connection with the nature of the peculiar forms of these pigments, which were indicated spectroscopically in the photoreduction by ascorbic acid.

According to Krasnovskii[7] and Evstigneev,[8] one must distinguish between the primary "yellow" form of the pigments with absorption maxima at 340 and 470 mμ (for pheophetene a) obtained in the first reduction step and supposedly corresponding to the charged molecule of the pigment with one additional electron, and the secondary "red" form obtained from the "yellow" form by addition of a proton, and possessing absorption maxima in the 525-530 mμ region. As was shown by Evstigneev and Gavrilova,[9] during the reduction (in the dark) of magnesion phthalocyanin by zinc in acetic acid, absorption bands characteristic of the secondary "red" form of the pigment appear. It was interesting in connection with this to design an experiment, analogous to those with p nuclear hydrocarbons, in which one would purposely re strict the reduction reaction to the first step in which only one electron would be added to the pigment with th resulting formation of the ion radical.

In order to eliminate oxygen, the experiments wer performed in a vacuum system at 10^{-5} mm pressure. Tetrahydrofuran or diethyl ether was used as solvent. The solvent was distilled over sodium and vacuum dri in the presence of anthracene, in the same way as described elsewhere.[1] A vacuum cell, shown in Fig. 1, w used for the experiments. A weighed amount of magne sium phthalocyanin was placed into compartment A, where after prolonged heating in vacuum it finally sub limed and condensed on the wall. Sodium azide was in troduced into compartment B, and was heated with con stant evacuation until the walls of this compartment w covered with a sodium mirror. With the stopcock K closed, the solvent was introduced into compartment C

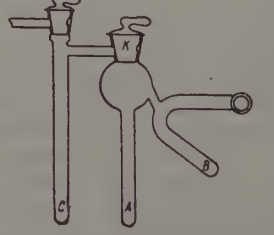

Fig. 1. Vacuum cell for the preparation of phthalocyanin and measurement of the absorption spectra.

ogether with some pieces of sodium and powdered anhracene and thoroughly degassed by repeated freezing nd pumping. The solvent was allowed to remain for 10-2 hr in compartment C, after which time it was disilled over into compartment A which contained the disilled phthalocyanin and which had been cooled to −40°C. The pigment concentration in the solvent amounted to bout 10^{-3} moles per liter. The phthalocyanin solution hus obtained was poured over into compartment B with he sodium mirror, where phthalocyanin anion formation ook place. The color change in the phthalocyanin soluion was observed in 5-10 min after it was brought into ontact with sodium.

The absorption spectra in the first experiments were ecorded with the SF-2M spectrophotometer immediately fter the contact between metallic sodium and tetrahydroran solution of phthalocyanin was made. At that time e observed the disappearance of the long wavelength aborption band at 676 mμ, the persistence of the 640 mμ and of magnesium phthalocyanin, and the appearance of 530 mμ band, which is somewhat different from the 70 mμ absorption band observed during the reduction of agnesium phthalocyanin by zinc filings in acetic acid.[9] More detailed measurements made with the SF-4 spectrohotometer allowed us to observe two stages of interacion between magnesium phthalocyanin and sodium.

The spectra taken immediately after the contact beween sodium and tetrahydrofuran solution of the pigment Fig. 2), indicated the formation of a product characterzed by a spectrum with absorption maxima around 570 nd 640 mμ, as well as a weak maximum at 950 mμ. This orm persists under vacuum condition for quite a conderable time. In a spectrum taken 40 hr later the 950 mμ band had completely disappeared and two new bands at 530 and 790 mμ had appeared. These changes are especially marked in the tetrahydrofuran solution but may e also observed in the solution of diethyl ether. After e introduction of air into the cell a rather rapid regenration of phthalocyanin with the characteristic maxima around 610, 640, and 675 mμ took place. Thus after

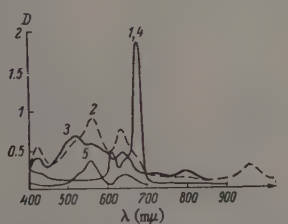

Fig. 2. Absorption spectra of the products of reaction of phthalocyanin with sodium. Curve 1—distilled solution in tetrahydrofuran; curve 2—immediately after reaction; curve 3—after 40 hr under vacuum; curve 4—after regeneration by introduction of air; curve 5—spectrum of magnesium phthalocyanin after reduction with zinc filings and acetic acid, according to the data of ref. 9.

interaction with sodium it is the spectrum of the secondary "red" photoreduced form of the pigment and not of the primary form which is observed.

It may be supposed that the primary product formed by the capture of an electron from sodium by the pigment molecules is initially adsorbed on the metal The appearance of absorption bands and the formation of a red color are apparently related to the interaction of the primary radical-ions among themselves and with the metal, which results in the formation of the more stable secondary reduced form. It must be noted that for Mg-phthalocyanin there was a failure to observe spectroscopically the primary form either during photoreduction[9] or during reduction in the dark due to its great reactivity.

Experiments with the chlorophyll derivatives did not give positive results, apparently because it was not possible to extract water completely.

During the reaction between the nonmetal-containing phthalocyanin and sodium some irreversible processes took place, which were evidenced by the appearance of new absorption bands characteristic of metal-containing phthalocyanin. Apparently the formation of sodium phthalocyanin was responsible for this.

Under the conditions of the experiments described above the presence of any kind of proton donors (water, acids) was completely excluded. In spite of this there was present in the spectrum the absorption maximum at 530-570 mμ, which is characteristic of the secondary form of the pigment which is observable in the second stage of photoreduction in the dark,[8] as well as during the reduction reaction in acid medium.[9] From this follows a general tentative conclusion, that the "red" form of the pigments does not result from the proton addition to the primary form, which is produced during the first stage of photoreduction.

We are very grateful to P. A. Moshkin for having provided us with pure tetrahydrofuran.

REFERENCES

1. D. Lipkin, D. E. Payl, I. Towsend, and S. I. Weissman, Science 117, 534 (1953); J. Am. Chem. Soc. 78, 119 (1956).
2. G. J. Hoijtink, E. de Boer, P. H. van der Meis, and W. P. Weijland, Rec. trav. chim. 74, 277 (1955); Ibid. 75, 487 (1956).
3. N. D. Scott, I. F. Walker, and V. U. Hansley, J. Am. Chem. Soc. 58, 2442 (1936).
4. Th. Chu and S. C. Yu, J. Am. Chem. Soc. 76, 3367 (1954).
5. E. de Boer, J. Chem. Phys. 25, 190 (1956).
6. G. J. Hoijtink, Colloque Intern. Calcul Fonctions d'Ondes Mol. Ed. C. N. R. S. p. 237. Paris, 1958; Mol. Phys. 2, 85 (1959).
7. A. A. Krasnovskii, Zhur. Fiz. Khim. 30, 968 (1956).
8. V. B. Evstigneev, Zhur. Fiz. Khim. 32, 969 (1958).
9. V. B. Evstigneev and V. A. Gavrilova, Doklady Akad. Nauk SSSR 108, 507 (1956).

THE NONISOTHERMAL RELAXATION OF THE LUMINESCENCE SPECTRA OF X-IRRADIATED KCl CRYSTALS ACTIVATED WITH Tl^+, In^+, Ag^+, AND Cu^+ IONS

I. K. Vitol

Received 31 October 1959

For the study of relaxation processes in crystal phosphors the integral method of thermal de-excitation is widely used (cf. refs. 1-3). By this method the light sum is measured in some specific region of the spectrum. However, the integral method will not enable one to obtain quantitative information about the composition of the luminescence spectra; i.e., to determine which electron-vibrational transitions are responsible for the emission of the light.

The results of an investigation of the thermoluminescence spectra of KCl crystals containing Tl^+, In^+, Cu^+, Ag^+, Pb^{++}, and Sn^{++} ions are given below. The measurements were made with a "relaxation combine,"—an apparatus which automatically records absorption emission, excitation or optical de-excitation spectra.

The optical-mechanical part of the "relaxation combine" was constructed around an SF-4 monochromator. The electronic part contained a synchronous detector for the measurement of weak luminous fluxes and a circuit for the measurement of absorbed light. For all types of measurements the crystal was placed in the cryostat at the location of the exit beam of the SF-4. To obtain absorption spectra, the light beam was alternately (with a frequency of 70 cps) passed through the sample and a reference sample (air) and measured with FEU-18 and FEU-22 photomultipliers. This arrangement made it possible to record an absorption spectrum from 240 to 1100 mμ in 10-20 sec on a linear optical density scale ranging from 0 to 1.5 (on the decimal scale).

Simultaneously with the recording of the absorption spectra, the apparatus provided for the possibility of continuously recording the integral thermoluminescence curve. Measurement of excitation spectra or optical de-excitation spectra could be made either with or without modulation of the exciting light. In the former case, none of the components with lifetimes greater than 10^{-1} sec have any real influence on the results of the measurements. For measurement of the thermoluminescence spectra, the light source is replaced by FEU-18 and FEU-22 photomultipliers (the direction of the 70 cps modulated light was backwards through the monochromator in these measurements).

The sensitivity of the apparatus used, with a synchronous detector having a band-width of 0.2-1.0 sec, made it possible to record luminescence spectra of most of the crystals investigated under the conditions which were most advantageous from the standpoint of the resolving power of the thermal de-excitation method; i.e., a warming rate of 0.1-0.3°C/sec. In all cases the spectra were recorded by photographing them on the screen of an oscillograph with a "Kiev" 16S-2 movie camera. The same curve was also recorded with a type PSR I-01 strip chart recorder (with a carriage transit time of 1 sec) or an N-375. The photographic form of recording is convenient for analysis of the position of maxima and the widths of emission bands, because the horizontal sweep of the oscilloscope beam is linearly related to the scale of the monochromator in electron volts, while the trace of the recorder is convenient for analysis of the heights of the different peaks under nonisothermal conditions.

Figure 1, for example, gives the thermoluminescence spectra of an x-irradiated KCl-Tl phosphor (0.03 mole %). Curve a of Fig. 1 shows the recorder's trace of the intensity of thermoluminescent light passed through the monochromator while the wavelength scale of the monochromator was traversed continuously back and forth from 1.5 to 6 ev. Curves b and c represent photographs taken of the thermoluminescence spectra on the oscilloscope. From Fig. 1 it follows that the thermoluminescence spectrum of KCl-Tl consists of two bands. The ratio of their intensities changes sharply as the crystal is heated. A comparison with data on the fluorescence of KCl-Tl indicates that the 300 mμ band in the thermoluminescence spectra corresponds to an electron-vibrational transition in Tl^+ ions which are located at regular lattice points (the transition is $^3P_1 \rightarrow {}^1S_0$), while the band whose peak is near 470 mμ corresponds to the same electron transition in Tl^+ ions located near lattice defects. The redistribution of band intensities upon heating the crystal is partly linked with the thermal quenching of luminescence centers. This quenching is observed even at room temperature.

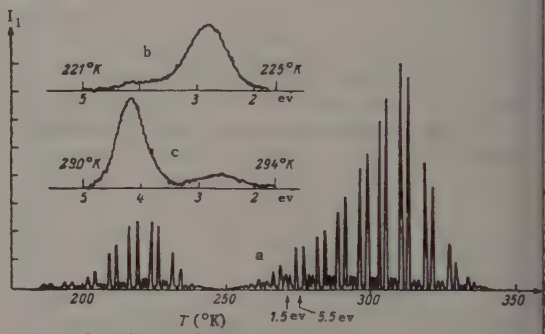

Fig. 1. Thermoluminescence spectra of a KCl-Tl crystal; curve b, in the 223° K region, and curve c, in the 292° K region. Curve a represents the change in intensity of the 300 and 470 mμ bands during the heating of the crystal (the warming rate was 0.2° C/sec). The numbers at the ends of curves b and c are the values of the temperature of the crystal at the moment of passing over the given portion of the spectrum.

We obtained similar results upon investigating the thermoluminescence spectra of KCl crystals activated with In^+, Cu^+, and Ag^+. The thermoluminescence spectra of these phosphors also clearly show emission bands corresponding to electron transitions in the activator ions. In the thermoluminescence spectrum of the KCl phosphor, there is an emission band at 270 mμ corresponding to the $^3P_1 \rightarrow {}^1S_0$ electron transition in the Ag^+ ion, and a band near 600 mμ corresponding to electron transitions in more complicated luminescence centers whose structure includes lattice defects, as well as A^+ ions. In this case too, upon increasing the temperatur

e relative intensity of the band changes in favor of the orter wavelength band. In the thermoluminescence ectrum of KCl-In one observes a primary emission nd with a maximum at 420 mμ. This band, according ref. 5, corresponds to the $^3P_1 \rightarrow {}^1S_0$ transition in In^+ ns. In the thermoluminescence spectra of KCl-Cu at w temperatures, one observes the Cu^+ ion's charac- ristic emission band at 297 mμ.

Investigation of x-irradiated KCl-Pb and KCl-Sn ystals shows that the thermoluminescence of phosphors th divalent activator ions is below the limit of sensitiv- of the apparatus. It is thus at least 10^3 times weaker an the thermoluminescence of a KCl-Tl crystal excited der the same conditions.

Study of the thermoluminescence spectra of KCl ystals with In^+, Cu^+, and Ag^+ activators, and also pure'' KCl, showed that in addition to the light due to e activators, new luminescence bands which are not aracteristic of the activator appeared at certain tem- ratures. In all the phosphors which have been investi- ted, a more or less well-defined band appears at ap- oximately 440 mμ; this band was also observed in f. 6. This band was clearly evident in our measure- nts of the x-ray luminescence spectra of activated and re KCl crystals.

Figure 2 shows the thermoluminescence spectra of

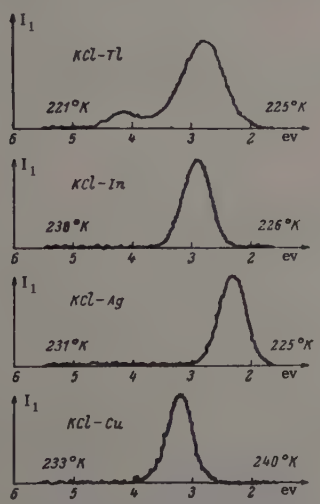

Fig. 2. Thermoluminescence spectra of KCl activated with Tl^+, In^+, Ag^+, and Cu^+ in the 220-240°K range. (The notation here is the same as in Figure 1.)

KCl-base phosphors activated with Tl^+, In^+, Ag^+, and Cu^+. These spectra were measured in the region of one of the primary thermoluminescence peaks near 220°K. It follows from these curves that when electrons are liberated from the same type of trap levels, the spectra of crystals containing various activator ions show an emission band corresponding to electron transitions in the activator ions. This result rigorously demonstrates the spatial distinctness of the electron traps and the emission centers; i.e., the recombination character of the phosphorescence of alkali halide crystals.

The author of this paper extends his profound thanks to Ch. B. Lushchik for proposing the topic and for his guidance.

REFERENCES

1. F. Urbach and O. Wien, Ber. **139**, IIa, 353 (1930); N. A. Brilliantov and Z. L. Morgenshtern, Zhur. Eksptl. i Teoret. Fiz. **8**, 401 (1938); M. L. Kats and R. E. Solomonyuk, Doklady Akad. Nauk SSSR **24**, 682 (1939); M. N. D'yachenko, Zhur. Eksptl. i Teoret. Fiz. **10**, 288 (1940); J. Randall and M. Wilkins, Proc. Roy. Soc. **A184**, 366 (1945); V. V. Antonov-Romanovskii, Izvest. Akad. Nauk SSSR, Ser. Fiz. **10**, 477 (1946); I. A Parfianovich, Zhur. Eksptl. i Teoret. Fiz. **26**, 697 (1954).
2. Ch. B. Lushchik, Trudy Inst. Fiz. i Astron., Akad. Nauk Eston.SSR No. 3, 3 (1955).
3. Ch. B. Lushchik, Zhur. Eksptl. i Teoret. Fiz. **30**, 488 (1956); Trudy Inst. Fiz. i Astron., Akad. Nauk Eston. SSR No. 1, 57 (1955); Ch. B. Lushchik, F. N. Zaitov, Kh. A. Myagi, and K. Yu. El'ken, Zhur. Eksptl. i Teoret. Fiz. **30**, 403 (1956); Ch. B. Lushchik and F. N. Zaitov, Trudy Inst. Fiz. i Astron., Akad. Nauk Eston.SSR No. 4, 53 (1956); F. N. Zaitov and V. Ya. Kark, Ibid., No. 6, 82 (1957).
4. W. Meyeren, Z. Physik **61**, 321 (1930); K. K. Shvarts, Trudy Inst. Fiz. i Astron., Akad. Nauk Eston.SSR No. 7, 153 (1957).
5. N. E. Lushchik, Trudy Inst. Fiz. i Astron., Akad. Nauk Eston. SSR No. 6, 149 (1957).
6. R. C. Dutta and A. K. Ghosh, Indian J. Phys. **30**, 570 (1956); A. Halperin and N. Kristianpoller, J. Opt. Soc. Am. **48**, 996 (1958).
7. Ch. B. Lushchik and V. I. Volin, Trudy Inst. Fiz. i Astron., Akad. Nauk Eston.SSR No. 7, 311 (1958).

ZONAL SENSITIVITY OF PbS PHOTOCONDUCTORS

M. N. Markov and E. P. Kruglyakov

Received 8 April 1960

The zonal sensitivity of radiation detectors plays a large part in their use for purposes of photometry, spectrometry, etc. Zonal sensitivity has often been studied in connection with detectors for photoelements, photomultipliers, and low inertia bolometers.[1,2] Lead sulfide photoconductors are of particular interest in this connection since the nature of their sensitivity has been shown by numerous investigations to be determined by the phenomena at the boundaries of the individual crystals, which create the detecting surface in the form of intercrystalline barriers.[3,4] Hence the study of zonal sensitivity has both practical and theoretical significance. The zonal sensitivity of standard lead sulfide photoconductors of the FSA-1 type was studied in the present investigation. In our case, light from a radiation source (a small incandescent lamp) was focused with the help of a lens and objective on the surface of the photoconductor. The photoconductor was moved at a uniform rate with respect to the fixed image of the light spot. The time required for passage of the spot over the entire length of the detector surface (3.5 to 4 mm) was 1.5 to 2 min. The light falling on the photoconductor was modulated at a frequency of 750 cps. The signal from the photoconductor was amplified by an ac amplifier and read on an LV-9M vacuum tube voltmeter and an EPP-09 automatic potentiometer connected in parallel with it. The illuminated spots were of two kinds: a circular spot with a diameter of about 30 μ, and a slit 3 to 4 mm long and approximately 0.1 mm wide (the second type is of practical interest in the use of photoconductors in spectroscopy). The total number of photoconductors studied was 35.

This study of the photoconductors showed that numerous sensitivity maxima and minima are disposed randomly over their surfaces. The mean diameter of the peaks is of the order of the size of the light spot. Increasing the diameter of the spot (by defocusing without changing the light flux) decreases both the number of peaks and their relative magnitude. Changing the current through the photoconductor within its rated range does not change the location and relative heights of the peaks. It is possible to divide the sensitive regions on the surface of the photoconductors into two approximately equal groups according to their distribution patterns. Photoconductors of the first group (Fig. 1) have well defined sensitivity maxima, usually located near the contacts. In some samples in this group the height of the maxima depends on the polarity of the power supply, and changes if the polarity is reversed. Photoconductors of the second kind have a multitude of maxima distributed randomly over the sensitive surface (Fig. 2). It should be pointed out, however, that the sensitivities of the two groups were similar (to within 20%) when the entire sensitive surface was uniformly illuminated.

Since the sensitivity of PbS photoconductors is connected with the phenomena occurring at intercrystalline barriers, local increases of resistance may be expected in these regions. We have compared the values of sensitivity and resistance.

For this purpose, additional contacts were placed at points b and c (cf. Fig. 1) and the distribution of voltage

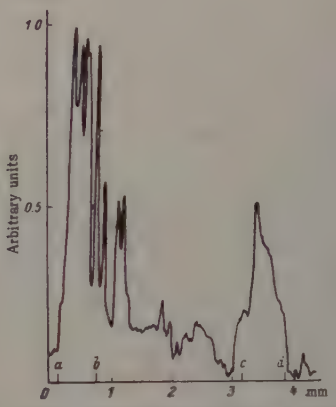

Fig. 1. Zonal sensitivity of FSA-1 photoconductor of the first group. Ordinates—sensitivity. Abscissae—distance from contact. The photoconductor contacts are at points a and d; the additional contacts are at points b and c.

between points a, b, c, and d measured, along with th total current through the photoconductor. Typical res are shown in the Table.

Type of Area	R_{ps} (ohms)	r_{ps} (ohms/mm)	R_{ab} (ohms)	r_{ab} (ohms/mm)	R_{cd} (ohms)	r_{cd} (ohms/mm)	R_{bc} (ohms)	(oh
1	194	51	57	82	92	102	45	
2	216	57	34	48	52	58	130	

R_{ps} is the total resistance of the sample and r_{ps} the resistance of a unit length of the photosensitive la R_{ab}, R_{cd}, and R_{bc} are the total resistances, and r_{ab}, and r_{bc} the resistance of a unit length of correspondi parts of the photosensitive layer. The first line gives for photoconductors of the first group; the second for photoconductors of the second group. As is seen in th first case, the resistance of the areas near the contac having higher zonal sensitivity is significantly greate than the resistance at the center. In the second case, both the sensitivity (on the average) and the resistanc are almost identical. Hence the values of the sensitiv and resistance are related not only for the photocondu as a whole, but for its separate parts as well.

Figure 3 shows the results of measuring the zona sensitivity of photoconductors of the first group by sc ning the surface parallel to the contacts of the photoc ductor with a light spot in the form of a slit 0.1 mm w and 4 mm high. It is seen in this case that the maxim near the contacts are quite broad, and that the sensiti at these maxima is more than three times as great a sensitivity at the center of the photoconductor. Comp ing the two types of illumination—defocusing but illun nating the whole surface, on the one hand, and focusin the same light flux on a 0.1×4 mm area near a conta on the other hand—we found that the sensitivity is als approximately three times higher in the latter case.

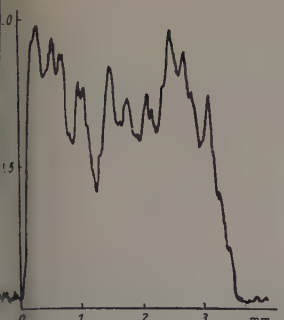

Fig. 2

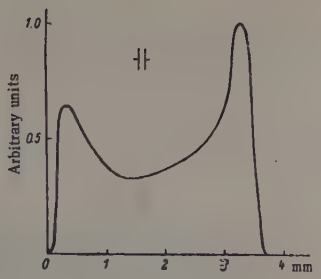

Fig. 3

Fig. 2. Zonal sensitivity of FSA-1 photoconductor of the second group. Notation same as in Fig. 1.

Fig. 3. Zonal sensitivity of FSA-1 photoconductor of the first group, scanned parallel to the contacts with a 0.1×4 mm spot. Notation same as in Fig. 1.

nsitivity threshold improves by the same amount. How-er, it is possible to reduce the threshold sensitivity ll more by taking the signal directly to the amplifier from the illuminated area (for example, cd, Fig. 1). An estimate will show that for photoconductors whose resistance distribution is shown in the Table, when the mean square noise value and resistance are related as $U_n = \text{const.}\sqrt{R^5}$ and $R_n \gg R_{ps}$, the ratio of the noise voltage of the whole photolayer to that of the part cd is $U_{nad}/U_{ncd} = \sqrt{R_{ps}/R_{cd}} \sim 1.5$. As a result the threshold sensitivity improves by at least a factor of 4. We note that under these conditions, the photoconductors of the second group show only a twofold improvement in threshold sensitivity. Thus a correct choice of illumination and circuit conditions will substantially improve the photoconductor sensitivity threshold.

REFERENCES

1. K. Kessler and R. Wolfe, J. Opt. Soc. Am. **37**, 133 (1947).
2. E. N. Wormser, J. Opt. Soc. Am. **43**, 15 (1953).
3. L. Sosnowski, J. Starkiewcz, and O. Simpson, Nature **159**, 818 (1947).
4. A. F. Gibson, Proc. Phys. Soc. **64** B, 603 (1951).
5. A. I. Goryachev and K. A. Yumatov, Radio and Electricity **1**, 1503 (1956).

FLUORESCENCE YIELDS OF ACETYLANTHRACENES IN SOME SOLVENT MIXTURES

A. S. Cherkasov

Received 27 April 1960

We have already demonstrated[1,2] that an addition of all amounts of hydroxyl-containing solvents to a solu-n of acetylanthracenes in hexane causes a sharp dis-acement of the fluorescence spectra. As a result of ther investigations, it has been established that the ectral displacement is accompanied simultaneously by ery marked change in fluorescence yields. Values of relative fluorescence quantum yields were determined ratios of the areas under fluorescence spectral curves tained under identical conditions. Solutions of identical ncentrations (2×10^{-5} mole/liter) were compared, as-ming that they all absorb the same amount of energy m the exciting light (366 mμ). The absence of a con-l oc the true absorption does not introduce a large ror, since it was established by preliminary measure-nts that the absorption spectra of acetylanthracenes, the various solvents, differ only insignificantly from ch other, and the absorption coefficients in the excita-n region do not differ by more than 10%. No correction as made for the difference in refractive index.

Curves of the change of fluorescence yields of 2-etylanthracene (the value of the fluorescence quantum eld in hexane was taken as unity) in various solvents d their mixtures,* are presented in Fig. 1. The smal-

he general nature of the dependence obtained for 1-etylanthracene is analogous to that presented here for acetylanthracene, only the absolute yield is 2 to 3 times ss.

st yield of the studied solvents (methanol, ethanol, n-tanol, benzyl alcohol, pyridine, acetone, dioxane, and hexane) is observed for n-hexane.* The addition of any

sing an absolute value of 0.70 for the quantum yield of acetylanthracene in ethanol (determined using a solu-on of anthracene in ethanol as a standard, the absolute yield of which, according to Bowen,[3] is 0.22), the absolute yield in hexane is 0.03.

of these solvents to a hexane solution of acetylanthracene produces an increase in fluorescence yield. With an increase in concentration of dioxane, pyridine, and acetone, the yield increases almost linearly, but upon addition of the alcohols,* a particularly sharp increase in yield is

*The addition of acetic acid has a similar effect.

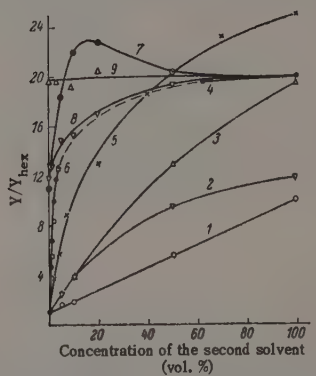

Fig. 1. The change in value of the relative fluorescence quantum yields of 2-acetylanthracene in relation to the solvents and their mixtures. Curve 1—hexane (I) + dioxane (II); curve 2—I + acetone (III); curve 3—I + pyridine (IV); curve 4—I + methanol (V); curve 5—I + n-octanol; curve 6—I + benzyl alcohol; curve 7—II + V; curve 8—III + V; curve 9—IV + V.

observed at small concentrations. The curves of fluorescence yield versus alcohol concentration are very similar to the curves showing the position of maximum fluorescence versus concentration, for the corresponding mixtures.[2] It is natural to assume that small additions of alcohols to hexane cannot produce such a substantial change in the macroscopic properties of the liquid (for example, ε and n) as to cause such a strong spectral displacement and increase in yield for that reason. In this instance, it is assumed that the effect is caused mainly by a specific interaction of the alcohols with the excited acetylanthracene molecules, which evidently results in the formation of hydrogen bonds. A similar increase in fluorescence yields, in solvents capable of hydrogen bond formation, is observed for acridine and its derivatives.[4]

A study of the fluorescence spectra of 2-acetylanthracene in mixtures of three solvents, has established[1] that the addition to a hexane solution, containing 0.2-0.5% methanol, of a third solvent, capable of hydrogen bond formation with methanol (pyridine, dioxane, etc.), can neutralize the effect of the alcohol to a certain extent. This gave rise to a fluorescence spectrum similar in position and shape to that of a mixture not containing alcohol. It was found that this effect produces a change in fluorescence yields. Thus, for example, the addition of acetone (10% by volume) to a hexane solution of 2-acetylanthracene, containing 0,5% methanol, increases the relative yield from 4.7 to 6.8. This is natural, since the addition of acetone to a hexane solution not containing alcohol also produces an increase in yield (from 1 in hexane to 3.8 in 10% acetone by volume). Acetone is a solvent which has a weak reaction with alcohol. However, if, to a solution containing alcohol, pyridine or dioxane are added (which, judging by their effect on the fluorescence spectra, react more strongly with alcohol than does acetone), the fluorescence yield is decreased, in spite of the fact that these solvents increase the yield of hexane solutions not containing alcohol.* This apparent

*For pyridine in a hexane solution, containing 0.5% methanol, the relative fluorescence yield is 4.1 as compared to 4.7 in the absence of pyridine; at the same concentration of dioxane in a hexane solution containing 0.25% methanol, the yield is 2.3 as compared to 2.9 in the absence of dioxane; at these same concentrations of pyridine and dioxane in a hexane solution not containing alcohol, the yields are 3.9 and 1.8 respectively.

anomaly may be explained by the interaction of pyridine and dioxane with alcohol which weakens its bond with the excited acetylanthracene molecules (or decreases the concentration of its complexes with acetylanthracene); this produces a value for the fluorescence yield similar to that for a mixture not containing alcohol.

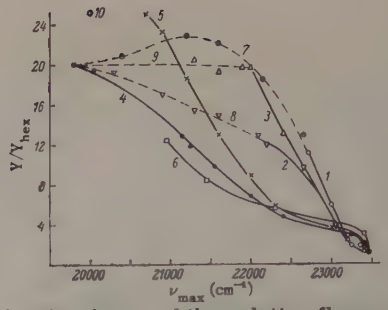

Fig. 2. The change of the relative fluorescence quantum yields in relation to the position of maximum fluorescence. The designations are the same as for Fig. 1.

Zelinskii and co-workers,[5] on the basis of their e perimental data, concluded that the value of the fluorescence yield for a substance is determined by the position of the fluorescence maximum, regardless of t solvent used. However, this rule is not verified in our instance. This is clearly evident from Fig. 2, in which the values of the relative fluorescence quantum yields various solvents and their mixtures are presented as function of the position of maximum fluorescence. Although for each given mixture of solvents there is a de nite relation between these values, there are marked differences between various mixtures (thus, for exam for a position of maximum fluorescence of 21,500 cm^{-1} the relative yield changes from 8 in a mixture of benz alcohol and hexane to 22 in a mixture of methanol and dioxane). In changing from pyridine to methanol, the position of the fluorescence maximum is shifted from 22,000 cm^{-1} to 19,800 cm^{-1}, whereas the fluorescence yield remains constant (~20) over this range. From th data examined, it follows that the conclusion regarding the determining role (for the value of the fluorescence quantum yield) of the position of maximum fluorescen has its limitations.

REFERENCES

1. A. S. Cherkasov, Doklady Akad. Nauk SSSR **130**, 12 (1960).
2. A. S. Cherkasov, Izvest. Akad. Nauk SSSR, Ser. Fi **24**, 591 (1960).
3. E. J. Bowen and A. Norton, Trans. Faraday Soc. 3 44 (1939).
4. N. Mataga and S. Tsuno, Naturwiss. **44**, 304 (1957)
5. V. V. Zelinskii, V. P. Kolobkov, and L. G. Pikulik, Opt. i Spektr. **1**, 161 (1956).

THE INFLUENCE OF TEMPERATURE ON TWO SERIES OF BANDS IN THE GREEN FLUORESCENCE SPECTRUM OF PURE CADMIUM SULFIDE AT LOW TEMPERATURE

M. Bancie-Grillot, E. F. Gross, E. Grillot, and B. S. Razbirin

Received 3 May 1960

Very pure cadmium sulfide, which does not luminesce at room temperature, displays an intense green fluorescence when the crystal is cooled to liquid air temperature. Kroeger[1] had shown in 1940 that the spectrum of this fluorescence has a characteristic structure, consisting of a series of bands separated by intervals of approximately 300 cm^{-1}. This phenomenon, which has considerable theoretical importance and is connected with the possibility of localizing this radiation in the crystal lattice, has been under discussion for some time.[2] Two of us discovered[3] a pronounced variability of different properties of this green fluorescence, which was dependent on the method of production of each crystal of pure cadmium sulfide and which is explained by a localization of the emission process at specific lattice defects.

It was shown on the CdS samples used by Furlong and Ravilious[2] to repeat the investigation of the properties of this fluorescence that the emission spectrum of the crystal was still more complex at 4°K. At this temperature, new bands of relatively low intensity appear among the intense bands observed at 77°K. According to the data of these authors, the whole spectrum, in this case, is represented by two vibrational series. In an investigation at 20°K, using pure CdS prepared by seven different methods, it was shown that two series of bands with maxima located (within an accuracy of 10 cm^{-1}) at $\nu_1 = 19450 - 300\,n\ cm^{-1}$ for the first series and $\nu_2 = 19310 - 300\,p\ cm^{-1}$ for the second series, can be observed either separately or simultaneously (n and p are small integers).

During our investigation of the luminescence of different cadmium sulfide crystals at different temperatures, we observed a peculiar influence of temperature on the relative intensity of the bands in the two series. We therefore undertook a qualitative investigation of this effect between 4° and 77°K.* The following facts were observed: In those crystals in which only the second series can be observed at 4°K the intensity of the bands depends on the temperature of the sample; the bands become weaker upon heating, but remain in their original positions. At the same time, the spectrum shows weak bands of the first series, whose intensity increases with increasing in temperature. The bands of the two series have comparable intensities at a certain fixed temperature. Finally, the bands of the second series completely disappear near the boiling point of liquid nitrogen, while the intensity of the first series approaches that which the second series had shown at 4°K. The resolution of the structure becomes noticeably poorer as the crystal is heated from 4° to 77°K.

When the green fluorescence spectrum at 4°K consists only of bands of the first series, heating the sample from 4° to 77°K does not lead to the appearance of second-series bands. Only bands of the first series are observed, and these do not noticeably change their position in the process of heating up. Likewise, the band intensity is not substantially changed by a rise in temperature, although some enlargement of the bands is noticeable. In crystals showing both series at 4°K, a redistribution of intensities is observed upon warming. Bands of the second series gradually fade and only the first series remains at 77°K, more intense, although somewhat diffuse. This effect is shown schematically in Fig. 1.

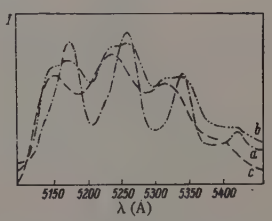

Fig. 1. Temperature dependence of the band intensity of two series in the green luminescence spectrum of a CdS crystal between 4° and 77°K. Temperature (in °K): curve a—4; curve b—$4 < T < 77$; curve c—77.

We observed a similar redistribution of intensities among the bands of the two series by applying an electric field to the crystal immersed in liquid helium. Increasing the strength of the applied field to approximately 1 kv/cm increased the intensity of first-series bands and considerably weakened the second series bands, as shown in Fig. 2. We reported this effect at the Conference on Energy Migration in Paris.[4] We are continuing our research in this direction in order to try to find out whether we are really dealing here with a specific action of the electric field and not with heating which is caused by the Joule effect, in spite of the immersion of the crystal in liquid helium.

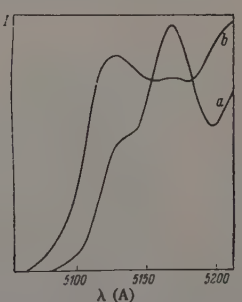

Fig. 2. Microphotometer tracing of the short-wavelength part of the green luminescence spectrum of pure CdS crystals at 4.2° (2 series of bands are present simultaneously). Curve a—in absence of an electric field; curve b—under the influence of an electric field (E = 1 kv/cm). Both spectra were obtained on the same photographic plate. The exposure used for curve a was one fifth of that used for curve b.

*The authors express their gratitude to the director of the cryogenic laboratory, N. M. Reinov, for his kind help in working with liquid helium.

REFERENCES

1. F. A. Kroeger, Physica 7, 1 (1940).
2. C. C. Klick, J. Opt. Soc. Am. 41, 816 (1951); Phys. Rev. 96, 274 (1953);
   C. Wendel, Fortschr. Physik 1, 4 (1953);
   F. A. Kroeger and H. T. G. Meyer, Physica 20, 1149 (1954);
   L. R. Furlong, Phys. Rev. 95, 1086 (1954);
   L. R. Furlong and C. F. Ravilious, Phys. Rev. 98, 9 (1955).
3. E. Guillot, J. phys. radium 17, 624, 795 (1956).
   E. Guillot and M. Bancie-Guillot, "Festkörperphys und Physik der Leuchtstoffe" (Physics of Solids an Physics of Luminescent Materials), Akademie Verl Berlin, 1958; Izvest. Akad. Nauk SSSR, Ser. Fiz. 22 1357 (1958).
4. E. Grillot, J. Chim. Phys. 55, 642 (1958).

NEW EXAMPLES OF A PRONOUNCED DEPENDENCE OF FLUORESCENCE YIELD ON THE POSITION OF THE EMISSION SPECTRUM

E. N. Viktorova, A. S. Kochemirovskii, N. D. Krasnitskaya, and I. I. Reznikova

Received 20 May 1960

Five derivatives of phthalimide investigated by Zelinskii, Kolobkov, and Pikulik[1] showed a regular relationship between the absolute quantum yield of fluorescence ($q_{fl.}$) at 20°C in various solvents and the frequency of the maximum of the fluorescence spectrum ($\nu_{fl.}^{max.}$). It was shown in refs. 2 and 3 that there is also a correlation between the values $q_{fl.}$ and $\nu_{fl.}^{max.}$ for aminochlormaleinimide and acridine.

It is demonstrated in the present paper that a similar dependence of $q_{fl.}$ on $\nu_{fl.}^{max.}$ exists in three compounds which are not phthalimide derivatives, and which belong to different classes of organic compounds.

The measurement of yields was made by the method described previously.[4] The dependence of the $q_{fl.}$ on $\nu_{fl.}^{max.}$ at 20°C is shown in the figure for dimethylnaphthyrhodine (I), 2-amino-acridine (II) and cyclohexylaminomaleinimide (III).

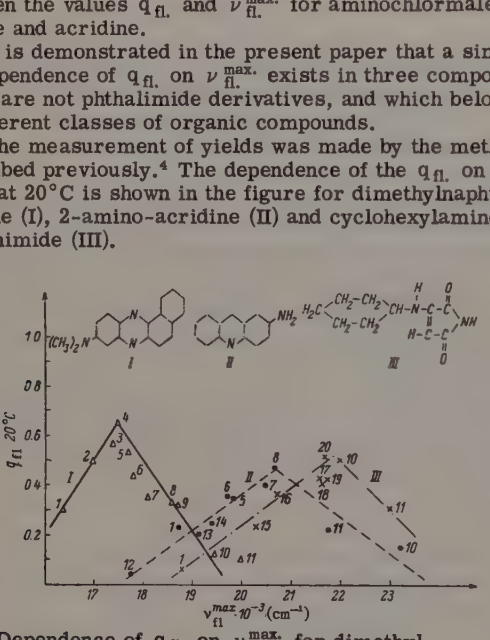

Dependence of $q_{fl.}$ on $\nu_{fl.}^{max.}$ for dimethylnaphthyrhodine (I), 2-aminoacridine (II) and cyclohexylaminomaleinimide (III). Numbering of solvents: 1—ethyl alcohol; 2—cyclohexanol; 3—cyclohexanone; 4—pyridine; 5—ethyl acetate; 6—dioxane; 7—chloroform; 8—benzene; 9—diethyl ether; 10—carbon tetrachloride; 11—n-octane; 12—water; 13—diisopropyl ether; 14—acetone; 15—orthoformic ether; 16—propyl acetate; 17—toluene; 18—meta-xylene; 19—Ortho-xylene; 20—Chlorobenzene.

As can be seen from the data, there is a clearly apparent dependence of $q_{fl.}$ on $\nu_{fl.}^{max.}$ in all compounds investigated. Thus in compound I there is a steady increase in $q_{fl.}$ as $\nu_{fl.}^{max.}$ is progressively increased (beginning with $\nu_{fl.}^{max.} = 16400$ cm^{-1} in ethyl alcohol). It should be emphasized that the increase of $q_{fl.}$ with increasing ν is of such a nature that the points fall near a straight line. In the case of compound I, $q_{fl.}$ increases to 0.05 pyridine ($\nu_{fl.}^{max.} = 17500$ cm^{-1}) and then begins to decre gradually with increasing $\nu_{fl.}^{max.}$. When $q_{fl.}$ decreases increasing $\nu_{fl.}^{max.}$, the points are also grouped about a straight line; in this case, nine points fall near the str line between 17500 cm^{-1} and 20000 cm^{-1}. The point co responding to the $q_{fl.}$ value in n-octane deviates some what from the straight line.

In the case of compound II, the points correspondi to values of $q_{fl.}$ between 17750 cm^{-1} and 20700 cm^{-1} i eight different solvents fall near the line with only a v insignificant scattering. The maximum value of $q_{fl.}$ f compound II is observed in benzene at $\nu_{fl.}^{max.} = 20700$ c $q_{fl.}$ decreases with a further increase of $\nu_{fl.}^{max.}$ to 232 cm^{-1}. Among the solutions of the compound measured point corresponding to the value of $q_{fl.}$ in pyridine fal considerably out of line, with $\nu_{fl.}^{max.} = 18750$ cm^{-1} and $q_{fl.} = 0.4$-0.42.

Compound III also shows a steady increase of q with increasing $\nu_{fl.}^{max.}$ between 18800 and 22000 cm^{-1}, dependence again being linear. The $q_{fl.}$ values in tolu meta-xylene, and ortho-xylene deviate somewhat from the straight line. The $q_{fl.}$ values tend to decrease wit further increase in $\nu_{fl.}^{max.}$.

It can also be seen in the drawing that in all of th newly investigated compounds (I, II, III) there are two fa clearly expressed branches of the dependence of $q_{fl.}$ $\nu_{fl.}^{max.}$ (the same was true in the dependence of $q_{fl.}$ on $\nu_{fl.}^{max.}$ for the previously investigated phthalimide deri tives). Let us call branch A the branch with the positi slope and branch B the branch with the negative slope Let us point out that only a single branch is present i some of the compounds investigated previously. Thus only branch A was found in aminochlormaleinimide.[2] branch B was found in acridine, according to ref. 3.

The existence of only one branch in the case of a dine indicates that the solvent which causes the large red shift of the fluorescence spectrum (trichloroaceti acid[3,5]) still does not displace the fluorescence spectr of this compound far enough to make branch A appear the case of aminochlormaleinimide, the presence of o a single branch is explained by the fact that in this ca the solvent giving the largest blue shift (octane) again does not shift the fluorescence spectrum far enough t make branch B appear.

The presence of two branches, A and B, of the de pendence of $q_{fl.}$ on $\nu_{fl.}^{max.}$ was interpreted as an expre

on of the existence of two independent deactivation ocesses. The supposition was advanced that each one these deactivation processes is determined solely by e relative positions of the potential surfaces of the ound and excited states of the fluorescent molecules. ne relative positions of the potential surfaces of the ound and excited states are changed by going over from ie solvent to another, so that the probabilities of the de- tivation processes are also changed. According to this terpretation, this dependence of $q_{fl.}$ on $\nu_{fl.}^{max.}$ must be latively general.

The absence of any specific action of solvents on the n. value is indicated by the fact that the experimental ints fall well on the branches A and B. This can only be consequence of the action of a single factor on the $q_{fl.}$ lue in all solvents.

It follows from the data given that, in studying the fluence of the solvent on the fluorescence spectra of ganic compounds, it is necessary to take particular count of the relative position of the potential curves of ie ground and the excited states of the fluorescent mole- ules in a given solvent. It seems to be necessary, in the ght of the data given above, to examine the influence of ie solvent on the yields described in refs. 6 and 7, where shift in the position of the spectrum was found, together ith a change in the luminescence yield.

The data obtained in the present paper thus indicate that the dependence of $q_{fl.}$ on $\nu_{fl.}^{max.}$ found for phthalimide derivatives in ref. 1 is not specific for these compounds, but appears to be a relatively general rule.

In conclusion, the authors wish to express their deep gratitude to V. V. Zelinskii, under whose immediate direction this work was carried out.

REFERENCES

1. V. V. Zelinskii, V. P. Kolobkov, and L. G. Pikulik, Opt. i Spektr. 1, 161 (1956).
2. V. V. Zelinskii, V. P. Kolobkov, and N. D. Krasnitskaya, Opt. i Spektr. 4, 417 (1959).
3. A. S. Kochemirovskii and I. I. Reznikova, Opt. i Spektr. 8, 399 (1960), Optics and Spectroscopy 8, 206 (1960).
4. V. V. Zelinskii, V. P. Kolobkov, and L. G. Pikulik, Opt. i Spektr. 1, 570 (1956).
5. I. A. Zhmyreva, V. V. Zelinskii, V. P. Kolobkov, and N. D. Krasnitskaya, Doklady Akad. Nauk SSSR 129, 1089 (1959).
6. V. A. Kizel and U. I. Safronova, Opt. i Spektr. 5, 482 (1958).
7. E. I. Bowen and S. F. A. Miskin, J. Chem. Soc. 3172 (1959).

THE INDICATRIX OF RAMAN SCATTERING

N. K. Sidorov

Received 27 May 1960

The Placzek formulas for the indicatrix of Raman cattering were deduced in a previous work under this tle.[1] However, starting from a knowledge of the inten- ity components of the scattered light, we can simply and raphically obtain these formulas from those obtained in ef. 2. For natural light, propagated along the x-axis, e have:[2]

$$I_{0z} \sim I_0 \frac{2}{15}(A-B)\sin^2\theta_z = I_0 \frac{2}{15}(A-B)\sin^2\varphi,$$

$$I_{0y} \sim I_0 \frac{1}{15}(4A+B)\sin^2\theta_y,$$

$$I_{0x} \sim I_0 \frac{1}{15}(4A+B)\sin^2\theta_x,$$

here $A = a_\xi^2 + a_\eta^2 + a_\zeta^2$, $B = a_\xi a_\eta + a_\eta a_\zeta + a_\zeta a_\xi$, and a_σ $\sigma = \xi, \eta, \zeta$) are the polarizability tensor components in ie molecular coordinate system. Considering that $\cos^2\theta_x + \cos^2\theta_y + \cos^2\theta_z = 1$, where θ_x, θ_y, and θ_z are ie angles between the direction of observation and the espective axes of the coordinate system x, y, and z, we btain

$$I = I_{0x} + I_{0y} + I_{0z} \sim I_0\left\{\frac{1}{15}(6A-B) + \frac{1}{15}(2A+3B)\cos^2\varphi\right\},$$

i.e., formula 10 of ref. 1. Here φ is the angle between he direction of propagation of the exciting light and the direction of observation.

For light polarized along the z-axis and propagated along the x-axis, we have:[2]

$$I_{0x} \sim I_0 \frac{1}{15}(A-B)\sin^2\theta_x,$$

$$I_{0y} \sim I_0 \frac{1}{15}(A-B)\sin^2\theta_y,$$

$$I_{0z} \sim I_0 \frac{1}{15}(3A+2B)\sin^2\theta_z = I_0 \frac{1}{15}(3A+2B)\sin^2\theta,$$

from which we obtain

$$I = I_{0x} + I_{0y} + I_{0z} \sim I_0\left\{\frac{1}{15}(4A+B) - \frac{1}{15}(2A+3B)\cos^2\theta\right\}$$

i.e., formula 12 of ref. 1. θ is the angle between the direction of observation and the electric vector.

REFERENCES

1. I. I. Kondilenko, P. A. Korotkov, and V. L. Strizhevskii, Opt. i Spektr. 8, 471 (1960), Optics and Spectroscopy 8, 249 (1960).
2. M. V. Vol'kenshtein, "Molekulyarnaya Optika" (Molecular Optics), pp. 220-221, 372. Gosudarst. Izd. Tekh.-Teoret. Lit., Moscow and Leningrad, 1951.

THE EFFECT OF VITRIFICATION ON THE POLARIZATION OF THE PERSISTENT LUMINESCENCE OF ORGANIC SUBSTANCES

E. V. Anufrieva

Received 12 April 1960

Vitrification of a polymer or of a low molecular weight liquid amounts to a freezing of some of the degrees of freedom of the molecule. The mobility of macromolecules or of some of their parts is almost completely lost in the vitreous state.[1,2] We selected the method of polarized luminescence in order to investigate the mobility of macromolecules in the block. It is known that the polarization of luminescence is determined by the viscosity and temperature of the medium, and also by the lifetime of the luminescent molecule in the excited state. The depolarization of luminescence can be used as a measure of the participation of the luminescent molecule in the Brownian rotational movement. It has been shown[3] that the method of polarized luminescence permits one to determine the conditions under which there is a Brownian rotation of a luminescent molecule introduced into the polymer. The polarization of the ordinary ($\tau \approx 10^{-8}$ sec) and the "retarded" ($\tau \approx 1$ sec) fluorescence of rhodulin orange in polyvinyl alcohol (PVA) does not change with temperature in the range $T < T_g$ of PVA. (T_g is the vitrification temperature.) In the range $T > T_g$ of PVA, the polarization of ordinary fluorescence remains constant, but the polarization of "retarded" fluorescence decreases with increasing temperature. This indicates that Brownian rotation of a luminescent molecule is not completed in vitreous PVA in 10^{-8} sec, or even in 1 sec. In a highly elastic state, this rotation requires a time of the order of ~1 sec, which is considerably longer than the fluorescence lasts. In order to study the depolarizing action of Brownian movement as a function of time, the change of polarization of the persistent luminescence of the polymer during decay has been investigated in the ranges $T < T_g$ and $T > T_g$.

The polarization of persistent luminscence during decay was measured on the systems polyvinyl alcohol (PVA)-rhodulin orange and glucose-rhodulin orange over the temperature interval 20-120°C, i.e., in the $T < T_g$ and $T > T_g$ ranges of the system. T_g of PVA is 80°C; T_g of glucose is 36°C.[4] The PVA samples investigated were prepared as 30μ films by dissolving rhodulin orange and PVA together and removing the solvent. A thin layer of glucose colored with rhodulin orange was applied to a glass plate at a temperature above the T_g of glucose. The concentration of rhodulin orange in PVA and in glucose was 0.1%. The samples were placed in a thermostating apparatus which was heated with water from an ultrathermostat.

An SVDSh-250-3 mercury lamp was used to excite the luminescence; a filter was used to isolate the mercury line at 436 mμ. The investigations were made on an apparatus consisting of a polarizer, an analyzer (Nicol prism), two photographic shutters, and an FEU-19 photomultiplier. The signal from the FEU-19 was fed to an ENO-1 oscilloscope. Decay curves of the persistent fluorescence were observed on the oscilloscope screen with the electrical vector parallel and perpendicular to the vector of the exciting light, $I_\parallel$ and $I_\perp$. The polarization of luminescence at the time t after excitation was determined from the ratio

$$P = \frac{I_\parallel - I_\perp}{I_\parallel + I_\perp}.$$

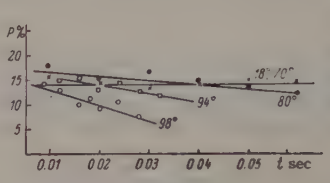

Fig. 1

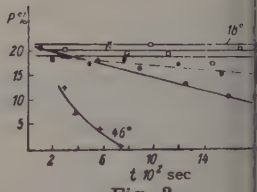

Fig. 2

Fig. 1. Change of polarization during decay of the persistent luminescence of rhodulin orange in polyvinyl alcohol at various temperatures.

Fig. 2. Change of polarization during decay of the persistent luminescence of rhodulin orange in glucose at various temperatures.

The P(t) functions obtained are shown in Figs. 1 and

It was found that the polarization of the persister luminescence remains unchanged during decay over t whole temperature interval below the T_g of the syste This is the case for polyvinyl alcohol as well as for g cose. The polarization of the persistent luminescenc decreases during decay at temperatures above the T the system.

The difference in the initial polarization values a different temperatures (Fig. 1) can be explained by a crease in the rate of decay of luminescence at high te peratures and by a substantial error in the determina of the absolute value of polarization brought about un these conditions by dissimilar operation of the photo- graphic shutters during the tracing of the afterglow c $I_\parallel$ and $I_\perp$. Initial polarization values of the persisten minescence of rhodulin orange in vitreous PVA and gl agree with the degree of polarization of the fluoresce

The results obtained can be explained by assumi that Brownian motion is the cause of the change of po larization during decay. The absence of change in the polarization of persistent luminescence during decay the vitreous state is due to the freezing of the motion the luminescent molecule and the macromolecules su rounding it. The increase in the mobility of the macr molecules during the softening of the glass causes a c crease in the polarization of the luminescence. This crease becomes greater as the temperature of the m increases. Thus the luminescence of glucose is almo completely depolarized after 0.07 sec at 46°C. Kudri shov and Svechnikov detected the same phenomenon w they investigated the persistent luminescence of acri orange in a piece of sugar candy.[5]

The P(t) functions make it possible to determine relaxation time $\rho = 3\eta V/RT$ of luminescent molecule troduced into the polymer and to determine the local viscosity η of a polymer or of a low molecular weigh vitreous system.

The author is grateful to M. V. Vol'kenshtein for interest in this work and for valuable advice.

REFERENCES

1. P. P. Kobeko, "Amorfnye veshchestva" (Amorpho Substances). Izd. Akad. Nauk SSSR, 1952.

. M. V. Vol'kenshtein and O. B. Ptitsyn, Zhur. Tekh. Fiz. 26, 2204 (1956).
. E. V. Anufrieva and A. D. Zaitseva, Izvest. Akad. Nauk SSSR, Ser. Fiz. 24, 755 (1960).
. E. V. Anufrieva, M. V. Vol'kenshtein, and T. V. Razgovorova, Opt. i Spektr. 7, 505 (1959), Optics and Spectroscopy 7, 318 (1959).
5. B. Ya. Sveshnikov and P. I. Kudryashov, Izvest. Akad. Nauk SSSR, Ser. Fiz. 22, 1403 (1958).

APODIZATION

D. Yu. Gal'pern

Received 15 August 1960

Much work has recently been devoted to apodization; at is, to attempts to reduce the diameter of the Airey sc (the central diffraction disc in the image of a bright ot). An amplitude-phase filter is designed for this purse; this type of filter consists of a glass plate whose rface has a certain shape and whose transmission is fferent at different locations. This plate is inserted into e optical system at a plane conjugate with the aperture p and introduces a definite wave aberration and the quired distribution of amplitude at the aperture.

It is well known[1] that the distribution of illuminance ρ) at the image of a point infinitesimally close to the tical axis is given by the equation:

$$E(\rho) = \sqrt{C^2(\rho) + S^2(\rho)}, \tag{1}$$

ere:

$$S(\rho) = \int_0^{\sigma_{edge}} A_1(\sigma) \sin\left[\frac{2\pi}{\lambda} l(\sigma)\right] I_0\left(\frac{2\pi}{\lambda}\sigma\rho\right)\sigma d\sigma, \tag{2}$$

$$C(\rho) = \int_0^{\sigma_{edge}} A_1(\sigma) \cos\left[\frac{2\pi}{\lambda} l(\sigma)\right] I_0\left(\frac{2\pi}{\lambda}\sigma\rho\right)\sigma d\sigma, \tag{2a}$$

here σ_{edge} is the angle between the axis and a ray from edge of the aperture stop to a point on the image axis; is the angle between the axis and a ray from an arbiry point in the aperture to a point on the image axis; is the wavelength; ρ is the radius vector of the point of e image for which the illuminance is being calculated; $A_1(\sigma)$ is a coefficient defining the transmission at the nt in the aperture; $l(\sigma)$ is the wave aberration of the ; I_0 is the zero order Bessel function.

Setting $l(\sigma) < (1/4)\lambda$ and $A(\sigma) > 0$, that is, assuming at the wave aberration is less than a quarter wavelength, e can easily demonstrate the following general theorem: o filter can reduce the central diffraction disc by a factor greater than 1.6.

Using the first mean value theorem we can write:

$$S(\rho) = I_0\left(\frac{2\pi}{\lambda}\sigma_1\rho\right)\int_0^{\sigma_{edge}} A_1(\sigma)\sin\left[\frac{2\pi}{\lambda} l(\sigma)\right]\sigma d\sigma, \tag{3}$$

$$C(\rho) = I_0\left(\frac{2\pi}{\lambda}\sigma_2\rho\right)\int_0^{\sigma_{edge}} A_1(\sigma)\cos\left[\frac{2\pi}{\lambda} l(\sigma)\right]\sigma d\sigma. \tag{3a}$$

From (2) and (2a) we get:

$$S(0) = \int_0^{\sigma_{edge}} A_1(\sigma)\sin\left[\frac{2\pi}{\lambda} l(\sigma)\right]\sigma d\sigma, \tag{4}$$

$$C_0 = \int_0^{\sigma_{edge}} A_1(\sigma)\cos\left[\frac{2\pi}{\lambda} l(\sigma)\right]\sigma d\sigma, \tag{4a}$$

here σ_1 and σ_2 are certain numbers lying in the anges $0 \leq \sigma_1 \leq \sigma_{edge}$, $0 \leq \sigma_2 \leq \sigma_{edge}$.

From this,

$$S^2(\rho) = I_0^2\left(\frac{2\pi}{\lambda}\sigma_1\rho\right) S^2(0), \tag{5}$$

$$C^2(\rho) = I_0^2\left(\frac{2\pi}{\lambda}\sigma_2\rho\right) C^2(0). \tag{5a}$$

Assuming that $\rho \leq \lambda/2\sigma_{edge}$, that is, that ρ is smaller than the radius of the Airey disc, and choosing the number $\sigma_{1,2}$ equal to the smaller of the numbers σ_1 and σ_2, each of which is less than σ_{edge}, we get:

$$S^2(\rho)+C^2(\rho) \geq I_0^2\left(\frac{2\pi}{\lambda}\sigma_{1,2}\rho\right)\cdot[S^2(0)+C^2(0)]. \tag{6}$$

Dividing both sides of (6) by $S^2(0) + C^2(0)$, we find:

$$\bar{E}(\rho) = \frac{S^2(\rho)+C^2(\rho)}{S^2(0)+C^2(0)} \geq I_0^2\left(\frac{2\pi}{\lambda}\sigma_{1,2}\rho\right). \tag{7}$$

Using (4) and (4a), we find that the quantity $\bar{E}^2(0) = 1$. Replacing $\sigma_{1,2}$ in (7) by σ_{edge}, we merely strengthen the inequality:

$$\bar{E}(\rho) \geq I_0\left(\frac{2\pi}{\lambda}\sigma_{edge}\rho\right). \tag{8}$$

The whole derivation is only valid for values of ρ less than the quantity:

$$\rho_0 < \frac{x_1 x}{2\pi\sigma_{edge}}, \tag{9}$$

where x_1 is the first root of the function $I_0(x_0)$, since the function I_0 is positive for these values only.

It follows from (8) that as ρ varies from zero to ρ_0 the function $E(\rho)$ is not less than the function $I^2(2\pi/\lambda\sigma_{edge}\rho)$ for the same values of ρ.

Therefore, the radius of the central diffraction disc for arbitrary values of the function $A_1(\sigma)$ defining the distribution of amplitude at the aperture, and for wave aberrations less than $l(\sigma) \leq (1/4)\lambda$ cannot be less than:

$$\rho_{lim} = \frac{x_0 x}{2\pi\sigma_{edge}}. \tag{10}$$

For the Airey disc obtained in a system with no aberration and with a completely transparent aperture,

$$\rho_{lim} = \frac{y_0\lambda}{2\pi\sigma_{edge}}, \tag{11}$$

where y_0 is the root of the first order Bessel function; consequently

$$\frac{\rho_{lim}}{\rho_{lim}} = \frac{y_0}{x_0} = \frac{3.83}{2.40} = 1.6. \tag{12}$$

Consequently, under the conditions given above, the central disc cannot be reduced by a factor greater than 1.6.

REFERENCES

1. G. G. Slyusarev, "Metody rascheta opticheskikh sistem" (Methods of Designing Optical Systems, pp. 667-671 Gosudarst. Izd. Tekh.-Teoret. Lit., Moscow, 1937.

PERSONALIA

ABRAM FEDOROVITCH IOFFE'S 80th BIRTHDAY

On October 29, 1960 Academician Abram Fedorovich Ioffe will be eighty. Abram Fedorovich has devoted more than fifty-five years of his life to intense scientific work. One can scarcely name another scientist who has enjoyed such fame and popularity, not only among scientists of very different disciplines, but among the whole Soviet people.

A. F. Ioffe is the father and acknowledged head of the great family of Soviet physicists. From the very beginning of his scientific career Abram Fedorovich has always been surrounded by talented students. Working under his guidance, they rapidly developed into outstanding scientsts, leading whole movements or schools of Soviet physics; they created new institutes and solved important scientific and engineering problems. Very many scientists, occupying leading positions in experimental and theoretical physics and its engineering branches, are students and colleagues of Abram Fedorovich.

All the scientific activity of Abram Fedorovich is characterized by the extraordinary breadth of his interests, combining depth of physical investigations with the ability to perceive current problems and to relate them to engineering needs. In the field of the mechanical properties of crystals, the electrical properties of dielectrics, and, finally, the physics of semiconductors, Abram Fedorovich together with his many students and colleagues carried out a series of broad investigations. Without any exaggeration it can be said that the state of these fields of science today is the fruit of the conception and realization of many ideas of A. F. Ioffe.

A. F. Ioffe created the Physico-Technical Institute and later founded ten other scientific research institutes in our country, thus beginning the work on nuclear physics, agro-physics, and metal physics.

Abram Fedorovich was responsible for much research of a fundamental nature. At the outset of his scientific career Ioffe turned to the quantum theory of radiation, which revolutionized physics at the beginning of the century. In 1912 he completed a classical work on the elementary photoeffect, in which he showed that the photoeffect is due to the expulsion of individual electrons from the surface of the metal by light. Later, in 1924 A. F. Ioffe showed by direct experiments that the creation and propagation of x-rays occurs in individual quanta. Ioffe attached great importance to the experimental verification of wave mechanics which appeared in 1925-1926, and in 1928 he worked successfully on the polarization of electron waves.

His eightieth birthday finds Abram Fedorovich full of creative power. As always, he communicates to his

colleagues enthusiasm and tireless energy; as always is in the forefront of scientific progress.

In the name of all Soviet workers in optics and spectroscopy, the staff of the journal "Optics and Spectroscopy" congratulates Abram Fedorovich on this happy anniversary and wishes him good health and many years of fruitful work for the benefit and fame of our science.

The present issue of the journal "Optics and Spectroscopy" was already printed when we received the news that on October 14, 1960

ABRAM FEDOROVICH IOFFE

died suddenly. A. F. Ioffe's services to Soviet physics were very great. By his many-sided and tireless activity he influenced the development of almost all its branches. All Soviet physicists will long remember Abram Fedorovich, eminent scientist and outstanding personality.

TRANSLITERATION OF CYRILLIC CHARACTERS

used by the Optical Society of America

А	а	a	Р	р	r
Б	б	b	С	с	s
В	в	v	Т	т	t
Г	г	g	У	у	u
Д	д	d	Ф	ф	f
Е	е	e	Х	х	kh
Ж	ж	zh	Ц	ц	ts
З	з	z	Ч	ч	ch
И	и	i	Ш	ш	sh
Й	й	i	Щ	щ	shch
К	к	k	Ъ	ъ	"
Л	л	l	Ы	ы	y
М	м	m	Ь	ь	'
Н	н	n	Э	э	e
О	о	o	Ю	ю	yu
П	п	p	Я	я	ya

(FILLER MATERIAL - NOT IN RUSSIAN ORIGINAL)

OPTICAL SOCIETY OF AMERICA

OSA proposes to issue a bimonthly publication in the areas of applied optics, infrared and closely related industrial and scientific fields, e.g. physical, electron, space, ion, infrared and ultraviolet optics, lens design, optical engineering and instrumentation, plasma and solid state physics, to meet the growing demands of OSA membership for a medium of publication emphasizing, in addition to research papers, those of topical state-of-the-art interest, news re instruments, people, OSA and other meetings, book reviews and many other features to keep the opticist aware of what is happening in his branch of optics throughout the world, both in industry and on the campus. The newpublication will supplement JOSA, which will remain the archival journal of the Society. In the interests of fast publication, OSA is considering producing this bimonthly by the photo offset process (see OPTICS AND SPECTROSCOPY) which should give a publication time of approximately two months from acceptance by the Editor.

OSA dues will continue to provide JOSA and OiS; the purpose of this Questionnaire is to determine membership reaction to the new project. Would all members therefore be good enough to complete the Questionnaire sent them in July and to mail it back to the Executive Office without delay. (The card is already stamped and addressed.) Also, please fill in your name, affiliation and mailing address in the way you would like to see these appear in the new Membership Directory.

QUESTIONNAIRE

Would you subscribe to APPLIED OPTICS (a tentative title) at a cost of approximately $6.00 a year to members? ( ) Yes ( ) No.

Would you contribute to APPLIED OPTICS? ( ) Yes ( ) No.

If invited, would you contribute review articles, meetings, reports or book reviews in your area of competence? ( ) Yes ( ) No.

What is your area of interest?
Are you interested more in: ( ) Basic research ( ) Applied research
( ) A mixture of these two.

Comments:

Name _____ Membership No. _____

Affiliation _____

Mailing Address _____

(FILLER MATERIAL – NOT IN RUSSIAN ORIGINAL)

The Spectrum of the Negative Molecular Ion of Phthalocyanin . . . . . A. V. Shablya and A. N. Terenin 280 (533)
The Nonisothermal Relaxation of the Luminescence Spectra of X-Irradiated KCl Crystals Activated with Tl^+, In^+, Ab^+, and Cu^+ Ions . . . . . I. K. Vitol 282 (535)
Zonal Sensitivity of PbS Photoconductors . . . . . M. N. Markov and E. P. Kruglyakov 284 (538)
Fluorescence Yields of Acetylanthracenes in Some Solvent Mixtures . . . . . A. S. Cherkasov 285 (540)
The Influence of Temperature on Two Series of Bands in the Green Fluorescence Spectrum of Pure Cadmium Sulfide at Low Temperature. . . . M. Bancie-Grillot, E. F. Gross, E. Grillot, and B. S. Razbirin 287 (542)
New Examples of a Pronounced Dependence of Fluorescence Yield on the Position of the Emission Spectrum . . . . . E. N. Viktorova, A. S. Kochemirovskii, N. D. Krasnitskaya, and I. I. Reznikova 288 (544)
The Indicatrix of Raman Scattering . . . . . N. K. Sidorov 289 (546)
The Effect of Vitrification on the Polarization of the Persistent Luminescence of Organic Substances . . . . . E. V. Anufrieva 290 (547)
Apodization . . . . . D. Yu. Gal'pern 291 (549)

PERSONALIA

Abram Fedorovitch Ioffe's 80th Birthday 292 (551)

EDITOR'S NOTE

Comments on the scientific content of the translated Russian articles published in OPTICS AND SPECTROSCOPY are invited. They should be addressed as a Letter to the Editor of the Journal of the Optical Society of America and forwarded to the Editor of that journal, Dr. W. R. Brode, National Bureau of Standards, Washington 25, D.C.

UNIVERSITY OF ILLINOIS 3
LIBRARY
UNDERGRADUATE DIV
NAVY PIER GRAND AVE

VOL. IX, NO. 4 OPTICS AND SPECTROSCOPY OCTOBER 19

CONTENTS

(Numbers in parentheses are original Russian page numbers)

A Spectroscopic Method for Studying the Diffusion of Atoms in an Electric Arc . . . . . Ya. D. Raikhbaum and V. D. Malykh 223 (42
Isotope Effect in the Singlet Spectral Bands of the BF Molecule . . . . . A. A. Mal'tsev 225 (42
Vibrational Spectra of Unsaturated Hydrocarbons IX. Calculation and Interpretation of the Vibrational Spectra of Methylallene and the Deuterioallenes . . . . . L. M. Sverdlov and M. G. Borisov 227 (43
Temperature Dependence of the Intensities of the Infrared Absorption Bands of Liquid Chloroform . . . . . M. P. Lisitsa and Yu. P. Tsyashchenko 229 (43
The Vibrational Spectrum and Molecular Structure of Crystalline Arsenic Oxide . . . . . N. N. Sobolev and V. P. Cheremisinov 223 (44
Vibrational Spectra of Silicates III. Equations of the Vibrations of Planar Silicon-Oxygen Rings in Silicates . . . . . A. M. Prima 236 (45
Infrared Absorption Spectra of the Complexes of Urea and Thiourea with Tin Chloride and Tin Bromide . . . . . D. S. Bystrov, T. N. Sumarokova and V. N. Filimonov 239 (46
Calculation of the Optical Activity of Molecules . . . . . M. V. Vol'kenshtein and M. P. Kruchek 243 (46
Use of Electron Paramagnetic Resonance for the Study of Eu-Activated SrS Phosphors . . . . . V. G. Dubinin and Z. A. Trapeznikova 246 (47
The Valence of Manganese as an Activator in Phosphors . . . . . V. V. Osiko and G. V. Maksimova 248 (47
The Properties of the Longest Wavelength Line in the Intrinsic Absorption of Cu_2O . . . . . I. S. Gorban' and V. B. Timofeev 250 (48
The Optical Properties of Bulk Bismuth in the 3-36μ Region . . . . . M. N. Markov and A. S. Khaikin 253 (48
Determination of the Optical Constants of Absorbing Substances from the Measurements of Stokes' Parameters of Reflected Light . . . . . A. P. Prishivalko 256 (49
Amplitude and Phase Characteristics of an Interference Light Modulator . . . . . I. I. Adrianova, Yu. V. Popov, and A. V. Lapina 260 (50
X-Ray Monochromator for Ultrasoft Radiation with the Recording of the Absolute Number of Quanta . . . . . A. P. Lukirskii, M. A. Rumsh, and L. A. Smirnov 262 (50
Measurement of the Photoelectric Yield for Ultrasoft X-Radiation . . . . . A. P. Lukirskii, M. A. Rumsh, and L. A. Smirnov 265 (51

SHORT COMMUNICATIONS

The Connection Between F-Band Half-Widths and Defects in Solid Solutions of Alkali Halide Crystals . . . . . I. Ya. Melik-Gaikazyan and E. K. Zavadovskaya 268 (51
Quantum-Mechanical Treatment of the Nonlinearity of a Molecule . . . . . S. M. Yazykova 269 (51
The Aging of ZnS Phosphors . . . . . I. K. Vereshchagin 270 (51
The Relationship Between Electronic-Vibrational Absorption and Emission Bands . . . . . K. K. Rebane and O. I. Sil'd 272 (52
Annular Low Pressure Mercury Lamp . . . . . I. I. Kondilenko and G. A. Vorob'eva 273 (52
The Effect of Temperature on the Decay of Phosphorescence in Boron Phosphors . . . . . M. D. Khalupovskii 274 (52
Approximate Wave Functions of Free Ions and of Ions in a Crystal . . . . . M. I. Petrashen', I. V. Abarenkov, and N. N. Kristofel' 276 (52
Low Temperature Thermal Radiation Detector . . . . . A. F. Mal'nev and L. S. Kremenchugskii 278 (53
The Effect of the Flux on the State of the Activator in a Phosphor: An Investigation by the Paramagnetic Resonance Method . . . . . V. G. Dubinin 297 (53

(Contents continued on inside back cover)